1967

Design of a marine nuclear power plant utilizing the direct Brayton cycle

Bruce Stephen Gathy
Iowa State University

DESIGN OF A MARINE NUCLEAR POWER PLANT UTILIZING THE DIRECT BRAYTON CYCLE

by

Bruce Stephen Gathy

A Dissertation Submitted to the
Graduate Faculty in Partial Fulfillment of
The Requirements for the Degree of
DOCTOR OF PHILOSOPHY

Major Subject: Nuclear Engineering

Approved:

Signature was redacted for privacy.

In Charge of Major Work

Signature was redacted for privacy.

Head of Major Department

Signature was redacted for privacy.

Dean of Graduate College

Iowa State University
Of Science and Technology
Ames, Iowa

1967

TABLE OF CONTENTS

INTRODUCTION

When the Nuclear Ship Savannah entered regular commercial service in August of 1965, nuclear power for merchant ships became a reality. There have been many studies on the application of nuclear power to all classes of merchant ships (1, 2)[1]. Such concepts as the direct and indirect boiling water reactors, pressurized-water reactors and organic- as well as gas-cooled reactors have been examined. These studies have shown that the problems associated with nuclear powered merchant ships are not technical but economic in nature and that the economics of nuclear power becomes better with longer trade routes and higher speeds.

Although the gas-cooled reactor is included in almost all comparisons between nuclear and conventional marine power, the emphasis has been placed on the pressurized water reactor which has proven itself in naval application. The few studies carried out on gas-cooled reactors have been for indirect cycles, with the production of propulsion steam as the primary objective. Their main application for conceptual designs have been the bulk, liquid cargo ships where fuel volume can be directly converted to useful cargo volume, and where long trade routes are the general rule.

The direct cycle concept had not been applied to

---

[1]Numbers in parentheses refer to references given in the bibliography.

nuclear power until the latter part of 1966 when a 25-MW stationary plant was designed by Gutehoffnungshatte (GHH) of West Germany in conjunction with the Escher Wyss Company of Switzerland.

The basic concept explored in this thesis is the direct cycle applied to a marine power plant. It is felt that a gas-cooled reactor, gas-turbines and a waste-heat boiler can be incorporated to provide heat energy, propulsive power and auxiliary steam, respectively, by utilizing the direct Brayton cycle.

This system was applied to a large passenger ship. This is one class of ship requiring large propulsive power and having high electrical as well as high steam loads in addition to demanding low cost. There are other motivating factors for applying nuclear power to a passenger ship, however. The impact on new design is readily apparent.

With nuclear power, large boiler uptakes can be eliminated making available large volumes of prime space, notably midships on the centerline. A few recent designs of conventionally powered passenger ships have moved the boiler rooms aft, and moved the uptakes outboard from the centerline. Canbarra and Rotterdam are two such examples. However, the very large steam ships with shaft horsepowers in the hundred thousand HP range still maintain midships boiler rooms with their uptakes on the centerline.

Passenger ships utilize their weather decks fully and soot and fumes are of great concern. Much time and effort is spent in stack design to eliminate this problem. This problem would be eliminated with nuclear power. Also, conventionally powered ships are dependent upon ports-of-call that have adequate fuel facilities. Passenger ships, when acting as cruise ships, have their itineraries based heavily upon this fact. Nuclear power would free a passenger ship from this consideration.

An existing ship was chosen, rather than arbitrarily selecting design criteria and parameters, primarily to insure a valid comparison with existing conventional power plants. This approach imposes some major limitations in design flexibility, notably machinery location, but this was accepted as being fair exchange for actual operating data.

The steam ship ROTTERDAM, flag-ship of the Holland-America Line, was chosen for this design study and is seen in Fig. 1.0. The ROTTERDAM entered commercial service in 1959 and is a fine example of a large, modern passenger ship. She is 748 feet long, displaces 31,040 tons, accomodates 1,456 passengers and requires 35,000 shaft horsepower to travel at a speed of 20.5 knots. Her power plant consists of four steam boilers, three geared-turbines on each of two shafts, four turbo-generators delivering 4,048 KW of electrical power, three distilling plants supplying 80,000 gallons

Fig. 1.0. Steam ship ROTTERDAM.

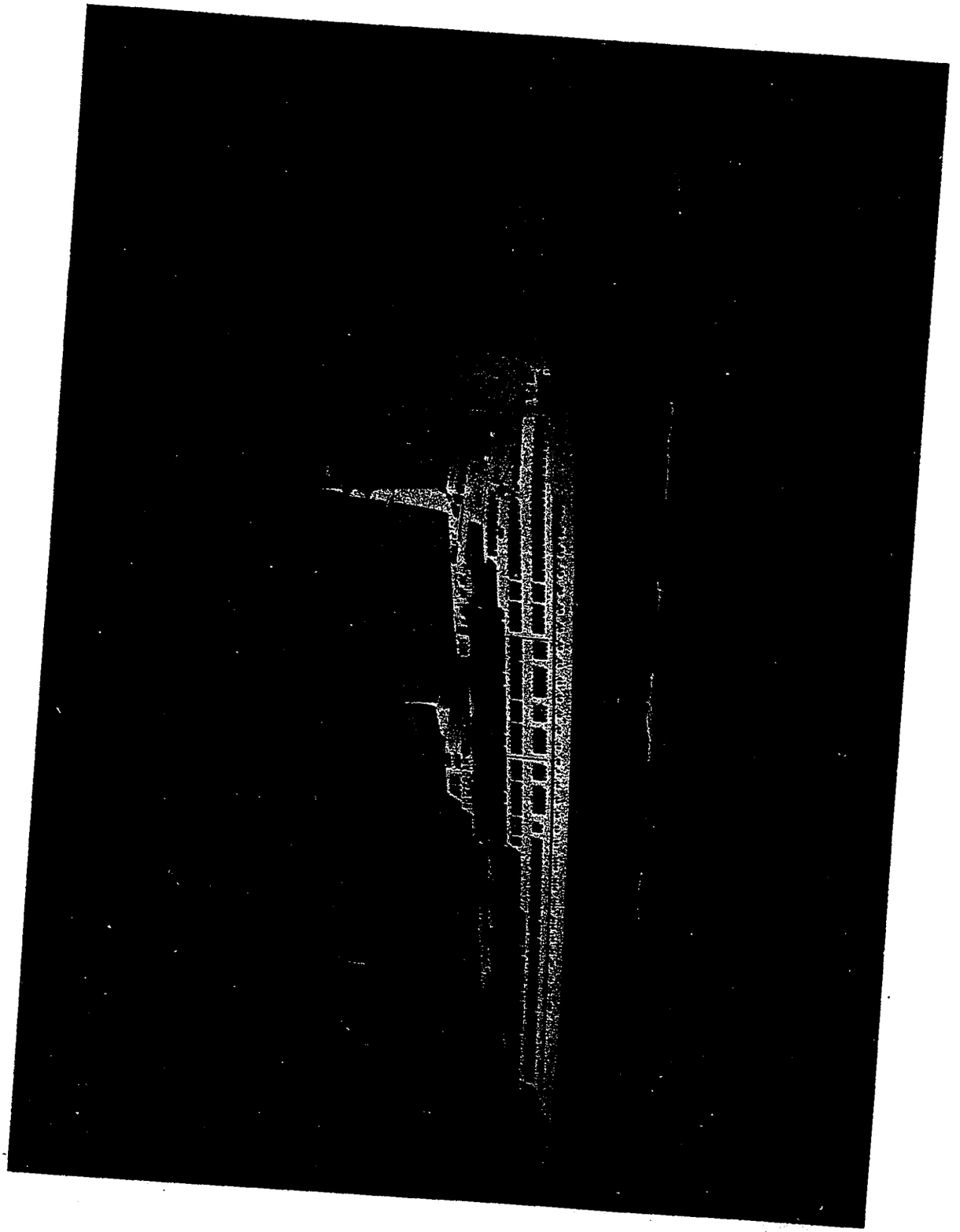

of fresh water per day and a 700 ton air conditioning plant. In addition, 11,000 pounds of steam per hour are utilized for hotel services such as cooking, laundering and heating[1].

It will be shown that the direct Brayton cycle is applicable to nuclear marine propulsion and that current, state-of-the-art technology is such that existing component machinery can, in fact, be employed. In addition, it will be shown that this system will require less total weight, occupy existing spaces, allow the ship unlimited cruising range and freedom from dependency on ports-of-call where adequate fuel supplies are available and provide a higher over-all plant efficiency.

This study is intended to adapt a specific nuclear system to a particular cycle configuration, and consider the space, weight, efficiency and economics of such a configuration. The following areas will be given detailed study:

1. Brayton cycle optimization to provide maximum cycle efficiency.
2. Control and cleaning of the working fluid.
3. Choice of a working fluid.
4. Adaptation of the General Electric 630A Mark V(B) nuclear steam generator to the design parameters.
5. Selection of the turbo-machinery and associated plant equipment.

---

[1]New Building Department of the Holland-America Line, Rotterdam, The Netherlands. Ship parameters. Private communication. 16 November and 30 December, 1965.

6. Machinery placement and ship stability.
7. Volume, weight and economic comparisons.

CHAPTER I. OPEN BRAYTON CYCLE

The least expensive and most abundant working medium for heat engines is air. Utilizing the atmosphere as a working medium reservoir and as a heat sink appears to be most desirable when dealing with mobile power plants. For these reasons an open Brayton cycle was studied and optimized for maximum efficiency.

As will be shown later the actual open cycle efficiency is a function of ambient temperature, maximum cycle temperature, compressor and turbine efficiencies, system pressure losses and cycle pressure ratio. Although the ambient air temperature varies within certain limits, a representative average value can be assumed and held constant. The maximum cycle temperature is dictated by the reactor fuel element metallurgy and lifetime, and for this study a value of 1250 ^{o}F is used as dictated by the design limitations described in Chapter IV. The compressor and turbine efficiencies chosen are representative of current state-of-the-art values and in addition, the various component pressure losses are based upon values experienced with actual operating components.

Brayton Cycle Theory

Nomenclature

The following nomenclature will be used in this chapter:

T = absolute temperature (^{o}R)

p = absolute pressure (psia)

k = ratio of specific heats

R = universal gas constant for air (BTU/# ^{o}R)

c_p = specific heat at constant pressure (BTU/# ^{o}R)

w = mass flow rate (# air/sec)

W_c = compressor work (BTU)

W_t = turbine work (BTU)

h = specific enthalpy (BTU/#)

Q = heat energy (BTU)

r_p = pressure ratio

η_c = compressor efficiency

η_t = turbine efficiency

η = cycle thermal efficiency

Numerical subscripts refer to state points on the Temperature-Entropy diagrams.

Isentropic Processes

Compression (between points 1 and 2)

$$\frac{T_2}{T_1} = \left(\frac{P_2}{P_1}\right)^{\frac{k-1}{k}} = \left(\frac{P_2}{P_1}\right)^{\frac{R}{c_p}} = (r_p)^{\frac{R}{c_p}} \qquad (1.1)$$

Expansion (between points 3 and 4)

$$\frac{T_3}{T_4} = \left(\frac{P_3}{P_4}\right)^{\frac{k-1}{k}} = \left(\frac{P_3}{P_4}\right)^{\frac{R}{c_p}} \qquad (1.2)$$

Work

Isentropic

Compressor (W_c)

$$W_c = wc_p(T_2-T_1) = w(h_2-h_1) \qquad (1.3a)$$

Turbine (W_t)

$$W_t = w c_p (T_3 - T_4) = w(h_3 - h_4) \tag{1.3b}$$

Actual (accounting for losses)

Compressor

$$W_c = w c_p (T_2' - T_1) = w(h_2' - h_1) \tag{1.4a}$$

Turbine

$$W_t = w c_p (T_3 - T_4') = w(h_3 - h_4') \tag{1.4b}$$

Isentropic efficiencies

Compressor

$$\eta_c = \frac{\text{isentropic work}}{\text{actual work}}$$

$$\eta_c = w c_p \frac{(T_2 - T_1)}{(T_2' - T_1)} = w \frac{(h_2 - h_1)}{(h_2' - h_1)} \tag{1.5a}$$

Turbine

$$\eta_t = \frac{\text{Actual work}}{\text{isentropic work}}$$

$$\eta_t = w c_p \frac{(T_3 - T_4')}{(T_3 - T_4)} = w \frac{(h_3 - h_4')}{(h_3 - h_4)} \tag{1.5b}$$

Temperature ratios

$$\frac{T_2}{T_1} = \frac{T_3}{T_4} = \alpha \tag{1.6}$$

$$\frac{T_3}{T_2} = \frac{T_4}{T_1} = \beta \tag{1.7}$$

$$\frac{T_3}{T_2} \times \frac{T_2}{T_1} = \frac{T_3}{T_1} = \alpha\beta = \nu \tag{1.8}$$

$$T_1 = T_1$$

$$T_2 = \alpha T_1$$

$$T_3 = \nu T_1$$

$$T_4 = \beta T_1$$

Actual work

Turbine

$$W_t = w c_p (T_3 - T_4') \tag{1.9a}$$

$$= w c_p \eta_t (T_3 - T_4) \tag{1.9b}$$

$$= w c_p \eta_t T_1 (\nu - \beta) \tag{1.9c}$$

$$= w c_p \eta_t T_1 \beta (\alpha - 1) \tag{1.9d}$$

Compressor

$$W_c = w c_p (T_2' - T_1) \tag{1.10a}$$

$$= \frac{w c_p}{\eta_c} (T_2 - T_1) \tag{1.10b}$$

$$= \frac{w c_p}{\eta_c} T_1 (\alpha - 1) \tag{1.10c}$$

Useful

$$W_u = (W_t - W_c) \tag{1.11a}$$

$$= \frac{w c_p T_1}{\eta_c} (\alpha - 1)(\eta_c \eta_t \beta - 1) \tag{1.11b}$$

Energy into cycle

$$Q = w c_p (T_3 - T_2') \tag{1.12a}$$

$$= w c_p [(T_3 - T_1) - (T_2' - T_1)] \tag{1.12b}$$

$$= w c_p \left[(\nu T_1 - T_1) - \frac{\alpha T_1 - T_1}{\eta_c}\right] \tag{1.12c}$$

$$= \frac{w c_p T_1}{\eta_c} [\eta_c (\nu - 1) - (\alpha - 1)] \tag{1.12d}$$

Cycle efficiency

$$\eta = \frac{\text{useful work}}{\text{energy in}} = W_u/Q \tag{1.13a}$$

$$\eta = \frac{\frac{w c_p T_1}{\eta_c}[(\alpha-1)(\eta_c\eta_t\beta-1)]}{\frac{w c_p T_1}{\eta_c}[\eta_c(\nu-1)-(\alpha-1)]} \tag{1.13b}$$

$$\eta = \frac{(1-\alpha)(\eta_c\eta_t\beta-1)}{\eta_c(\nu-1)-(\alpha-1)} \tag{1.13c}$$

Variations from the Simple Cycle

The simple cycle is varied to improve cycle efficiency or useful work. Efficiency can be improved by increasing W_u while holding Q constant; decreasing Q while holding W_u constant; or increasing W_t while decreasing W_c. These variations can be brought about with the use of intercooling, regeneration or reheat.

Intercooling

Work of an isentropic compression

$$w\ c_p(T_2-T_1) \tag{1.14}$$

is greater than the work for an isothermal compression

$$wRT_1\ \ln(p_1/p_2). \tag{1.15}$$

Intercooling is isentropic compression in two or more stages while cooling the fluid between stages, to approach isothermal compression. This is seen in Fig. 1.2, where

1-2 Ideal Isentropic compression
1-2' Actual Isentropic compression
1-2a Ideal Isothermal compression
1-c-d-2b two stage actual Isentropic compression with intercooling from c-d

Regeneration

Regeneration entails returning heat energy to the cycle that would normally be lost in the exhaust gases. This reduces the quantity of heat required from an outside source, thus reducing Q and increasing cycle efficiency. Referring to Fig. 1.3, the maximum heat energy that is available to the cycle from the exhaust gas is proportional to

$$\Delta T = (T_{4'}-T_{2'}). \tag{1.16}$$

This heat energy would be available with an ideal heat exchanger. However, there must be a temperature difference between two fluids in order to transfer heat energy. Setting δt equal to that minimum temperature difference required, the maximum temperature difference available to transfer heat is

$$\Delta T' = \Delta T - \delta t \ . \tag{1.17}$$

In Fig. 1.3 T_9 is the highest temperature possible through regeneration and Q equals

$$Q = w\ c_p(T_3-T_9) \ . \tag{1.18}$$

The EFFECTIVENESS of a heat exchanger (ϵ) is defined as

$$\epsilon = \Delta T'/\Delta T \ . \tag{1.19}$$

Cycle Optimization

Design criteria

Usually η_c, η_t, T_3 and T_1 are known and r_p is allowed to be the design independent variable. Because W_u and η are functions of r_p, a plot of W_u and η versus r_p can be made and

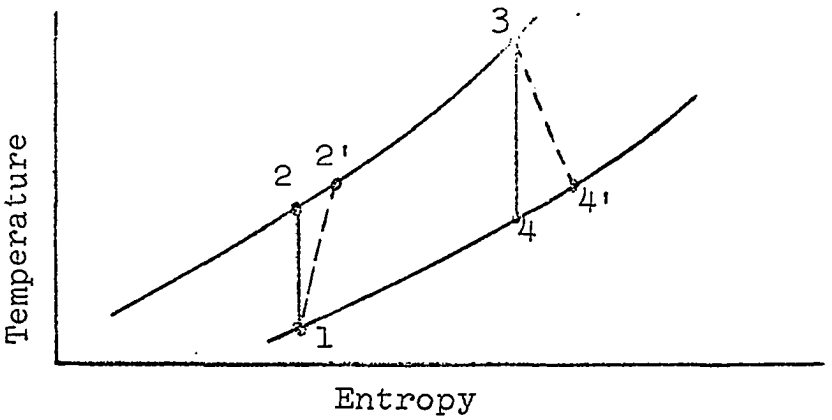

Fig. 1.1. Simple Brayton cycle.

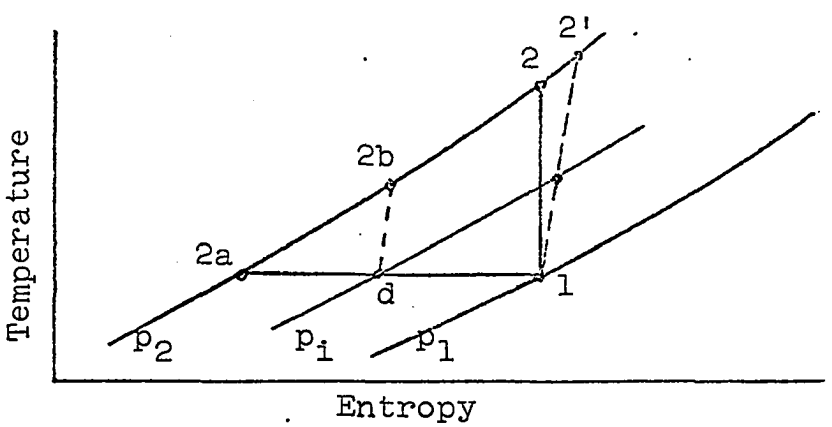

Fig. 1.2. Intercooling.

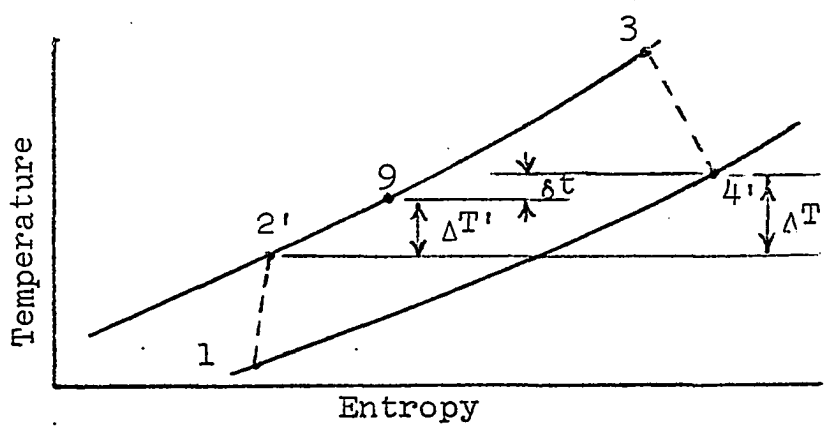

Fig. 1.3. Regeneration.

r_p chosen based on best W_u or η. Because component pressure losses cause a decrease in turbine work (decrease the turbine expansion ratio), they must be accounted for. Pressure losses experienced anywhere within the cycle can be expressed in terms of a percent of the individual losses. The sum of the individual losses is the total pressure loss and is applied to the cycle between the compressor discharge and the turbine inlet.

This cycle analysis was carried out utilizing the following pressure losses which are considered to be well within the limits of existing equipment:

1. Regenerator (3)	4.0%
2. Intercooler	1.0%
3. Intake and exhaust filters (4), 0.18 psia	1.5%
4. Waste-heat boiler[1] (5); 2.9 psia	2.0%
5. Reactor (values allowed to vary)	2, 4, and 6%

From the above list the total percent pressure loss is 8.5% plus that across the reactor. The pressure drop across the reactor was considered a variable.

Gas from either the turbine exhaust or regenerator will be entering the waste-heat boiler and is of concern, for it determines the maximum steam temperature that is possible to

---

[1]Hedges, R. B., Marine Department, Combustion Engineering Corporation, Winsor, Connecticut. Waste-heat boilers. Private communication. 15 May, 1965.

achieve. The stack temperature is determined by the temperature of the gas leaving the last component, i.e., the boiler or regenerator. This temperature should be as low as possible to avoid thermal stresses within the stack.

The pressure ratio dictates the number of stages in the turbo-machinery and the maximum system pressure. In order to keep the machinery size and component weights down, a low pressure ratio is sought. Because W_u dictates the mass flow rate, it should be high to keep the ducting sizes small and flow velocities low. From the economic point of view cycle and plant efficiency should be as high as possible.

Design parameters

The maximum cycle temperature is 1250 ^{o}F. The ambient air temperature was chosen as 60 ^{o}F. Values of compressor and turbine efficiencies of 88% and 90% respectively, were used. It was assumed that sea water is available to intercool to the ambient temperature and that the regenerator effectiveness is 80%.

The power requirements of the ship at normal cruising speed are as follows:

1. 35,000 shaft horsepower
2. 4,048 KW of electricity
3. 6.24 # steam/sec @ 620 psia or less for all other auxiliary use.

In order to determine the amount of power that must be produced to deliver 35,000 HP to the shaft, the method of

power transmission from primemover to shaft must be known. The gas-turbine is unidirectional and cannot be reversed to produce backing power. There are three methods available to accomplish this: electric drive; reversing reduction gears; and controllable pitch propellers.

The electric drive and the reversing reduction gear systems can utilize the existing propeller. For AC motors and generators, efficiencies of 97% are attainable[1], while efficiencies of 98% per toothmesh can be achieved with large marine gears (6). This would result in a 94% efficient transmission system for the electric drive and 96% for the double reduction gear system. Controllable pitch propellers are of lower efficiency than that of varying pitch propellers, which is inherent in their designs. The varying pitch propeller presently installed on the ROTTERDAM has three blades, is 18 feet in diameter, weighs 23 long tons and has an efficiency of 71% at 131 RPM and 20.5 knots[2]. This can be replaced by a four bladed, 14 foot, 11.6 ton controllable pitch propeller, delivering the same shaft horsepower, which

---

[1]Lory, M. R., Engineering Manager, Large Rotating Apparatus Division, Westinghouse Electric Company, East Pittsburgh, Pennsylvania. Marine motors and generators. Private communication. 10 January, 1966.

[2]Van Veen, G., New Building Department of the Holland-America Line, Rotterdam, the Netherlands. Propeller efficiency. Private communication. 2 May, 1967.

has an efficiency of 64% at 240 RPM and 20.5 knots[1]. This would then result in a transmission efficiency of 86.5%. For this study the lowest transmission value was used so as to determine an upper limit on power production.

Design study

Utilizing Equations 1.11b, 1.12b, and 1.13b and allowing α to vary from 1.0 to 2.2, a plot of W_u and η was prepared and is seen in Fig. 1.4. This plot shows that W_u peaks before η and, therefore, it is impossible to obtain maximum work and efficiency at the same value of r_p. As discussed earlier under design criterior, high values of W_u, along with low values of r_p are desirable. Three pressure ratios will be examined further; 4.5, 5.5 and 7.0, to determine the optimum pressure ratio to be utilized. In addition, because the pressure drop across the reactor is not accurately known at this time, it will assume values of 2%, 4%, and 6%.

With the utilization of a waste-heat boiler for steam production, the gas temperature at the boiler inlet dictates the maximum steam temperature and is of primary importance. Also of importance is the inlet gas temperature to the regenerator for it has a direct bearing on the quantity of heat added to the cycle, or put another way, the temperature

---

[1]Naulty, A. M., Project Engineer, Baldwin-Lima-Hamilton Corporation, Philadelphia, Pennsylvania. Controllable pitch propellers. Private communication. 7 April, 1967.

Fig. 1.4. Useful work and cycle efficiency versus pressure ratio to the (k-1)/k power for the simple, open Brayton cycle. $\eta_c = 0.88$, $\eta_t = 0.90$, $T_1 = 520\ ^{o}R$, $T_3 = 1710\ ^{o}R$.

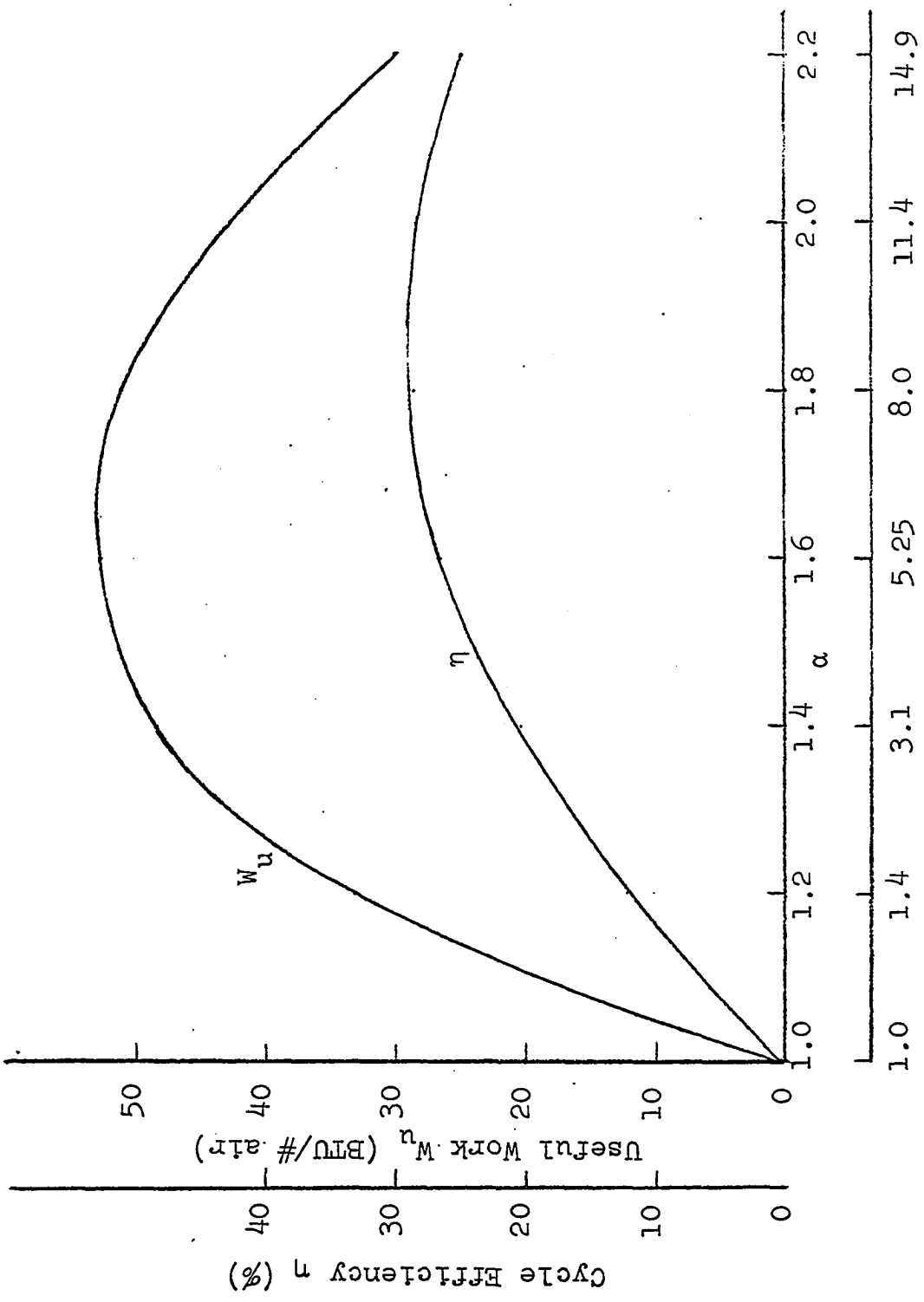
Cycle Efficiency η (%)
Useful Work W_u (BTU/# air)
0
10
20
30
40
50
W_u
η
1.0
1.2
1.4
1.6
1.8
2.0
2.2
α
1.0
1.4
3.1
5.25
8.0
11.4
14.9
r_p

change across the reactor. Another state point of concern is the exhaust temperature to the stack.

It is possible to place the boiler before or after the regenerator but it must be remembered that superheated steam at 620 psia is required for the turbo-generators. This means steam temperatures of at least 490 ^{o}F. If a minimum of 100 degrees between gas and steam temperatures is assumed, the minimum gas temperature is 590 ^{o}F. The only gas at this temperature is the gas from the power turbine. But placing the boiler immediately after the turbine will result in a decrease in the cycle efficiency from that which would otherwise be attainable with only regeneration. As can be seen in Fig. 1.7, if the turbine exhaust gas went directly to the regenerator the gas temperature entering the reactor (T_9) would be higher, the heat energy entering the cycle would be less and the cycle efficiency would be greater, because the useful work is the same. This difference in cycle efficiency amounts to 9.6% in the case of the intercooled and regenerated cycle at a pressure ratio of 5.5.

However, when considering the plant efficiency, which is defined as the total heat energy out divided by the total heat energy in, the difference is within one to two percent with the waste-heat boiler giving the higher efficiency. For example, if the same cycle as above is used along with a conventional boiler of 88% efficiency (7), the plant efficiency is 52.0% while that for the cycle utilizing the

waste-heat boiler before the regenerator is 52.4%. In both cases steam with 140 degrees of superheat was produced.

The turbine exhaust temperature varied with changing Δp and r_p, and resulted in a varying maximum steam temperature in the boiler. This brought about a variation in the steam rate through the turbo-generators for a constant electrical load. A steam balance had to be made for each set of operating conditions.

With varying compressor discharge temperature ($T_{2'}$), and varying boiler exit temperature (T_{bex}) the minimum gas temperature difference within the regenerator (δt), also varied with each set of operating conditions. The minimum temperature difference was determined from the expression

$$\delta t = (1-\varepsilon)(T_{bex}-T_{2'}), \qquad (1.20)$$

where the regenerator effectiveness (ε) was kept constant at 80%.

Based on the above criterion and utilizing the chosen parameters, a study was carried out to determine the optimum pressure ratio and cycle. The cycles examined were the simple cycle Fig. 1.5, intercooled cycle Fig. 1.6, regenerative cycle Fig. 1.7, and intercooled and regenerative cycle Fig. 1.8. For all of the calculations the thermodynamic properties of air were taken from "Gas Tables" by J. A. Keenan and J. Kaye (8) and those for steam were taken from "Thermodynamic Properties of Steam" by J. H. Keenan and F. G. Keyes (9).

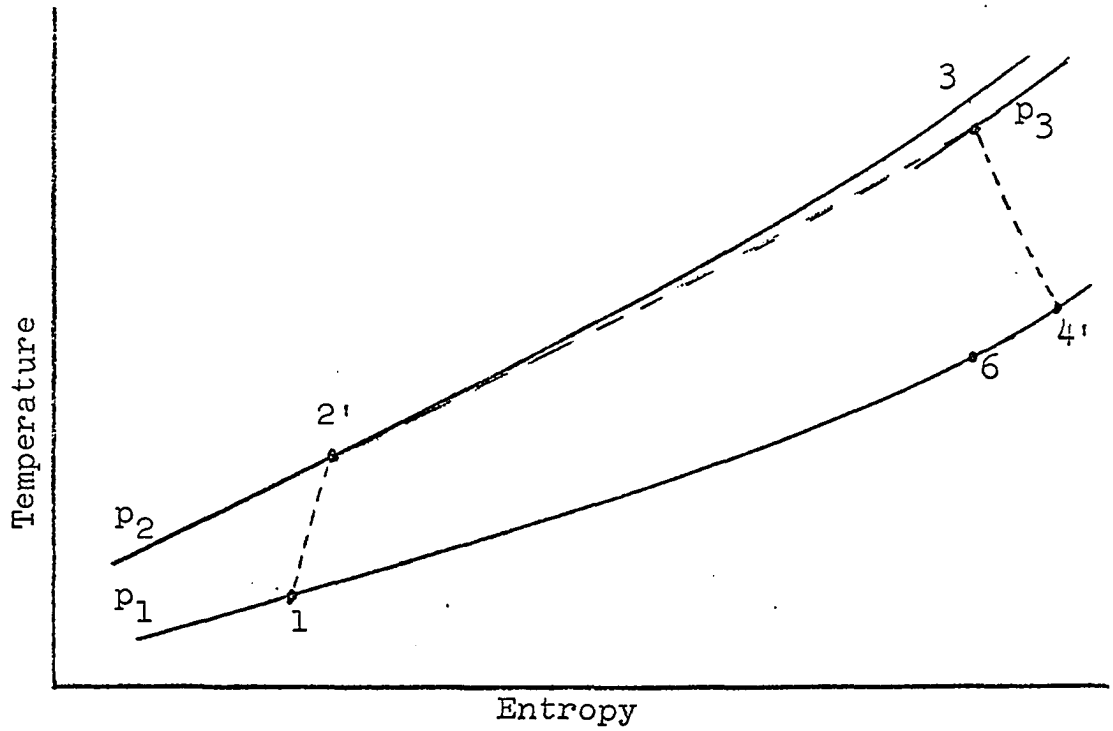

Fig. 1.5. Simple cycle.

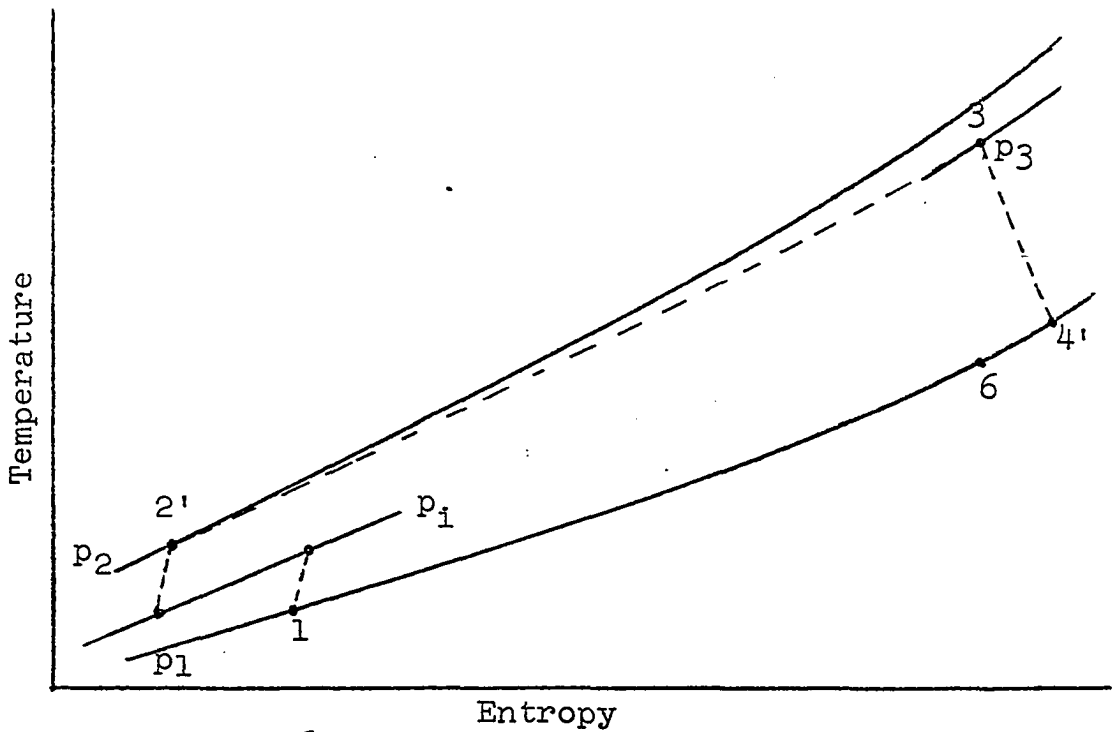

Fig. 1.6. Intercooled cycle.

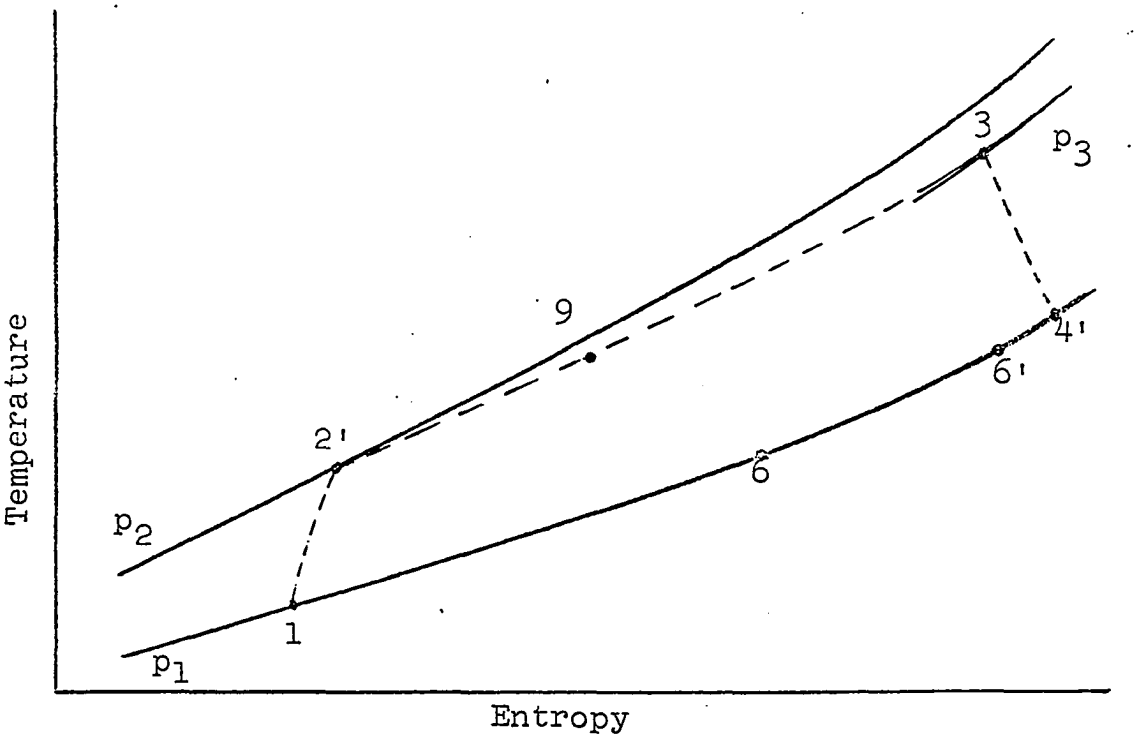

Fig. 1.7. Regenerative cycle.

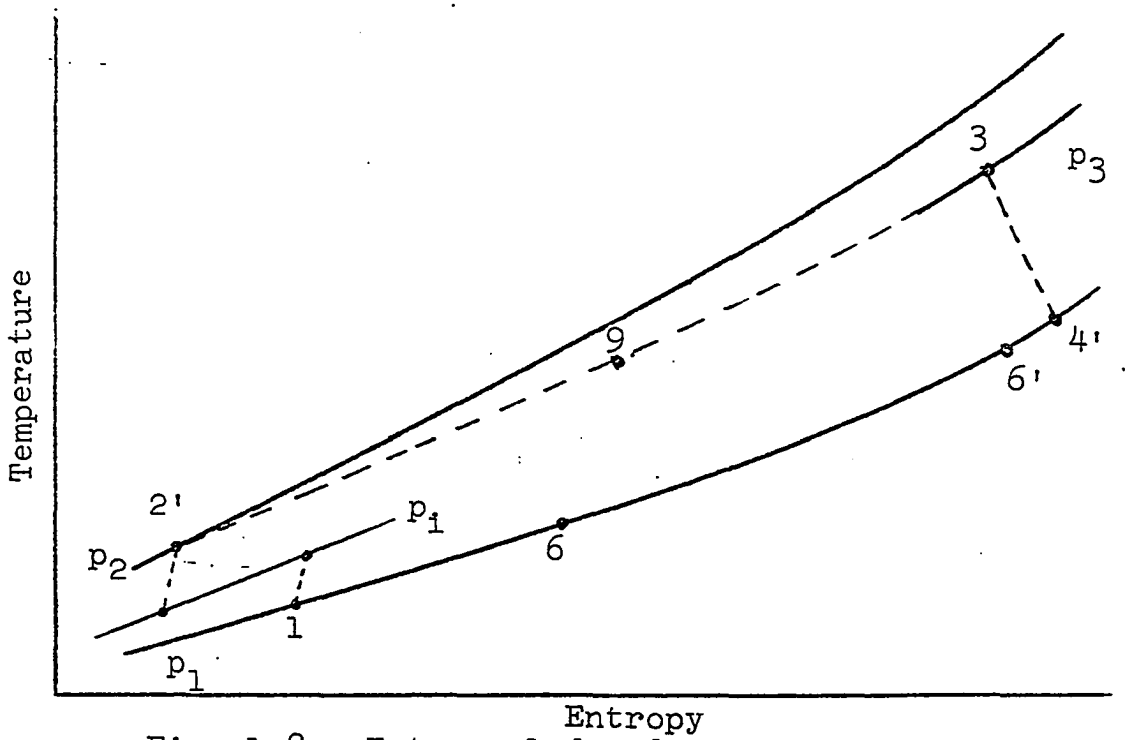

Fig. 1.8. Intercooled and regenerative cycle.

Conclusions and selection

This study showed that with an increasing pressure ratio, the cycle efficiency increased for the simple and intercooled cycles, fell with the regenerative cycle and remained essentially constant for the cycle with both intercooling and regeneration. The total mass flow rate decreased in every case with an increase in pressure ratio. Increasing the total pressure losses lowered the cycle efficiency and raised the total mass flow rate in every case. The results are plotted in Figs. 1.9, 1.10, 1.11, 1.12.

When the cycle efficiency and mass flow rate for each cycle are plotted versus the pressure ratio for a constant reactor pressure drop, the intercooled and regenerative cycle gave the highest cycle efficiency and the second lowest mass flow rate as can be seen in Figs. 1.13 and 1.14. Based on these results the cycle chosen is the one incorporating intercooling and regeneration.

Because the cycle efficiency remains essentially constant, as seen in Figs. 1.12 and 1.13, it is not a factor in selecting the operating pressure ratio. As can be seen in Fig. 1.14, however, increasing the pressure ratio from 4.5 to 5.5 decreases the mass flow rate 7.8% where as, increasing the pressure ratio from 5.5 to 7.0 only brings about a further 5.9% decrease in the mass flow rate. Also examining the boiler inlet temperature and the stack temperature plotted versus the pressure ratio, at a constant reactor pressure

Fig. 1.9. Cycle efficiency and mass flow rate versus pressure ratio, with varying total system pressure drop, for the simple open cycle.

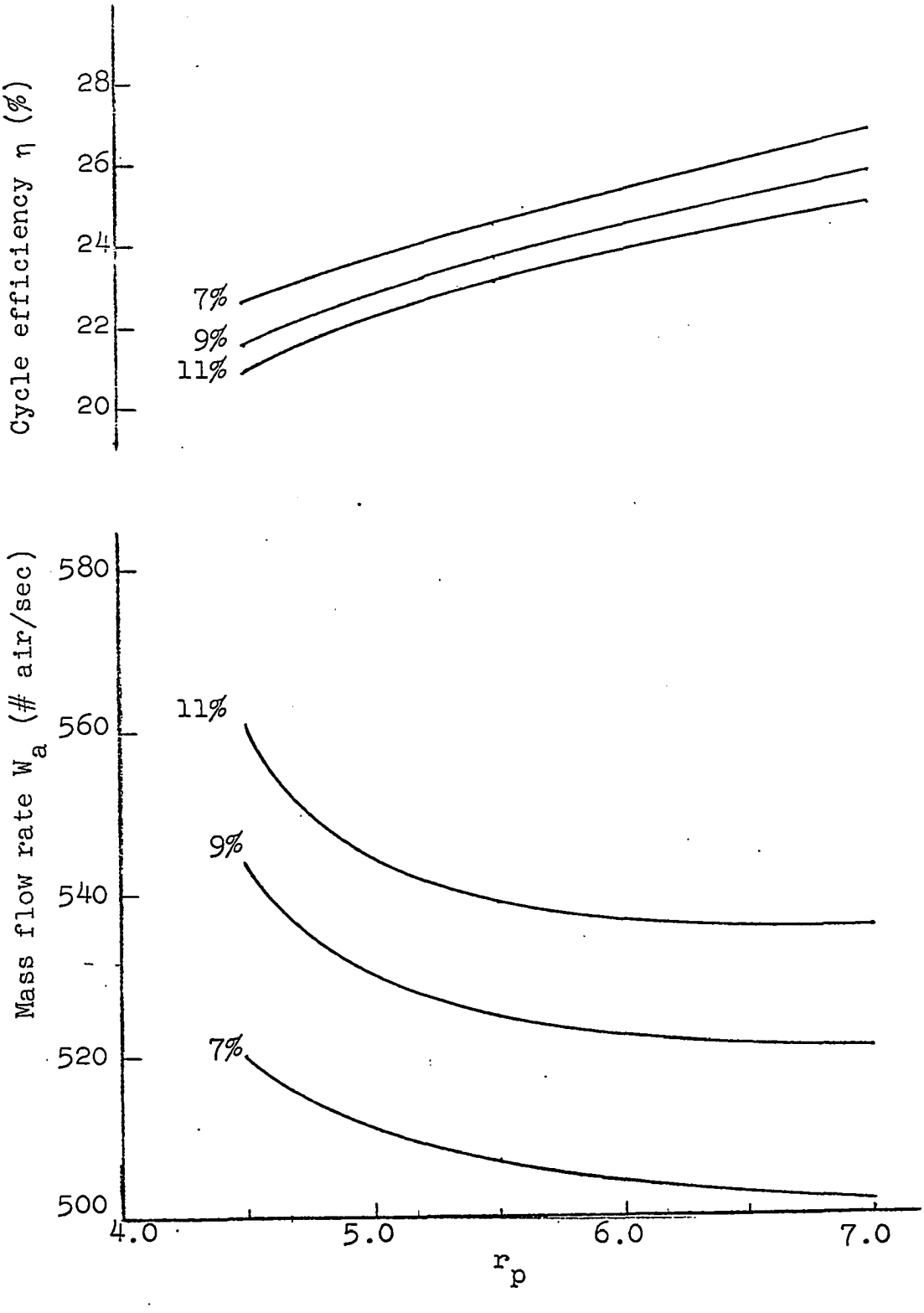
Cycle efficiency η (%)
28
26
24
22
20
7%
9%
11%
Mass flow rate W_a (# air/sec)
580
560
540
520
500
11%
9%
7%
4.0
5.0
6.0
7.0
r_p

Fig. 1.10. Cycle efficiency and mass flow rate versus pressure ratio with varying total system pressure drop, for the intercooled open cycle.

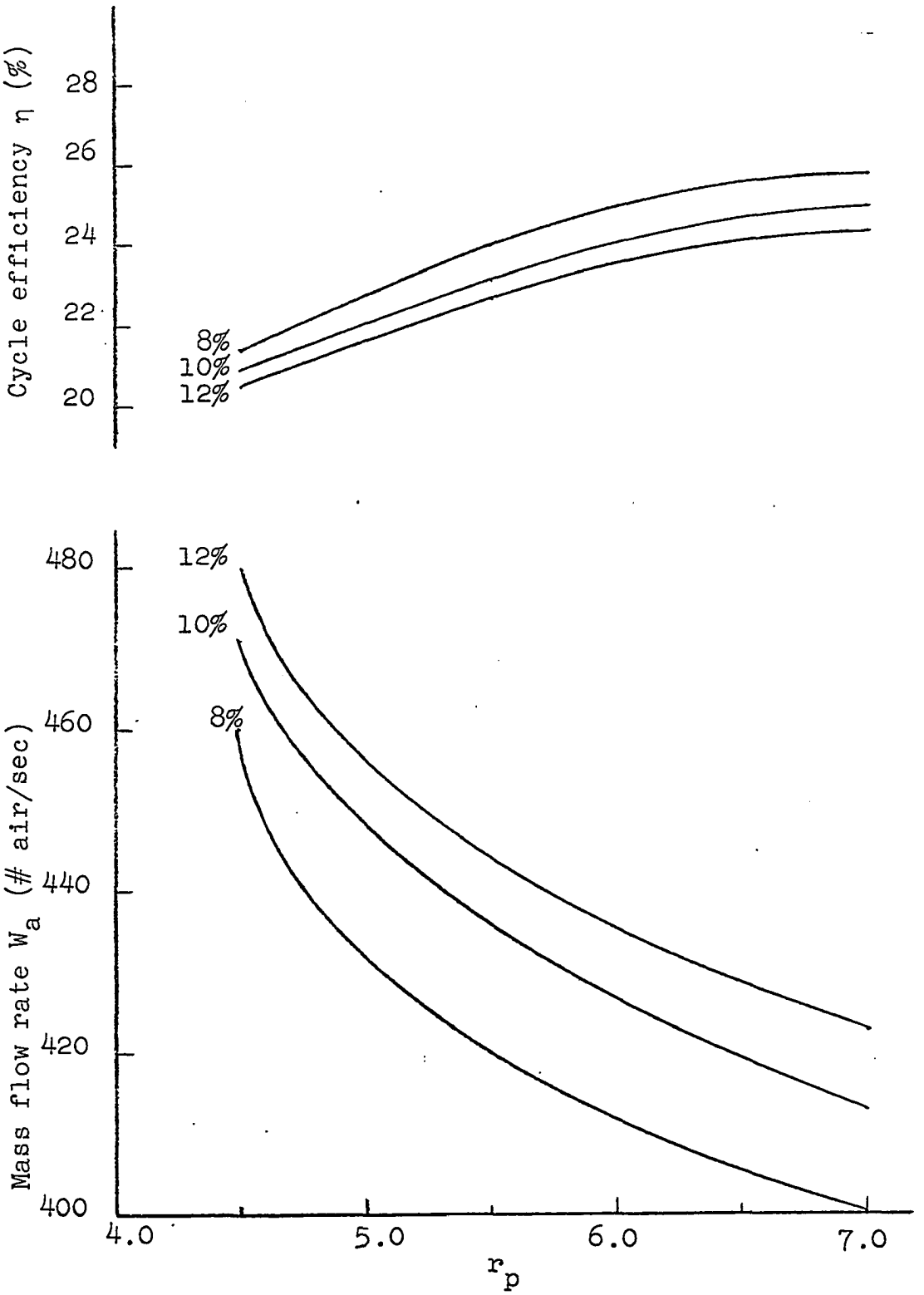
Cycle efficiency η (%)
28
26
24
22
20
8%
10%
12%
Mass flow rate W_a (# air/sec)
480
460
440
420
400
12%
10%
8%
4.0
5.0
6.0
7.0
r_p

Fig. 1.11. Cycle efficiency and mass flow rate versus pressure ratio with varying total system pressure drop, for the regenerative open cycle.

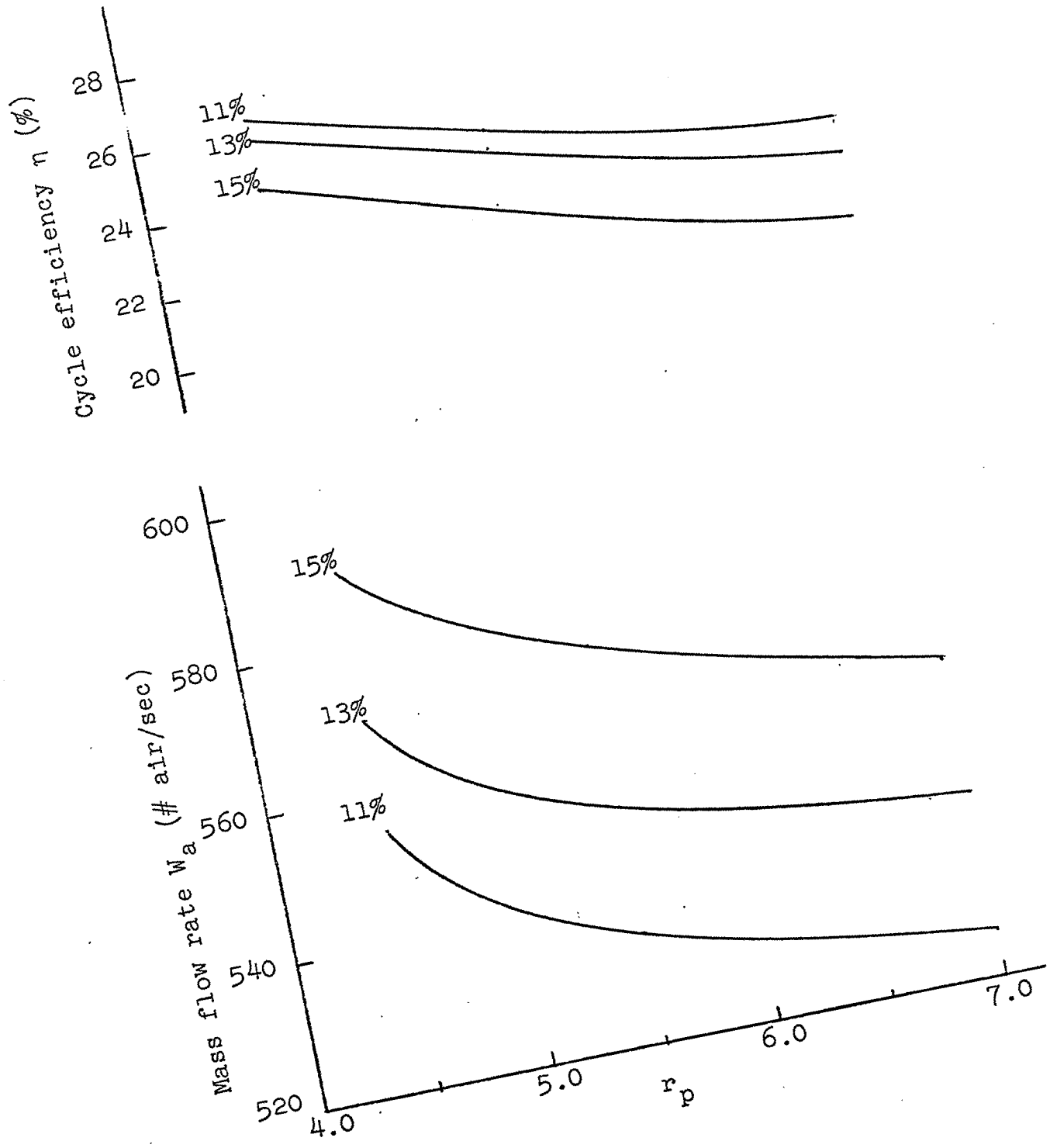
Cycle efficiency η (%)
28
26
24
22
20
11%
13%
15%
600
580
560
540
520
Mass flow rate W_a (# air/sec)
15%
13%
11%
4.0
5.0
6.0
7.0
r_p

Fig. 1.12. Cycle efficiency and mass flow rate versus pressure ratio with varying total system pressure drop, for the intercooled and regenerative open cycle.

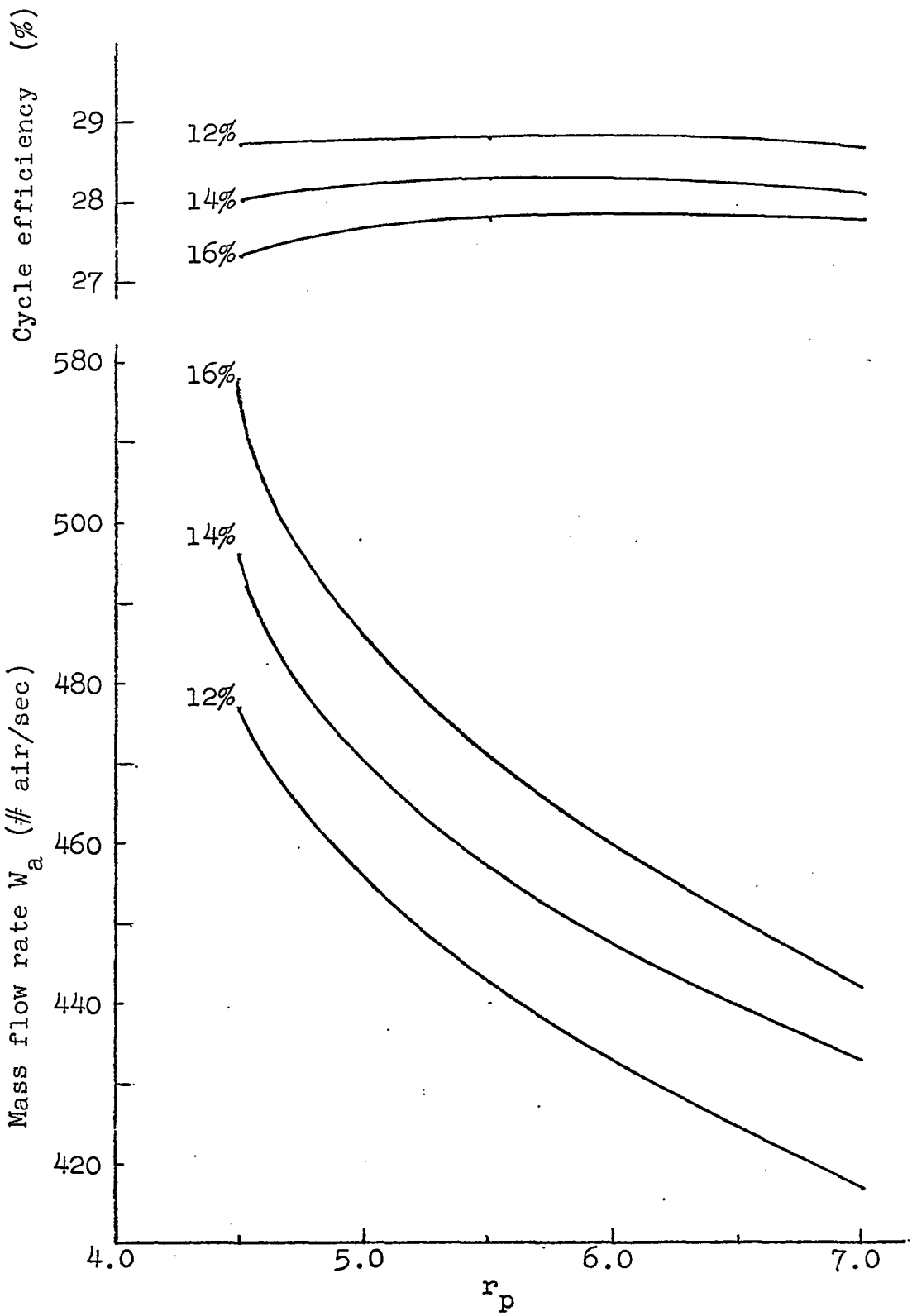
Cycle efficiency (%)
29
28
27
12%
14%
16%
580
500
480
460
440
420
16%
14%
12%
Mass flow rate W_a (# air/sec)
4.0
5.0
6.0
7.0
r_p

Fig. 1.13. Cycle efficiency versus pressure ratio for a 2% pressure drop in the reactor for the various cycles.

A. Intercooled and regenerative cycle.

B. Regenerative cycle.

C. Simple cycle.

D. Intercooled cycle.

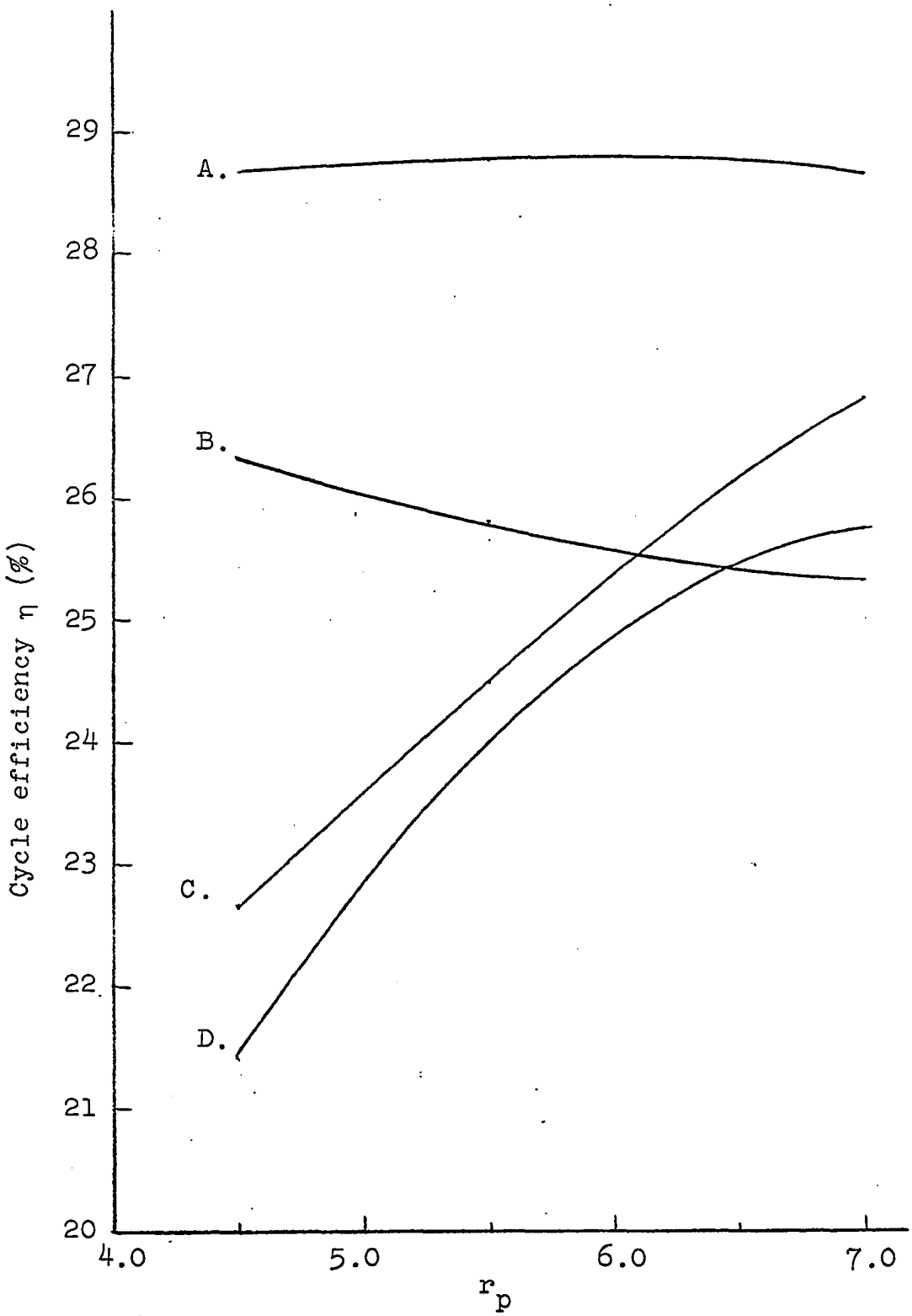
29
28
27
26
25
24
23
22
21
20
Cycle efficiency η (%)
A.
B.
C.
D.
4.0
5.0
6.0
7.0
r_p

Fig. 1.14. Mass flow rate versus pressure ratio for a 2% pressure drop in the reactor for the various cycles.

A. Regenerative cycle.

B. Simple cycle.

C. Intercooled and regenerative cycle.

D. Intercooled cycle.

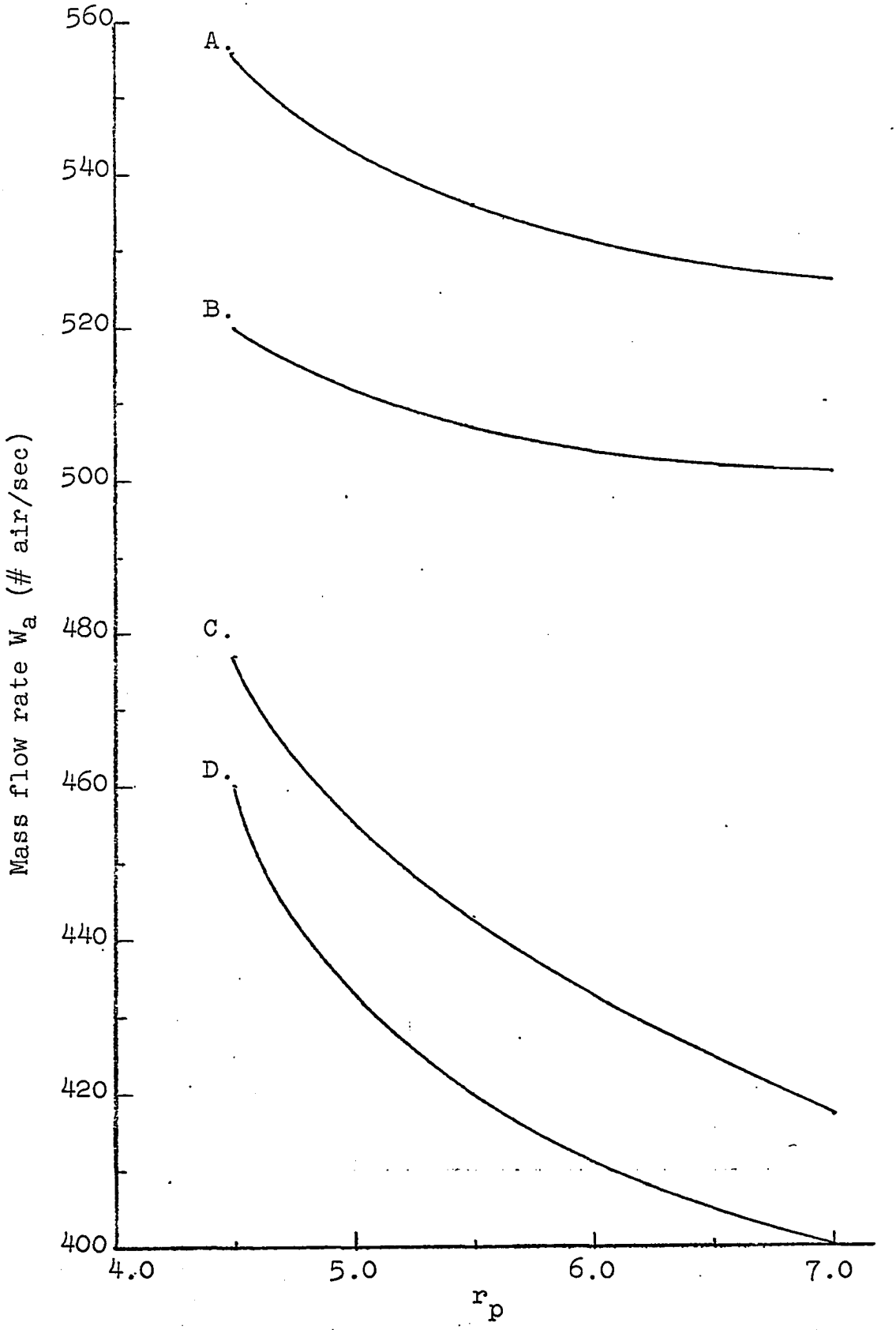
560
540
520
500
480
460
440
420
400
A.
B.
C.
D.
Mass flow rate W_a (# air/sec)
4.0
5.0
6.0
7.0
r_p

drop, certain trends can be seen. The boiler inlet temperature decreases at a constant rate of 6.6% for every unit change in the pressure ratio while the stack temperature increases slightly more than 1% for every unit change in the pressure ratio (Fig. 1.15).

Another consideration is the overall plant efficiency. A plot of plant efficiency versus the pressure ratio, for varying pressure drops, is seen in Fig. 1.16.

Based on Figures 1.12, 1.13, 1.14, 1.15, and 1.16 an operating pressure ratio of 5.5 was chosen and utilized for the open Brayton cycle with intercooling and regeneration.

Fig. 1.15. Boiler inlet and stack temperatures versus pressure ratio for the intercooled and regenerative cycle.

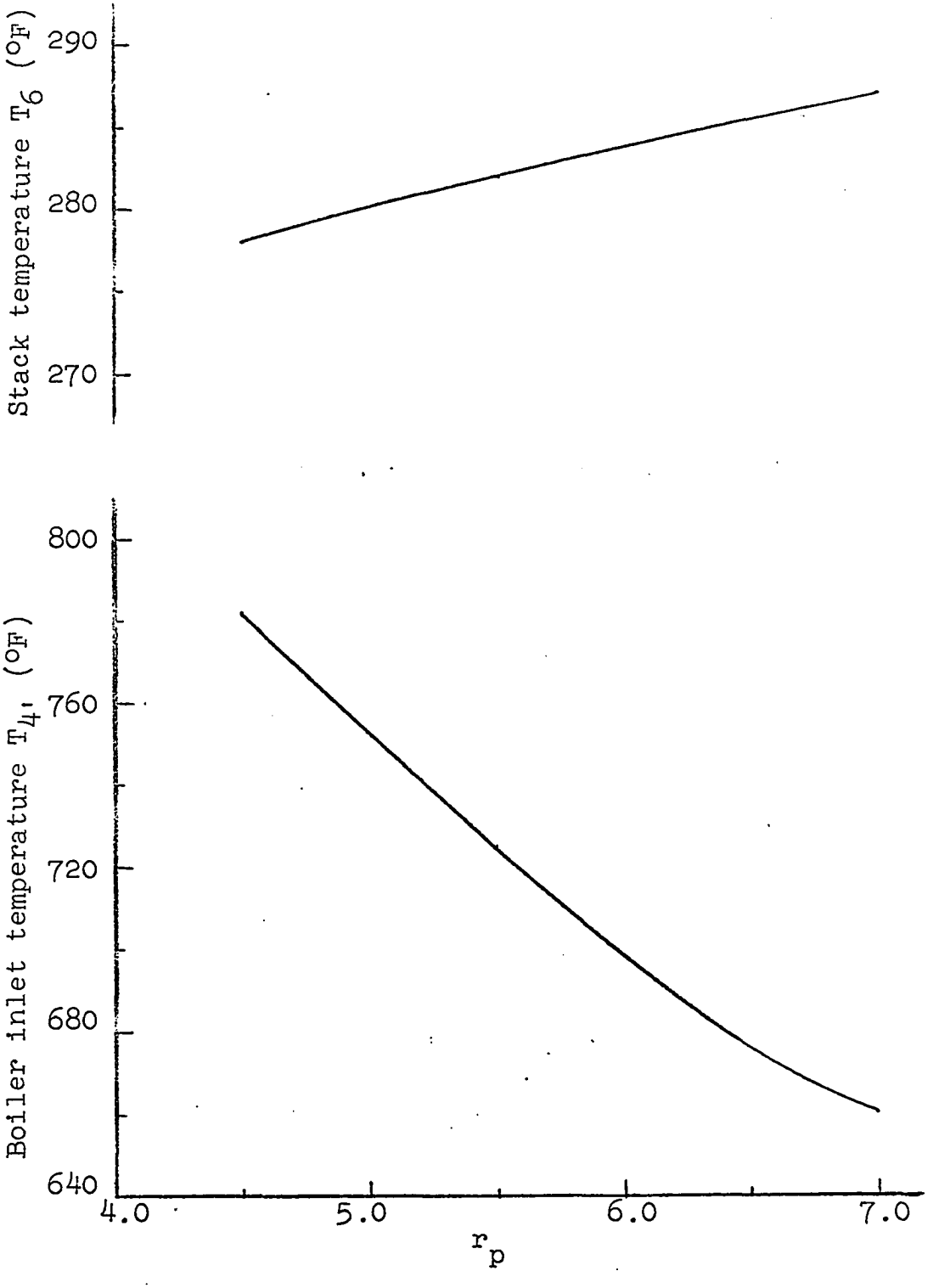
Stack temperature T_6 (°F)
290
280
270
Boiler inlet temperature $T_{4'}$ (°F)
800
760
720
680
640
4.0
5.0
6.0
7.0
r_p

Fig. 1.16. Plant efficiency versus pressure ratio for the intercooled and regenerative cycle with varying total system pressure drop.

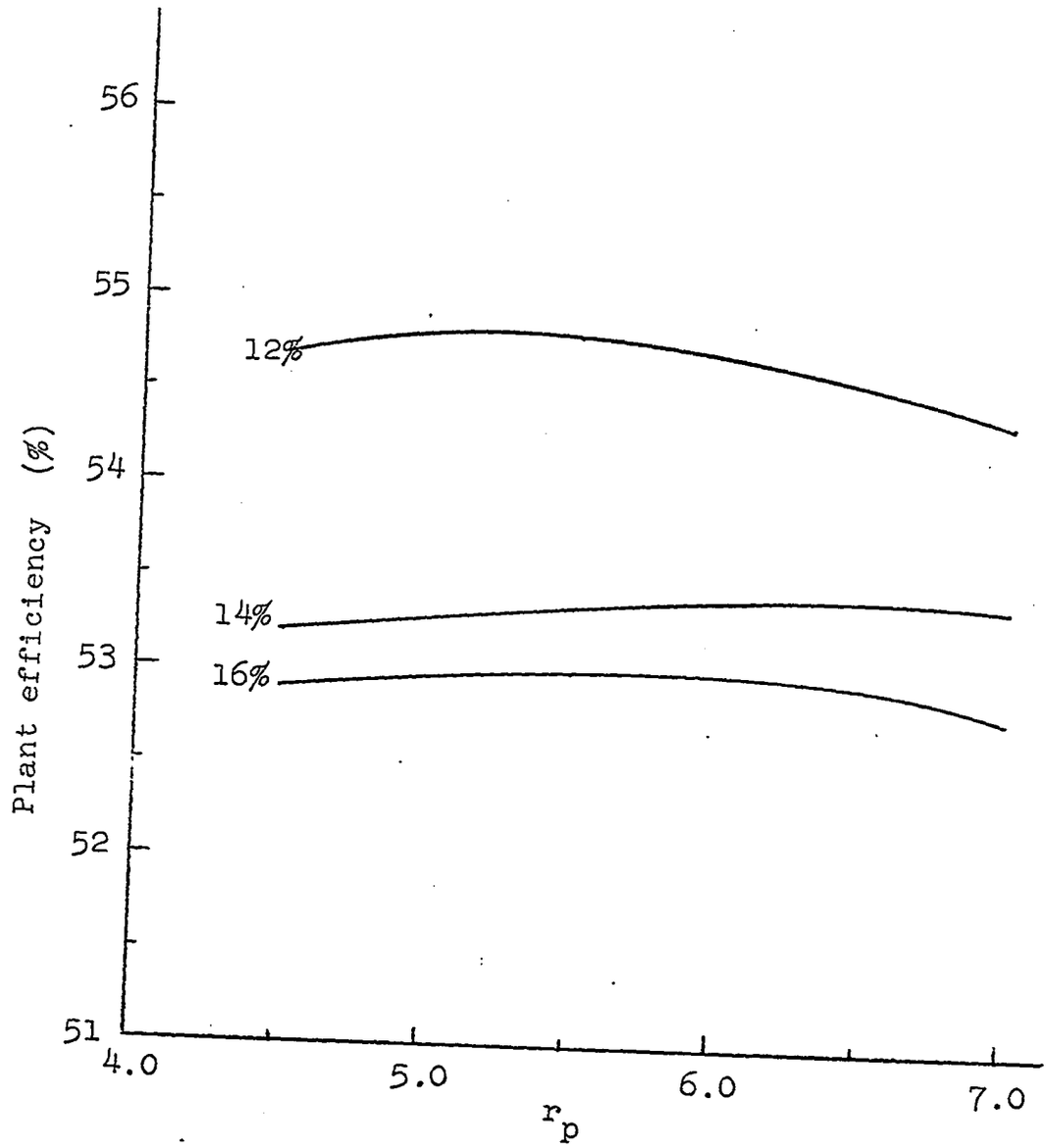
56
55
54
53
52
51
Plant efficiency (%)
12%
14%
16%
4.0
5.0
6.0
7.0
r_p

CHAPTER II. AIR FILTERING SYSTEM

An open cycle will require an air-filtering system. The damaging effects of dust on the blades of compressors and turbines are well known. Erosion and deposits are of primary concern, both of which lead to a change in the blade profile with accompanying loss of efficiency.

Cleaning of the blades is technically feasible and because of this plant will be shut-down periodically, it might be felt that blade fouling is of little consequence, however, due to the high probability of radioactivity, cleaning might not be desirable except after long periods of shut-down. Another major reason for removing particulate matter from the air stream is to lessen the quantity of solid matter entering the reactor core where fouling of the fuel element surfaces will result in decreasing the heat transfer properties. In addition, these particles will be in a neutron environment where neutron activation is highly probable. It is essential that the inlet-air be filtered. The demands normally placed upon filters for high dust-holding capacity are lessened here because of this plant's periodic operation which will permit frequent cleaning.

Particulate Matter

Dust can be separated into two basic types; errosive (larger than ten microns) and sticky (less than ten microns). These two types do not normally occur together. Ernst (10)

categorized the sources of dust by particle size and showed that particle concentration is inversely proportional to height above the ground. The environment that this system will be operating in contains particles of three microns or less. For this size particle high efficiency or "absolute" filters are used. Investigation (4, 11) has shown that this type of filter has efficiencies of 99.99% for three micron particles, develops a pressure drop in the neighborhood of 2" of water (0.072 psia) and operates with maximum face velocities of five feet per second[1,2]. Based on the maximum face velocity and a required total volume flow 4,250 ft^3/sec per shaft, a frontal area of 1,850 ft^2 would be needed and would have an approximate cost of $12,000.

The author is of the opinion that such a filtering system could be installed within the design ship. One, 30 ft by 30 ft filter one foot thick could be located directly below each of the existing air up-takes and leave adequate room for the necessary machinery.

---

[1]Bryant, L. P., Manager, Engineering Sales, Continental Air Filters Incorporated, Louisville, Kentucky. Air filters. Private communication. 2 March, 1966.

[2]Labadie, P. A., Farr Air Filter Company, Los Angeles, California. Air filters. Private communication. 8 March, 1966.

Moisture

Dry, desalted air is essential to avoid salt attack and can be insured against by providing a moisture separator at the air inlet (12, 13). One method requires a 90° bend in the ducting which causes entrained droplets to separate by inertial forces. Velocities of 66 ft/sec would provide efficiencies of 60% on 5 micron droplets; 75% on 10 micron droplets and 90% on 20 micron droplets. This type of separator offers a minimum pressure loss (0.33" water) as well as low weight, volume and cost.

Radioactive Effluent

The greatest filtering problems arise with the exhaust gas. Beta and gamma-emitting fission and activation products found in the exhaust gas can be a health hazard. Those of interest can be divided into three main groups: particulate matter; the noble gases; and the halogens.

The primary source of particulate matter would be injestion from the outside air. The gaseous fission products are primarily bromine, iodine, xenon and krypton while argon 41 and nitrogen 16 are the activation products of primary concern.

The quantity of particulate matter entering the reactor should be nill because of the inlet filtering system, but any matter that does enter the reactor can become a source of radioactivity and, therefore, should be

filtered. Absolute filters can be employed here, also.

Various methods have been developed to remove the inert gases from air streams (14). Formation of clathrate compounds between rare gases and organic compounds is one, condensation of the gases is another while a third is adsorption on activated carbon. Because formation of clathrate compounds requires long periods of time (12 hours) and condensation requires temperatures below -241 °F, the dynamic adsorption method will be the only one considered for the open cycle filtering system.

Adsorption with permanent retention or adsorption-desorption can be used. The former requires no interruption in filtering while the latter operates cyclicly. While one adsorber is being striped or regenerated another must be used. This requires duplication of equipment for continuous operation. Although the plant under consideration will operate periodically, it is not of constant period and the shut-down time is of short duration usually 24 to 36 hours. This would rule out the adsorption-desorption method as being impractical. Other undesirable features of the adsorption-desorption system are that scrubbing is achieved with saturated or superheated steam or under a vacuum. Either case involves transfer and storage of the gaseous activity.

The halogens can also be removed from air streams by activated carbon (15) and the choice of activated charcoal for the filtering absorber material allows only one medium to adsorb both the halogens and the noble gases.

Based on work by Ackley, Adams, and Browning (16), the breakthrough times of the inert gases can be determined for given quantities of activated carbon, effluent flow rates, filter shape and various types of sweep and inert gases. Utilizing their expression

$$t_b = \frac{m\ k\ (t_b/t_m)}{F} \quad , \tag{2.1}$$

where

t_b = the breakthrough time of the fission gas (min).

t_m = the average retention time for the fission gas atoms passing through the filter (min).

m = the mass of the absorbent (grams).

k = the dynamic adsorption coefficient (cm^3/gm).

F = the flow rate of the sweep gas (cm^3/min).

calculations of t_b will be carried out for various quanties of carbon.

The ratio t_b/t_m is a function of the filter length and approaches an asymptote of 0.8 at about a length of 72 feet (16) as can be seen in Fig. 2.3. The dynamic adsorption coefficient k, is a function of the inert gas to be adsorbed, the type of sweep gas, the adsorbent, and the temperature of the sweep gas. In all cases, k decreases with and increase in temperature, as can be seen in Figs. 2.1 and 2.2.

Fig. 2.1. Dynamic adsorption coefficient versus reciprocal absolute temperature for xenon and krypton (from ORNL CF-61-2-32, page 10, Reference 17).

A. Columbia G activated carbon.

B. Columbia ACC activated carbon.

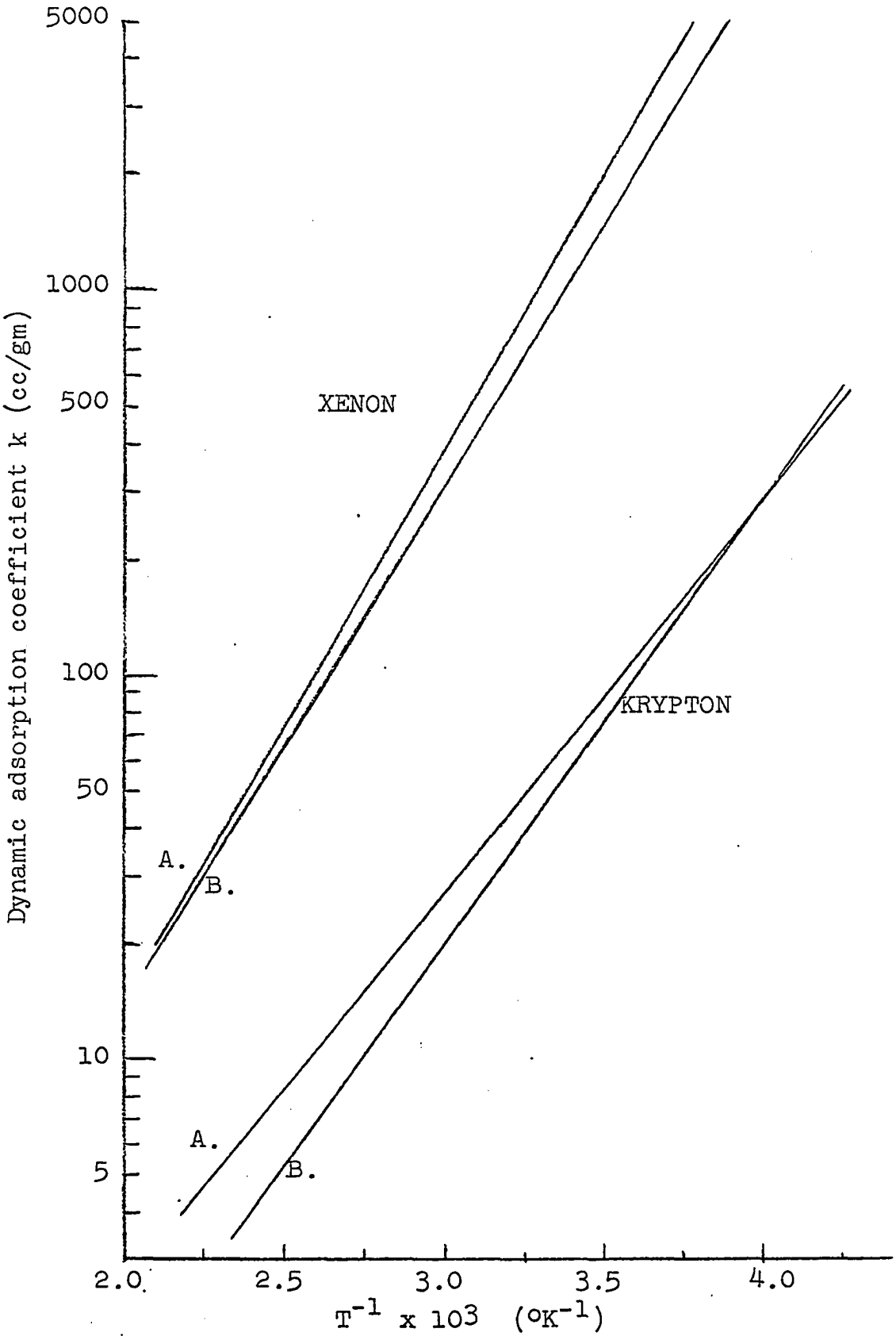
5000
1000
500
100
50
10
5
Dynamic adsorption coefficient k (cc/gm)
XENON
KRYPTON
A.
B.
A.
B.
2.0
2.5
3.0
3.5
4.0
T-1 x 103 (oK-1)

Fig. 2.2. Dynamic adsorption coefficient versus reciprocal absolute temperature for xenon, air and krypton (from TID-7593, pages 209 and 213, Reference 16).

A. Xenon on charcoal.

B. Krypton on charcoal.

C. Air on activated carbon.

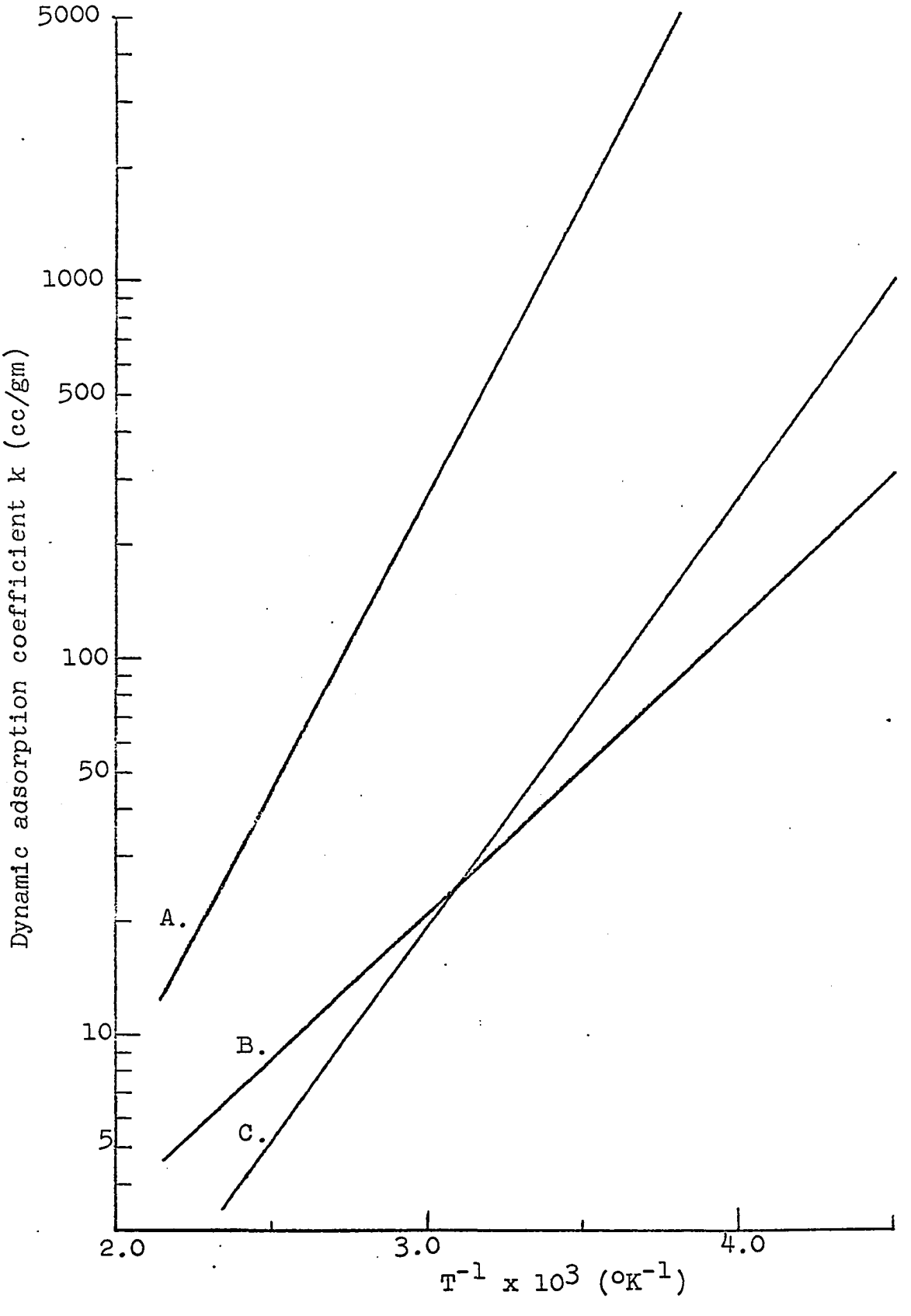
5000
1000
500
100
50
10
5
Dynamic adsorption coefficient k (cc/gm)
A.
B.
C.
2.0
3.0
4.0
T-1 x 10³ (°K-1)

Fig. 2.3. Ratio of breakthrough time to holdup time versus adsorber length (from TID-7593, page 212, Reference 16).

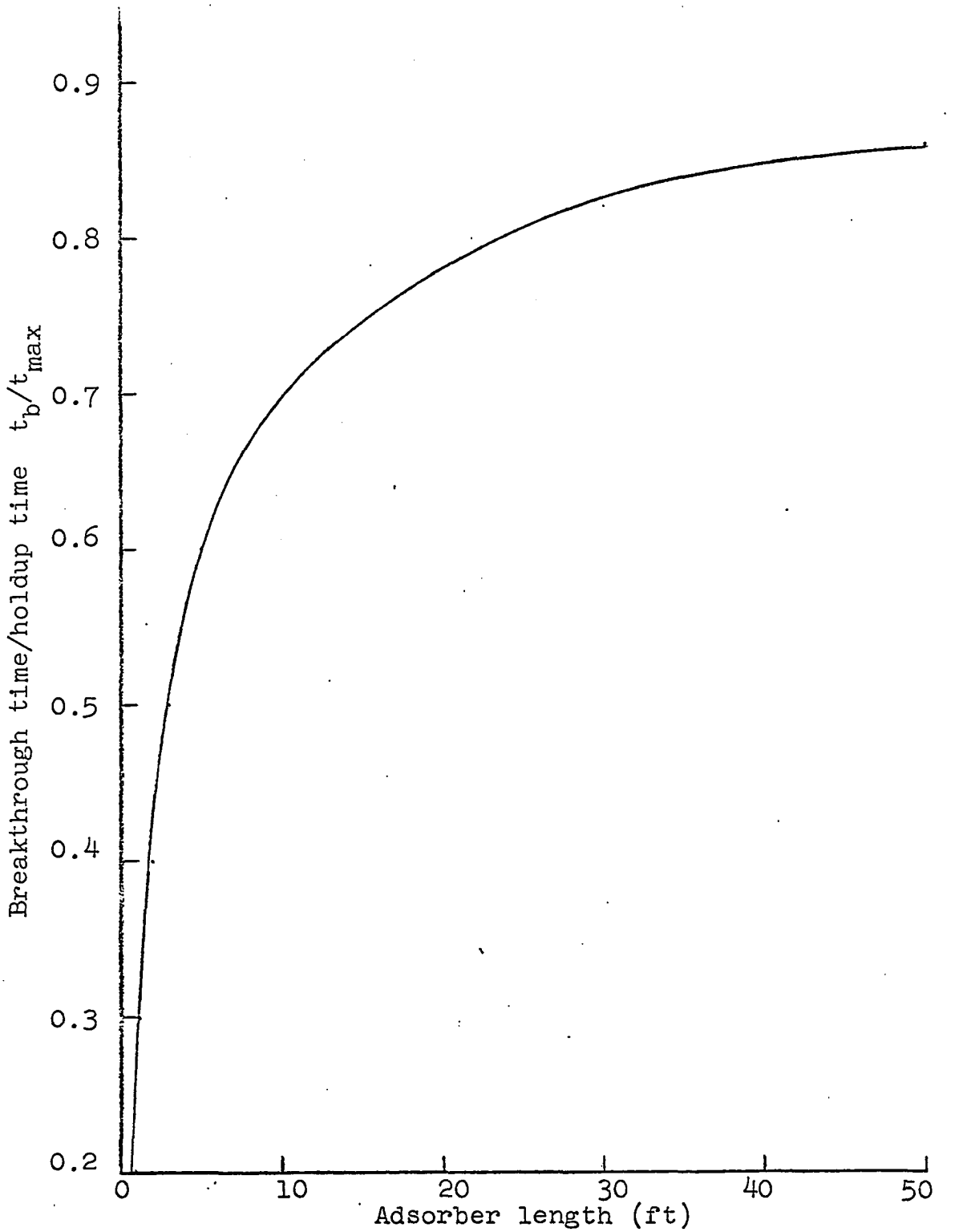
Breakthrough time/holdup time t_b/t_{max}
0.9
0.8
0.7
0.6
0.5
0.4
0.3
0.2
0
10
20
30
40
50
Adsorber length (ft)

There are two air uptakes aboard the ROTTERDAM, one to port and one to starboard of the centerline. These would be ideal locations for such a filtering system for it was found that vertical columns adsorb more effectively than horizontal ones. The uptakes are each 11 ft wide and 19 ft long and have a vertical height, from the top of the main engine room to the upper-most deck, of 54 ft. This space will have to contain the intake ducting also. Knowing that this filter will require shielding, a cylindrical configuration will be chosen, having a diameter of 10 ft and whose length will be allowed to vary from 10 ft to 50 ft.

In this manner the breakthrough times for krypton and xenon were determined as a function of the filter length. The volume flow rate, for the operating conditions chosen in Chapter I, was 230 # air per second per shaft at 280 ^{o}F and 15 psia. A density of 30.2 #/ft^{3} for carbon was used, the dynamic adsorption coefficient was taken from Figs. 2.1 and 2.2, while the ratio of breakghrough to holdup times was taken from Fig. 2.3.

The calculated breakthrough times for xenon and krypton, as a function of filter length are seen in Fig. 2.4. The extremely short breakthrough times are a direct result of the large flow rates and the very low values of k, due to the high operating temperatures. Even with the curves optimistically drawn with constant slope beyond an absorber length

Fig. 2.4. Calculated breakthrough time versus adsorber length for xenon and krypton.

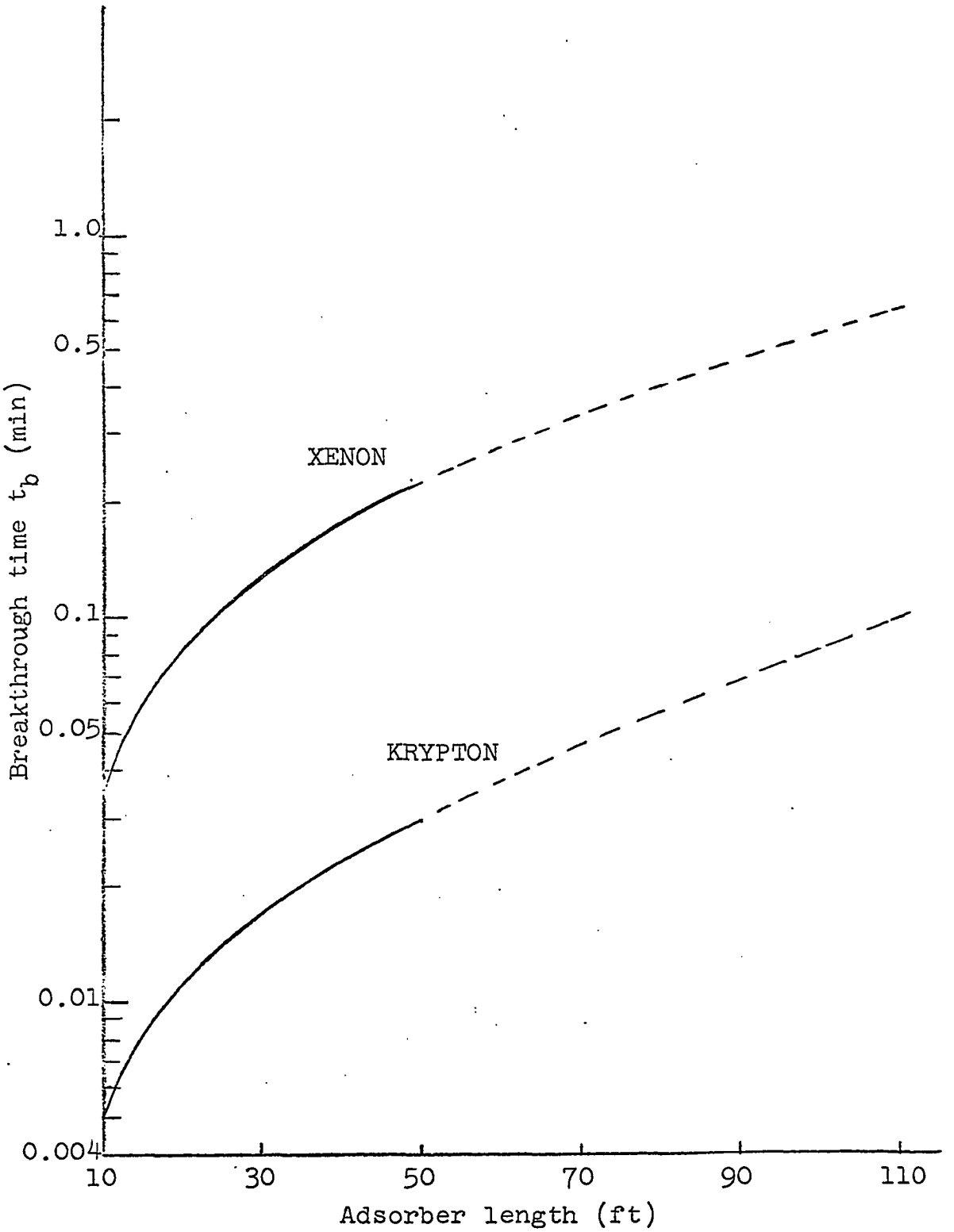
1.0
0.5
0.1
0.05
0.01
0.004
Breakthrough time t_b (min)
XENON
KRYPTON
10
30
50
70
90
110
Adsorber length (ft)

of 50 ft, the breakthrough times do not get longer than one minute for xenon and two tenths minute for krypton at a filter length of 150 ft which would not be useful for radioactive isotope holdup. In addition to the poor breakthrough times, there are other reasons why this filtering system would be unacceptable for shipboard use. First is the large weight of the filter plus the shield. Second is the fact that the charcoal will have to be cooled to prevent ignition at the operating temperatures and finally is the very large pressure drop (126 psia per foot of filter length for 2-4 mesh charcoal with the existing flow velocities (Fig. 2.5)).

Conclusions

This study showed that the adsorption method for noble gas filtering would be unexceptable for the open cycle due to excessive size, weight, pressure drop and low retention times. An open cycle is impractical for this type of plant and dictates going to a closed cycle.

Fig. 2.5. Pressure drop through charcoal filter versus gas velocity (from ORNL-2872, page 6, Reference 15)).

A. 6-8 mesh charcoal.

B. 4-6 mesh charcoal.

C. 2-4 mesh charcoal.

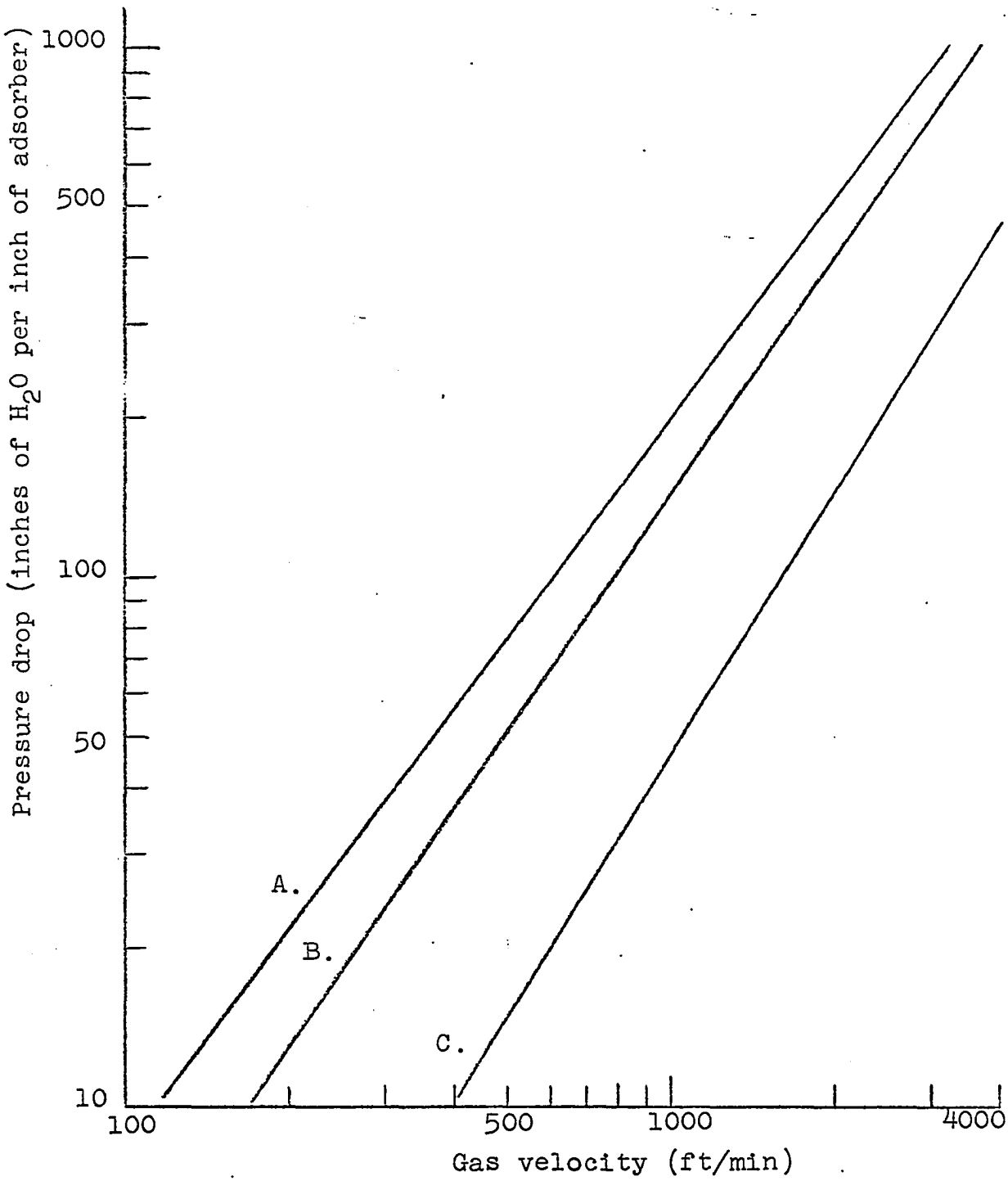
Pressure drop (inches of H_2O per inch of adsorber)
1000
500
100
50
10
A.
B.
C.
100
500
1000
4000
Gas velocity (ft/min)

CHAPTER III. CLOSED BRAYTON CYCLE

Once the cycle is closed many advantages become evident. No longer requiring air as the working fluid, a gas can be chosen based on optimum characteristics. Higher operating pressures can be employed yielding lower specific volume with more work per unit flow area, while improving the heat transfer properties. The medium can be kept clean and one of the most important benefits is that power regulation can be accomplished by varying the density of the working fluid, which achieves power variation with constant state point temperatures, resulting in a flatter efficiency curve.

Working Fluid Characteristics

Selection of a working fluid should be based on thermodynamic as well as nuclear properties. Three gases, carbon dioxide, nitrogen and helium were compared and a selection of the working medium made. Other gases such as air, hydrogen and water vapor, have been investigated (18, 19, 20, 21) and found to be undesirable for nuclear closed-cycle application. They were not considered here. In addition to gas properties, gas performance should be evaluated. For example: the network, which has a direct bearing on the quantity of gas required to do a specific amount of work; the energy specific volume, which directly effects the size of the components; and the cycle efficiency.

Heat transfer components

The study of the open-cycle showed decided advantages to intercooling and regeneration. These innovations will produce a similar improvement in the closed-cycle. In addition to the intercooler, and regenerator, a precooler will now be required. All are heat transfer devices and, therefore, the heat transfer characteristics of the gases should be compared. To best compare the heat transfer qualities of the gases under consideration, a heat exchanger should be chosen where one medium gaining or losing heat is the same in each case. The precooler is one such component where the common medium is cooling water. In addition, all of the gases must be cooled to the same temperature, that of the compressor inlet temperature.

One basic expression for heat flow rate is (22)

$$Q = U\ A\ \Delta T\ , \tag{3.1}$$

where

Q = the rate of heat transfer (BTU/hr)

U = the over-all heat transfer coefficient (BTU/hr-ft^2-$^\circ$F)

ΔT = over-all temperature difference ($^\circ$F)

U is equal to the reciprocal of the total resistance R_t, where

$$R_t = R_{H_2O} + R_{tube} + R_{gas}\ . \tag{3.2}$$

R_{h_2O} and R_{tube} can be considered to remain constant because the inlet water temperature, tube material and the tube wall thickness are all constant.

The constant of proportionality in Newton's Law of Cooling is the film coefficient, h_c. McAdams (23) gives an expression of h_c for turbulent flow inside of tubes, for cooling, as

$$h_c = 0.023\ k/D\ (R_e)^{0.8}\ (P_r)^{0.3}\ , \qquad (3.3)$$

with

R_e = Reynolds number = $Dv\rho/\mu$

P_r = Prandtl number = $c_p\mu/k$

D = inside diameter of tube (ft)

ρ = fluid density ($\#_m/ft^3$)

v = fluid velocity (ft/hr)

μ = fluid dynamic viscosity ($\#_m$/hr-ft)

c_p = specific heat at constant pressure (BTU/# ^oF)

k = fluid thermal conductivity (BTU/hr-ft^2 ^oF-ft)

The fluid properties are functions of temperature and will be evaluated at the mean fluid temperature t_m, which is the average of the average fluid temperature and the tube wall temperature. For this study the tube wall temperature will be assumed constant.

Because the fluid velocities are unknown and functions of volume flow rate and passage area, a Reynolds number of 3,000 was assumed for all gases. The gas temperatures entering the precooler were those of the turbine exhaust.

A comparison of the heat transfer coefficients, listed in Table 3.1, shows that helium is the best gas, by a factor

Table 3.1. Gas properties, film coefficients and heat exchanger area per horsepower

Property	CO_2	N_2	He
molecular weight (m). ($\#_m$/mole)	44.0	28.0	4.0
gas constant (R). (ft $\#_f/\#_m$ ^oF)	35.1	55.2	386.0
specific heat ratio (k). (low pressure)	1.3	1.4	1.66
thermal neutron absorption (σ_a) (24). (cm^2/nucleous)	$C^{12}=(3.7)10^{-27}$ $O^{16}=(0.2)10^{-27}$	$(1.9)10^{-24}$	
density (ρ). (from ideal gas law @ STP) ($\#_m/ft^3$)	0.0465	0.0345	0.0059
dynamic viscosity (μ). ($\#_m$/hr ft)	0.055	0.058	0.055
specific heat at constant pressure (c_p). (BTU/$\#_m$ ^oF)	0.256	0.249	1.24
thermal conductivity (k). (BTU/ft^2 hr ^oF-ft)	0.0197	0.0214	0.094
Prandlt number (P_r).	0.74	0.70	0.71
film coefficient (h_c). (BTU/hr ft^2 ^oF)	4.00	4.25	18.8
heat exchanger surface per HP. (ft^2/HP)	4.85	4.9	1.9

of four, for heat transfer. This indicates that less surface area was required to transmit the same quantity of heat energy. But each gas does not give up the same quantity of heat to the precooler. A more meaningful comparison would be one of the heat transfer area per useful work developed.

For one pound mass of working fluid flowing per hour the heat transfer rate can be determined using Equation 3.1. Once again helium requires less heat transfer area per horsepower as can be seen in Table 3.1.

System Ambient Pressure

System pressure drop

The system pressure drop and the film coefficient must be considered when choosing an ambient cycle pressure because they are both functions of the fluid density. The fundamental expression for pressure drop in fluid flow is (18)

$$\Delta p = f(L/D)\ (\rho\ v^2/2g_c)\ , \qquad (3.4)$$

where

Δp = pressure loss ($\#_f/ft^2$)

f = Fanning friction factor

L/D = length to diameter of tube

ρ = fluid density ($\#_m/ft^3$)

If the wetted tube surface (S) is expressed as π DL and the cross sectional area (A), as $\pi\ D^2/4$, Equation 3.4 can be rewritten as

$$\Delta p = f\ (S/A)\ (\rho\ v^2/2g_c). \qquad (3.5)$$

For a given mass flow rate ($\dot{m}$), the flow velocity is $\dot{m}/\rho\ A$, and Equation 3.5 becomes

$$\Delta p = f\ S\ \dot{m}/2g_cA3)\ (1/\rho)\ . \qquad (3.6)$$

Heat transfer coefficient

With respect to the film coefficient, the relationship between Reynolds, Nusselt and Prandtl numbers for turbulent flow inside of tubes, for cooling, is (23)

$$N_u = K_1 (R_e)^{0.8} (P_r)^{0.3} , \qquad (3.7)$$

where

K_1 = a constant

N_u = Nusselt number = hD/k

Solving for the film coefficient yields

$$h_c = K_1 \, k/D \, (D\rho v/\mu)^{0.8} \, (c_p \mu/k)^{0.3} . \qquad (3.8)$$

Substituting for $v = 4 \dot{m}/D^2 \rho \pi$ in Equation 3.8 yields

$$h_c = (K_1 \, D^{-1.8} \, \pi^{-0.8} \, 4^{0.8}) \, k^{0.7} \, c_p^{0.4} \, \mu^{-0.5} \qquad (3.9)$$

k, c_p and μ are functions of temperature and pressure. k and μ vary at about the same rate while c_p varies slower. There will, therefore, be a slight increase in h_c as pressure is increased. It can be concluded that the higher the system ambient pressure the higher will be the heat transfer rate and the smaller will be the pressure drop.

Closed cycle studies by General Dynamics Corporation (25), General Electric Corporation (26) and Escher Wyss Limited (27) utilized maximum cycle pressures of 850 psia, 830 psia and 1,000 psia, respectively. A maximum cycle pressure of 1,000 psia is well within the limits of present day technology and this value was used for this design.

Cycle Efficiency

Of the three gases under consideration, helium is the only one whose thermal properties are independent of pressure and, therefore, pressure effects must be taken into account when utilizing thermodynamic properties of the other gases. For the studies carried out on carbon dioxide and nitrogen, the thermal properties were taken from the U.S. National Bureau of Standards Circular #564 (28) and those for helium were taken from the National Aeronautics and Space Administration publication SP-3001 (29).

Component pressure losses

It now becomes evident that the component pressure drop will vary with the type of gas used. The values of the component pressure losses assumed for air in Chapter I will be used as a reference and are listed below for convenience. The value for the waste-heat boiler is up-dated based on calculations of Clay[1]. That for the reactor was calculated utilizing an expression taken from page 77 of GEMP-342 (26) and is

$$dP_o = \left(\frac{-k\, M^2\, P_o}{2}\right)\left(\frac{dT_o}{T_o} + \frac{4f}{D}\, dX\right), \qquad (3.10)$$

where

P_o = initial pressure (psia)

---

[1]Clay, P. E., Senior Engineer, AMP Beaird Incorporated, Sheveport, Louisiana. Waste-heat boilers. Private communication. 30 March, 1967.

k = average specific heat ratio

M = average Mach number

T_o = inlet temperature (^oR)

f = friction factor = $(0.046)R_e^{-0.2}$

dX = incrimental length in flow direction

D = hydrolic diameter

Then for air:

precooler	1.0%
intercooler	1.0%
regenerator	4.0%
waste-heat boiler	4.0%
Reactor	1.0%

Following the development of Keller and Schmidt (30), a comparison of the pressure losses between air and helium can be made. It was assumed that the temperature ratios were the same for both gases. If $T_{2'}$ and $P_{2'}$ are the temperature and pressure respectively, resulting from pressure losses and T_2 and P_2 are the isentropic temperature and pressure respectively, then

$$\frac{T_{2'}}{T_2} = \left(\frac{P_{2'}}{P_2}\right)^{\frac{k-1}{k}} . \tag{3.11}$$

Defining the pressure loss as

$$\frac{P_{2'}-P_2}{P_2} = \frac{\Delta P}{P_2} = \delta . \tag{3.12}$$

For the same energy loss compared to the turbine work for air and helium

$$(1 + \delta_H)^{(\frac{k-1}{k})_H} = (1 + \delta_A)^{(\frac{k-1}{k})_A} \qquad (3.13)$$

But because δ is small Equation 3.13 can be expressed as

$$(\frac{k-1}{k})_H \delta_H = (\frac{k-1}{k})_A \delta_A , \qquad (3.14)$$

Substituting the proper values for k yields

$$\delta_H = (0.675) \delta_A, \qquad (3.15)$$

which can be applied to the component losses assumed for air. This results in the following component losses for helium:

precooler	0.675%
intercooler	0.675%
regenerator	2.70%
waste-heat boiler	2.70%
reactor	0.675%

The pressure losses resulting with carbon dioxide, can be estimated by employing the ideal equation of state and Equation 3.5. It is seen from the equation of state that the density is directly proportional to the molecular weight. The molecular weight of CO_2 is about 50% greater than that for air, and utilizing Equation 3.5, the pressure drop expected for CO_2 should be about 15% lower than that experienced for air at any state point. This is justified because air and CO_2 will normally be operating at about the same pressure and temperature. This results in the following expected component pressure losses for CO_2:

precooler	0.85%
intercooler	0.85%
regenerator	3.4%
waste-heat boiler	3.40%
reactor	0.85%

When considering the component pressure losses for nitrogen, the similarity of its properties to those of air can be put to use. Their molecular weights are within 3% of each other and therefore, the pressure losses associated with air will be used for those of nitrogen.

This leads to the following cycle pressure losses associated with each of the gases:

CYCLE	HELIUM	CO_2	NITROGEN
simple	4.05%	5.10%	6.0%
intercooled	4.725%	5.95%	7.0%
regenerative	6.75%	8.5%	10.0%
Intercooled and regenerative	7.425%	9.35%	11.0%

Cycle variation

A computer program was written (a copy is on file in the Nuclear Engineering Department Library) to solve the simple, intercooled, regenerative and intercooled and regenerative cycles. The same design parameters were used as earlier in this chapter with the addition of the maximum pressure of 1,000 psia and the new assumed pressure losses of each of the gases under consideration.

It must be remembered that the turbine exhaust gas is utilized to produce steam and its temperature dictates the maximum possible steam temperature. The higher the steam temperature (degree of superheat) the lower the steam rate to the turbo-generators and, therefore, a high turbine exhaust temperature is desirable. Most marine turbo-generators operate with at least 200-300 degrees of superheat and pressures of from 450 psia to 900 psia. Reduced performance will result as the degree of superheat is decreased. The ROTTERDAM'S turbo-generators utilize 620 psia steam with 300 degrees of superheat. To meet the requirements of the ROTTERDAM, the design criteria established in Chapter I were maintained. That is, there is a minimum gas to steam temperature difference of 100 degrees in the boiler and steam of no less than 100 degrees of superheat was produced. These two requirements dictate the lowest acceptable value of turbine exhaust temperature that can be tolerated for this design.

The turbine exhaust temperature is compared to that of the minimum acceptable, namely 690°F. If the turbine exhaust temperature is greater than 690 °F a steam balance is performed and the gas temperature entering the regenerator is that of the boiler exhaust. If the turbine exhaust temperature is lower than 690 °F the gas is sent directly to the regenerator. This gives rise to higher cycle efficiencies as described in the design study

of Chapter I and discontinuities in the plot of cycle efficiency. The cycle efficiency versus the compressor pressure ratio is plotted for the various gases and cycles in Figs. 3.1 through 3.12. A summary of the maximum cycle efficiencies, while producing at least 100 degrees of superheat, along with the compressor pressure ratio at which it occurs is seen in Table 3.2.

Table 3.2. Maximum cycle efficiency

Gas	Cycle							
	Simple		Intercooled		Regenerative		Intercooled and Regenerative	
	η	r_p	η	r_p	η	r_p	η	r_p
Nitrogen	26.5%	5.5	26.5%	5.5	30.0%	3.5	32.5%	4.5
CO_2	22.5%	8.5	22.5%	8.5	27.5%	4.5	28.7%	8.5
Helium	23.8%	3.0	22.7%	3.0	25.5%	3.0	28.5%	3.0

Cycle and Working Fluid Selection

Cycle

It is evident from Table 3.2 that the intercooled and regenerative cycle provides the highest cycle efficiency for each of the gases considered. Nitrogen had the highest value of 32.5% while carbon dioxide and helium each had a value of about 28.5%. This cycle variation will be chosen as the operating cycle for this design.

Fig. 3.1. Cycle efficiency versus pressure ratio for simple closed cycle with helium.

Fig. 3.2. Cycle efficiency versus pressure ratio for regenerative closed cycle with helium.

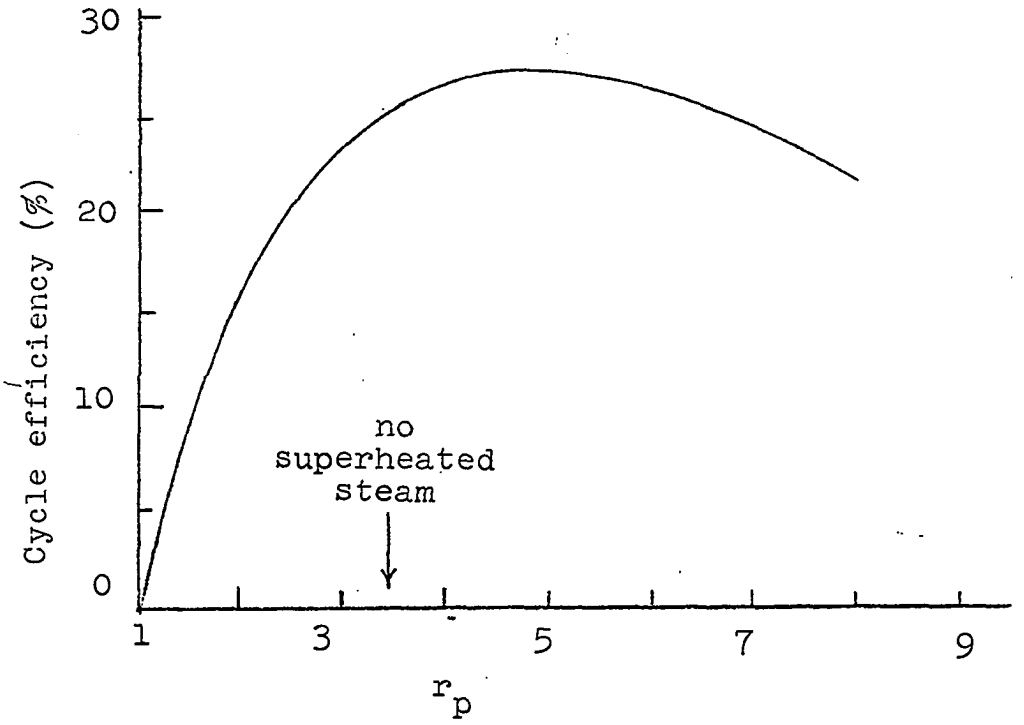
30
20
10
0
Cycle efficiency (%)
no
superheated
steam
1
3
5
7
9
r_p

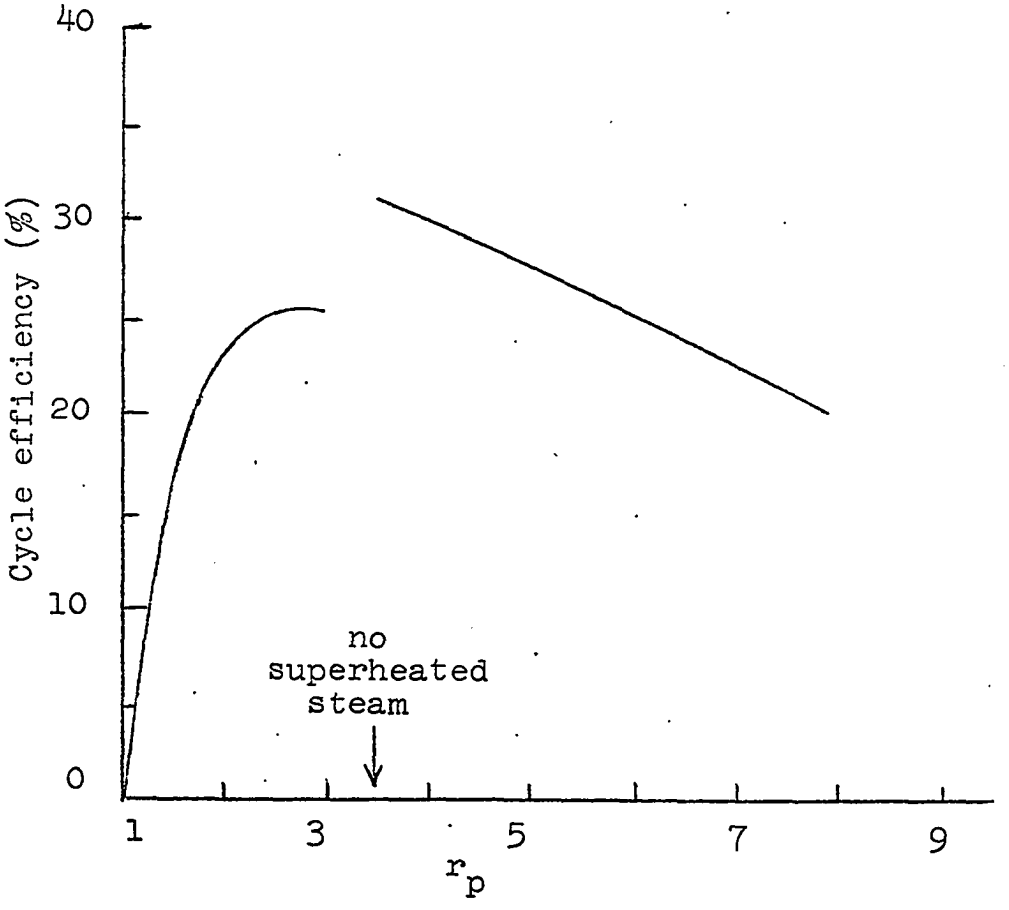
40
30
20
10
0
Cycle efficiency (%)
no
superheated
steam
1
3
5
7
9
r_p

Fig. 3.3. Cycle efficiency versus pressure ratio for intercooled closed cycle with helium.

Fig. 3.4. Cycle efficiency versus pressure ratio for intercooled and regenerative cycle with helium.

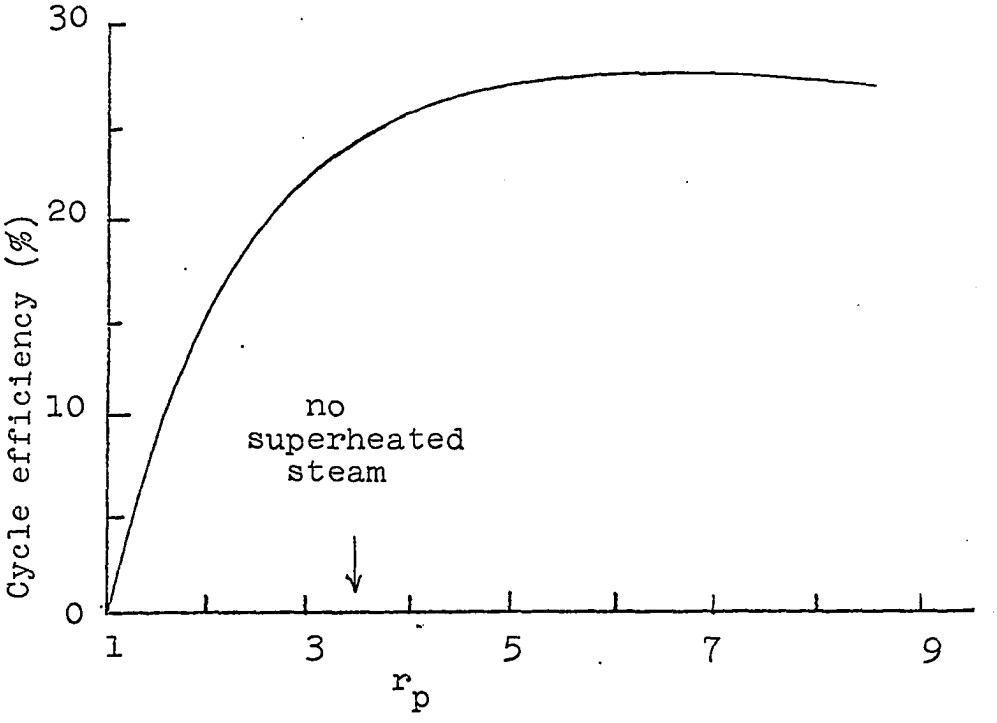
30
20
10
0
Cycle efficiency (%)
no
superheated
steam
1
3
5
7
9
r_p

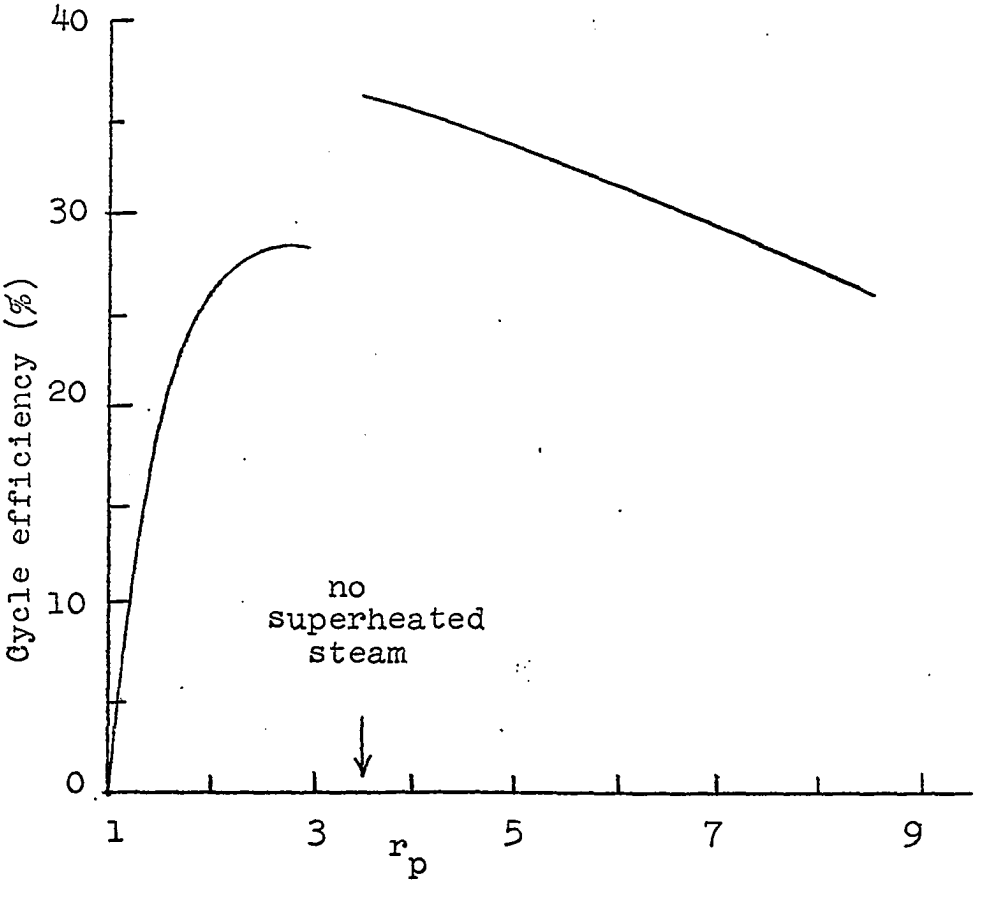
40
30
20
10
0
Cycle efficiency (%)
no
superheated
steam
1
3
5
7
9
r_p

Fig. 3.5. Cycle efficiency versus pressure ratio for simple closed cycle with carbon dioxide.

Fig. 3.6. Cycle efficiency versus pressure ratio for regenerative closed cycle with carbon dioxide.

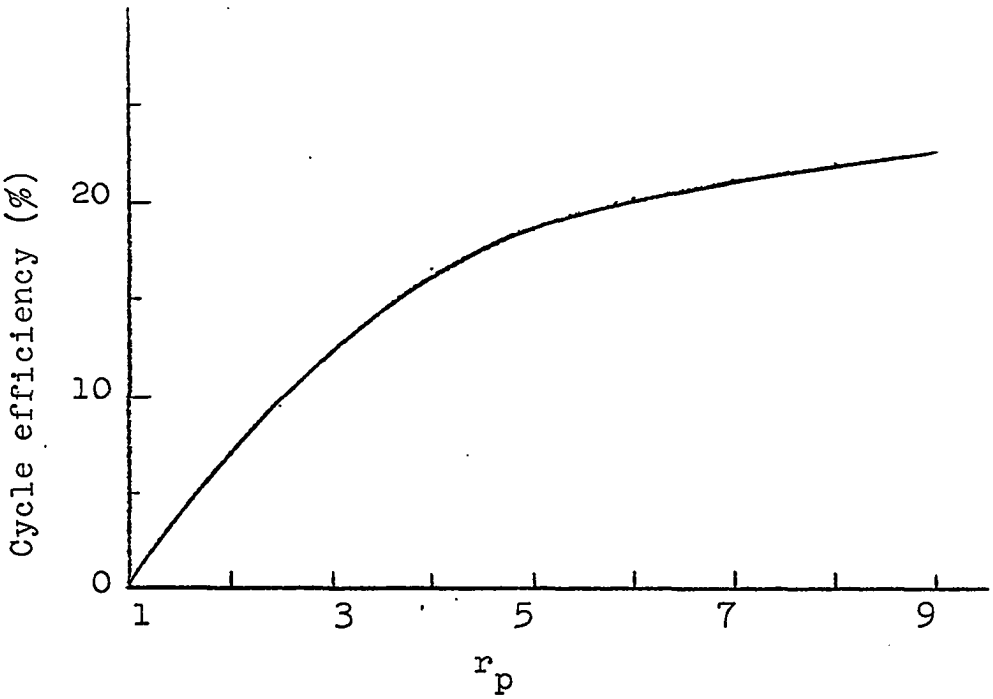
Cycle efficiency (%)
0
10
20
1
3
5
7
9
r_p

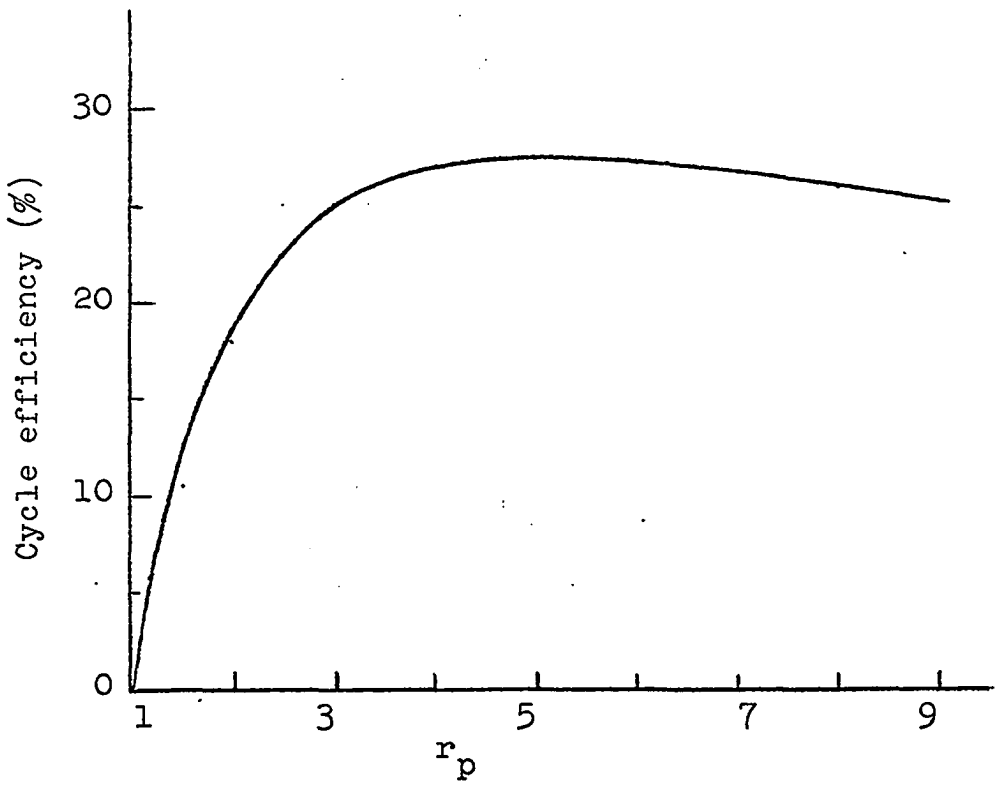
Cycle efficiency (%)
0
10
20
30
1
3
5
7
9
r_p

Fig. 3.7. Cycle efficiency versus pressure ratio for intercooled closed cycle with carbon dioxide.

Fig. 3.8. Cycle efficiency versus pressure ratio for intercooled and regenerative closed cycle with carbon dioxide.

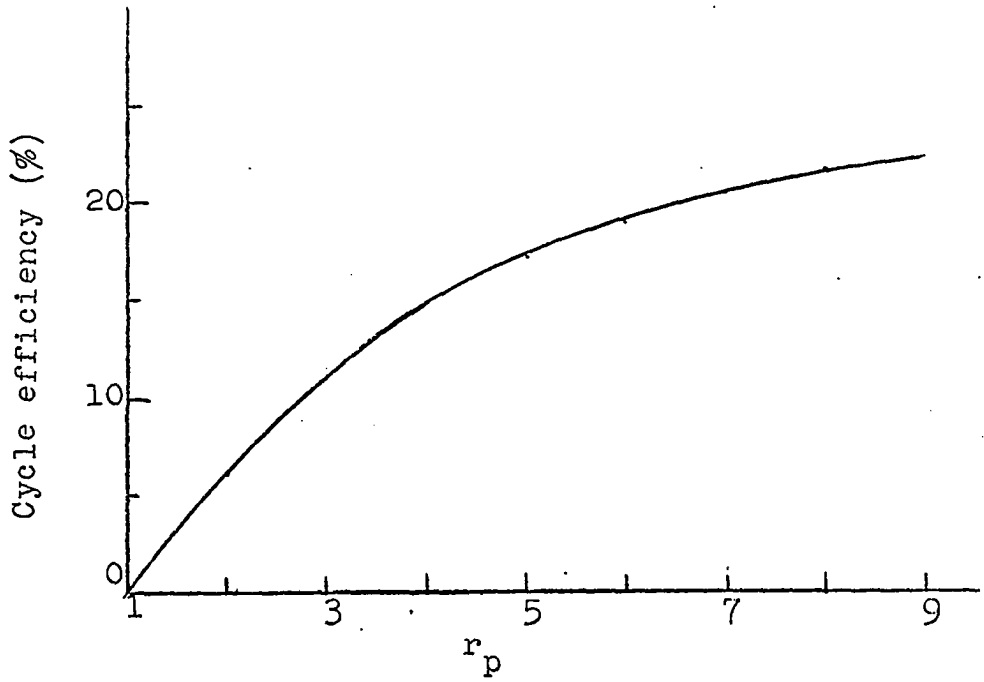
Cycle efficiency (%)
20
10
0
1
3
5
7
9
r_p

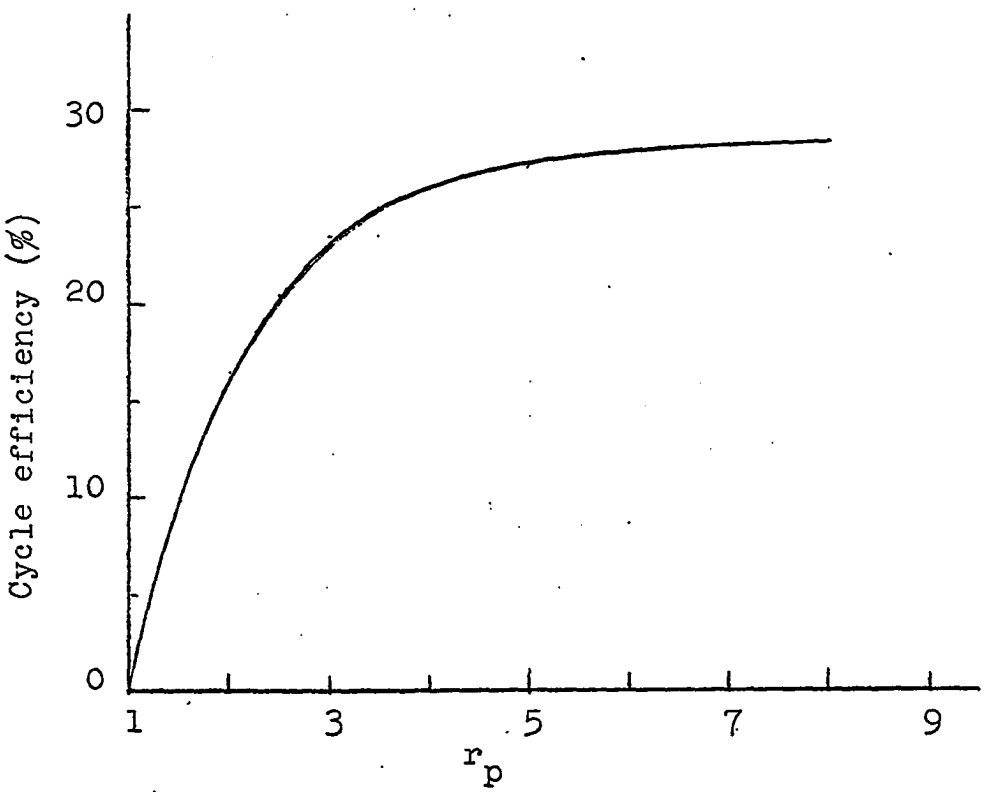
Cycle efficiency (%)
30
20
10
0
1
3
5
7
9
r_p

Fig. 3.9. Cycle efficiency versus pressure ratio for simple closed cycle with nitrogen.

Fig. 3.10. Cycle efficiency versus pressure ratio for regenerative closed cycle with nitrogen.

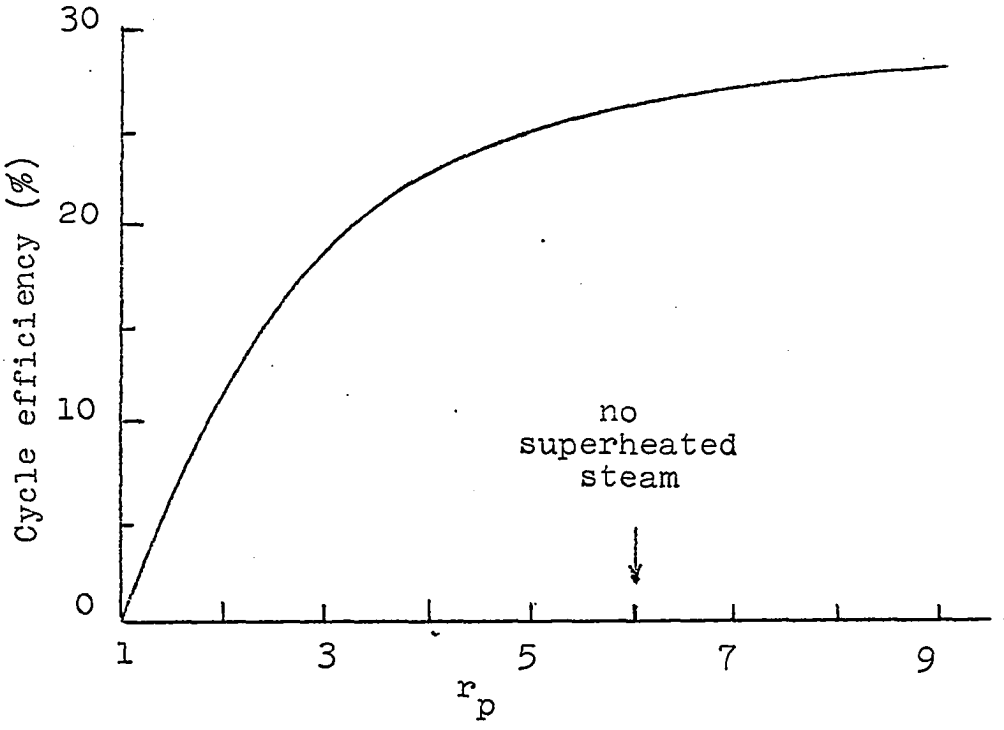
30
20
10
0
Cycle efficiency (%)
no
superheated
steam
1
3
5
7
9
r_p

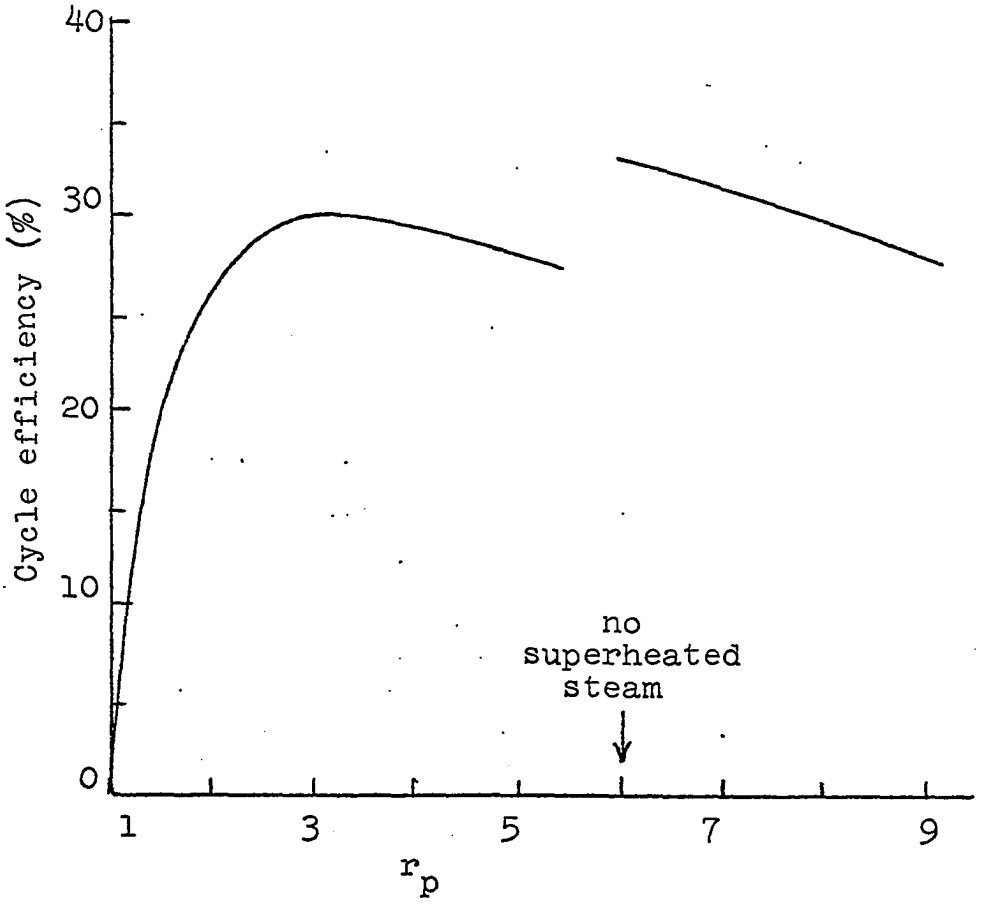
40
30
20
10
0
Cycle efficiency (%)
no
superheated
steam
1
3
5
7
9
r_p

Fig. 3.11. Cycle efficiency versus pressure ratio for intercooled closed cycle with nitrogen.

Fig. 3.12. Cycle efficiency versus pressure ratio for intercooled and regenerative closed cycle with nitrogen.

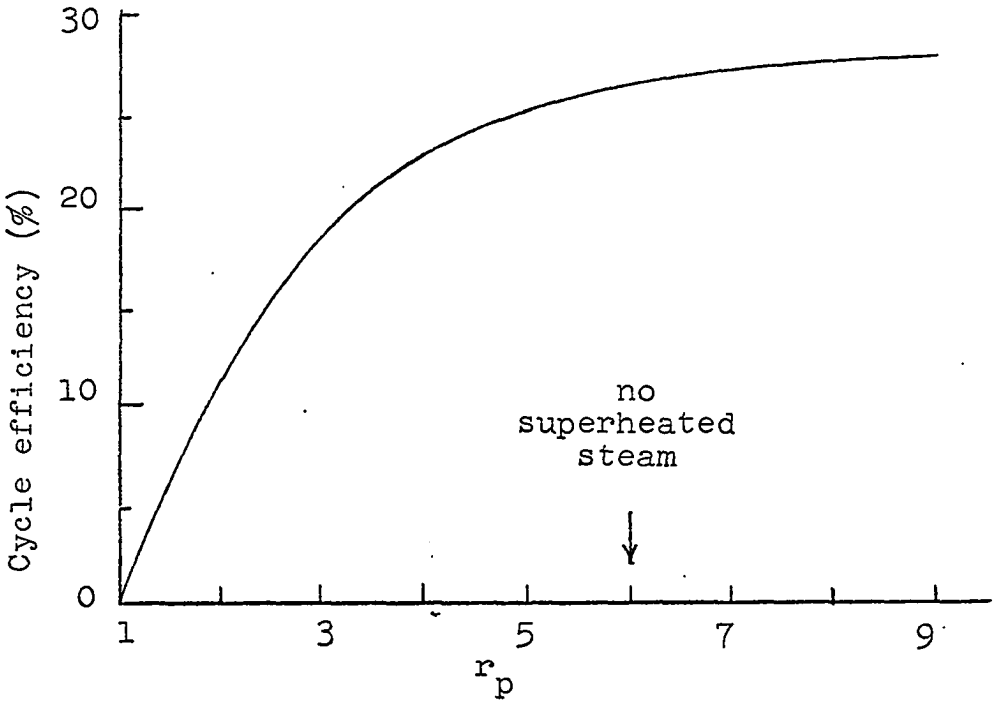
30
20
10
0
Cycle efficiency (%)
no
superheated
steam
1
3
5
7
9
r_p

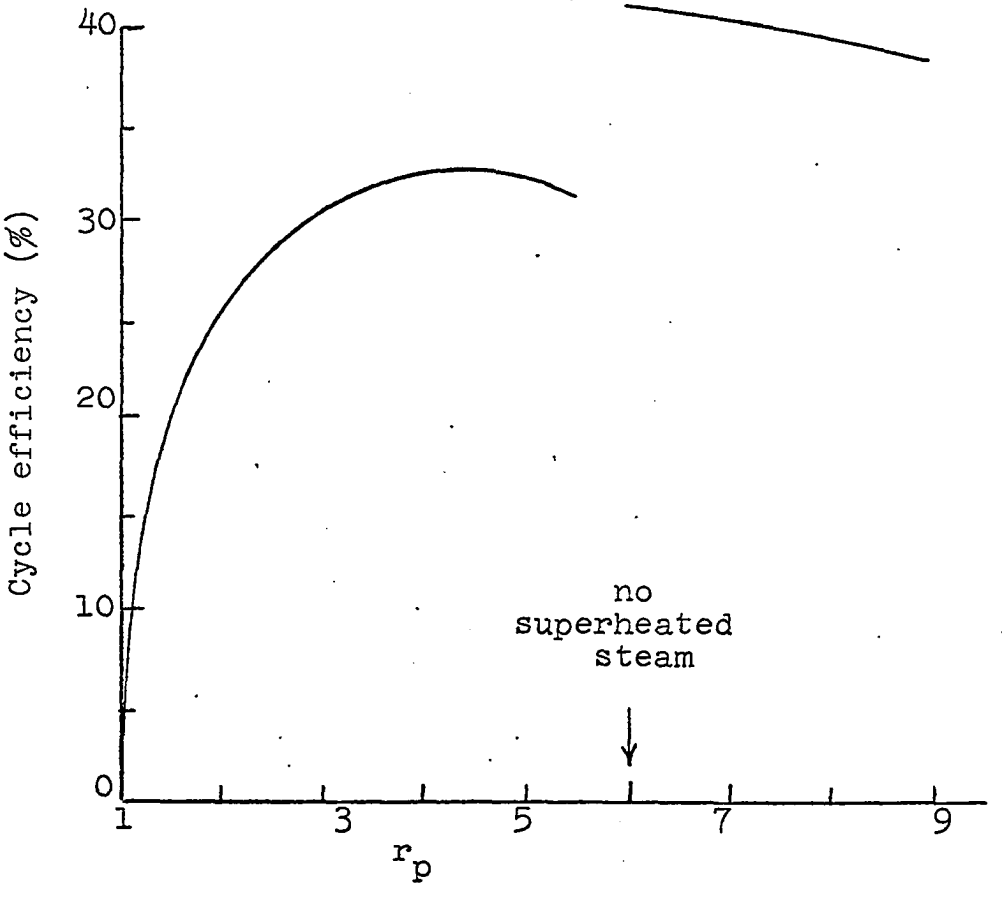
40
30
20
10
0
Cycle efficiency (%)
no
superheated
steam
1
3
5
7
9
r_p

Working fluid

Based on work by Frieder (20) the diameter and number of stages of axial-flow compressors and turbines can be approximated. Nitrogen is used as the reference gas for his study. The following data are abstracted from Table, page 7 of his report:

		N_2	He	CO_2
Diameter Ratio:	Turbine	1.0	1.118	1.318
	Compressor	1.0	1.77	1.318
Stage Number Ratio:	Turbine	1.0	5.02	1.33
	Compressor	1.0	2.23	1.33
Speed Ratio		1.0	0.898	0.652

Also included in Frieder's report is a comparison of the heat exchanger parameters. The below listed data are abstracted from Table 3, page 10, of his report:

	N_2	He	CO_2
Length:	1.0	0.89	0.95
Diameter:	1.0	0.80	1.10
Relative Volume:	1.0	0.40	1.143

Some conclusions can be drawn from the above information. Nitrogen provides the smallest turbo-machines while helium requires the largest size. Helium requires the smallest exchangers while CO_2 the largest. Because there are three heat exchangers required for each turbine-compressor, their size has a stronger influence on the choice of working medium than that of the turbo-machinery.

The last aspect to be considered is the nuclear and chemical properties of the gases. Here, helium provides the most desirable qualities because it is chemically inert and practically insensitive to neutron interaction.

The choice of working fluid is helium which is based on the compromise of cycle efficiency, component machinery size and compatability.

CHAPTER IV. REACTOR ADAPTATION

During the period 1958 to 1960 the General Dynamics Corporation was engaged in developing a Maritime Gas-Cooled Reactor which resulted in a helium-cooled, UO_2 fueled, beryllia moderated and reflected reactor of 64.7 MW_t. This plant was incorporated in a conceptual design of a nuclear tanker (31).

In 1961 the General Electric Corporation began design work on a maritime gas-cooled reactor based on their work with the Aircraft Nuclear Propulsion plant. This work resulted in a reactor called, "The 630A Maritime Nuclear Steam Generator". The 630A is a UO_2 fueled, light water moderated, air-cooled, beryllium oxide and graphite reflected reactor rated at 60.4 MW_t, which produces superheated steam in an intergrated boiler. It has undergone five major modifications since 1961 and by the end of 1964 the 630A Mark V emerged in two forms, "A" and "B". The Mark V(A) is an air-cooled, calandria-type reactor while the Mark V(B) is a helium-cooled, tube-type reactor. It is the 630A Mark V(B) that will be utilized as the prototype for this design and it will be referred to as the 630A.

The 630A Mark V(B)

The fuel rods are UO_2 pellets enriched to 6% and clad in Incoloy. A sketch of a fuel rod can be seen in Fig. 4.1.

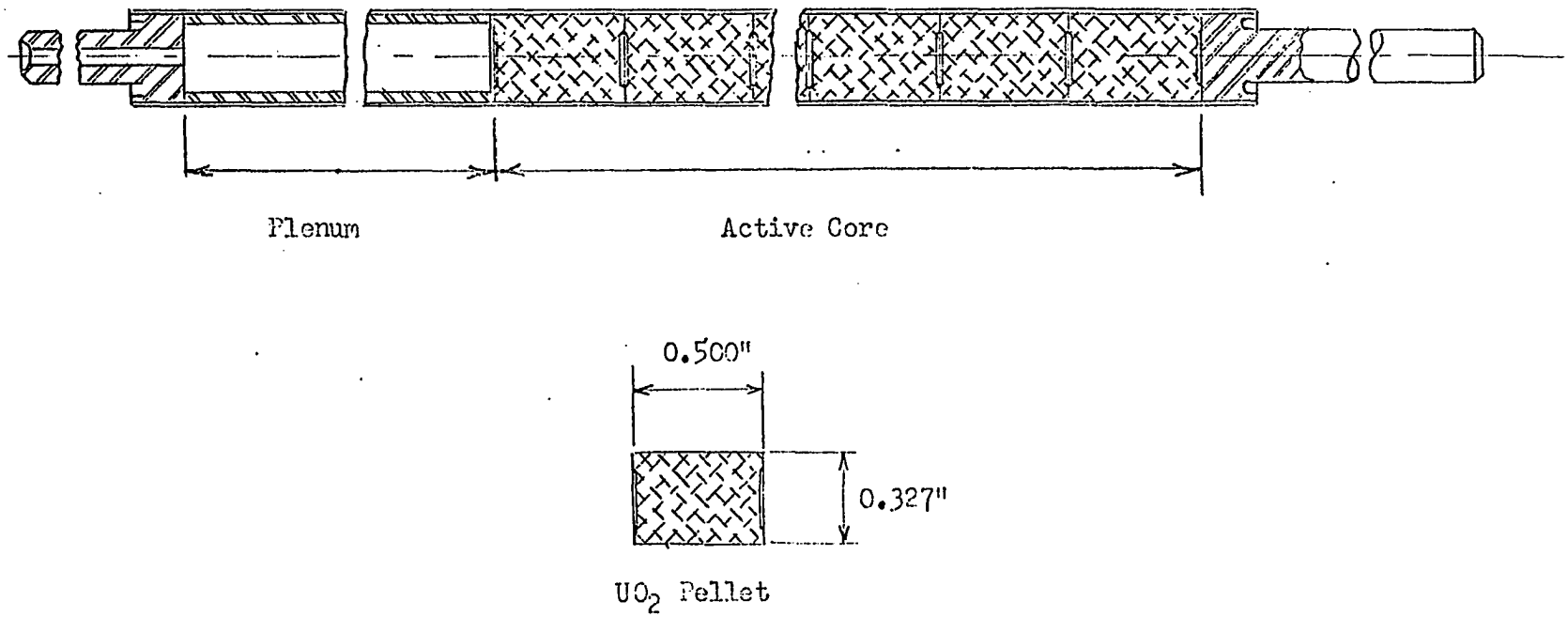

Fig. 4.1. Cross section of fuel rod (from GEMP-342, Reference 26).

There are 27 rods per fuel assembly, arranged in a 0.433 inch triangular pitch as can be seen in Fig. 4.2. The active core is hexagonal in shape, 26 inches on a side and 42 inches long. The active core is surrounded by an inner beryllium oxide reflector, with an average thickness of 4.8 inches, followed by an eight inch graphite reflector, which is pierced by cooling holes and separated from the inner reflector by a one inch annulus. A perspective view of the upper portion of the core can be seen in Fig. 4.3. The void between the fuel elements and the moderator tubes is filled with helium.

A cross sectional view of the 630A can be seen in Fig. 4.4. Noticeable are the borated-water shield tanks both inside and outside the containment vessel. The coolant flow is from the circulator up the outside of the core, through the annulus and the graphite reflector, into the coolant inlet flow plenum. From there, down through the active core through the boiler and back to the circulator.

The reactor is controlled by means of shim rods that displace the moderator for their reactivity effect. This control by water displacement, results in an increase of the mean energy of the neutron spectrum with resultant greater absorption in the fertile U238 in the fuel. This, in effect, allows the excess reactivity to be held in conversion ratio of fertile to fissile material rather than in burnable

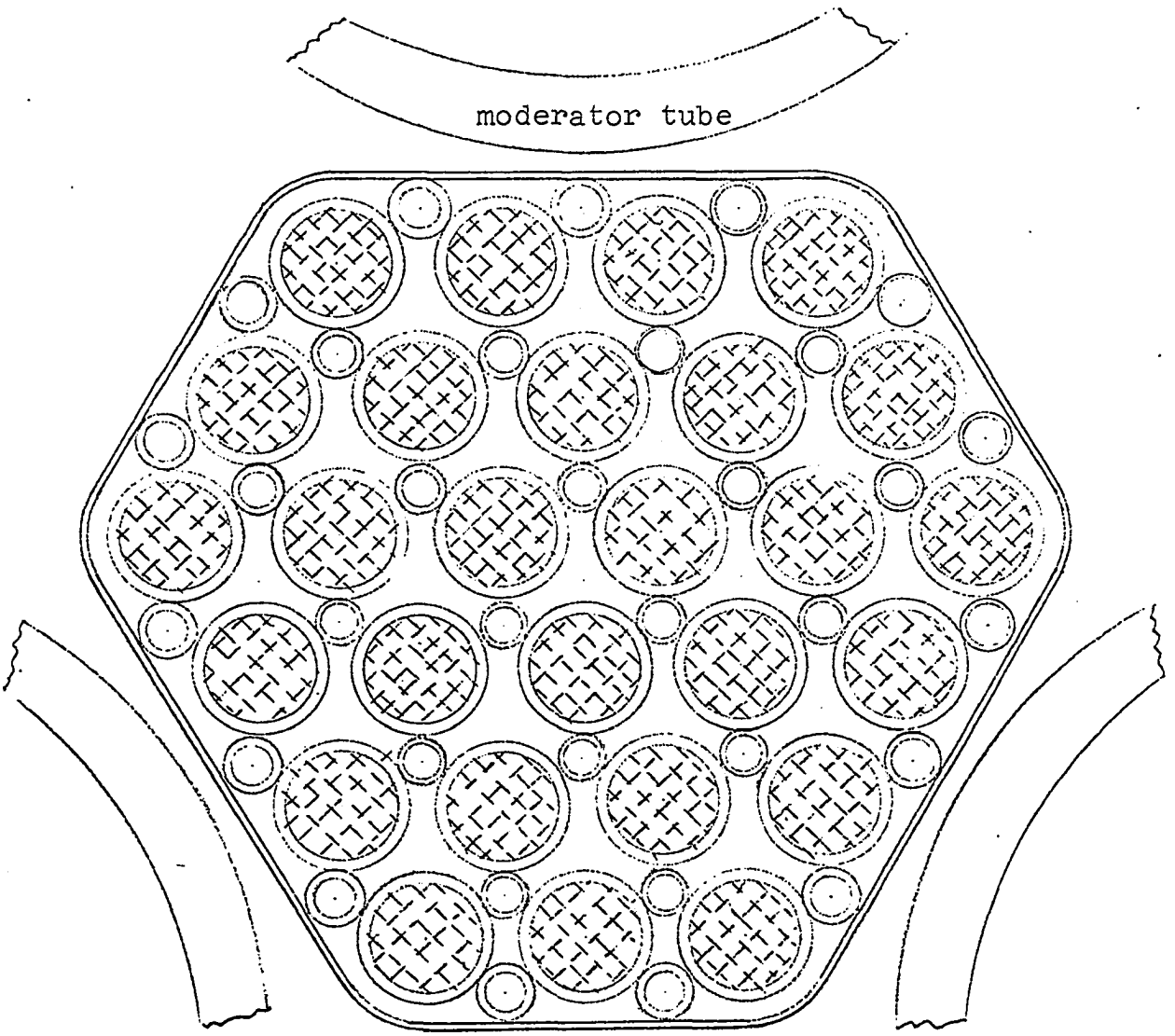

Fig. 4.2. Cross section of fuel element (from GEMP-342, Reference 26).

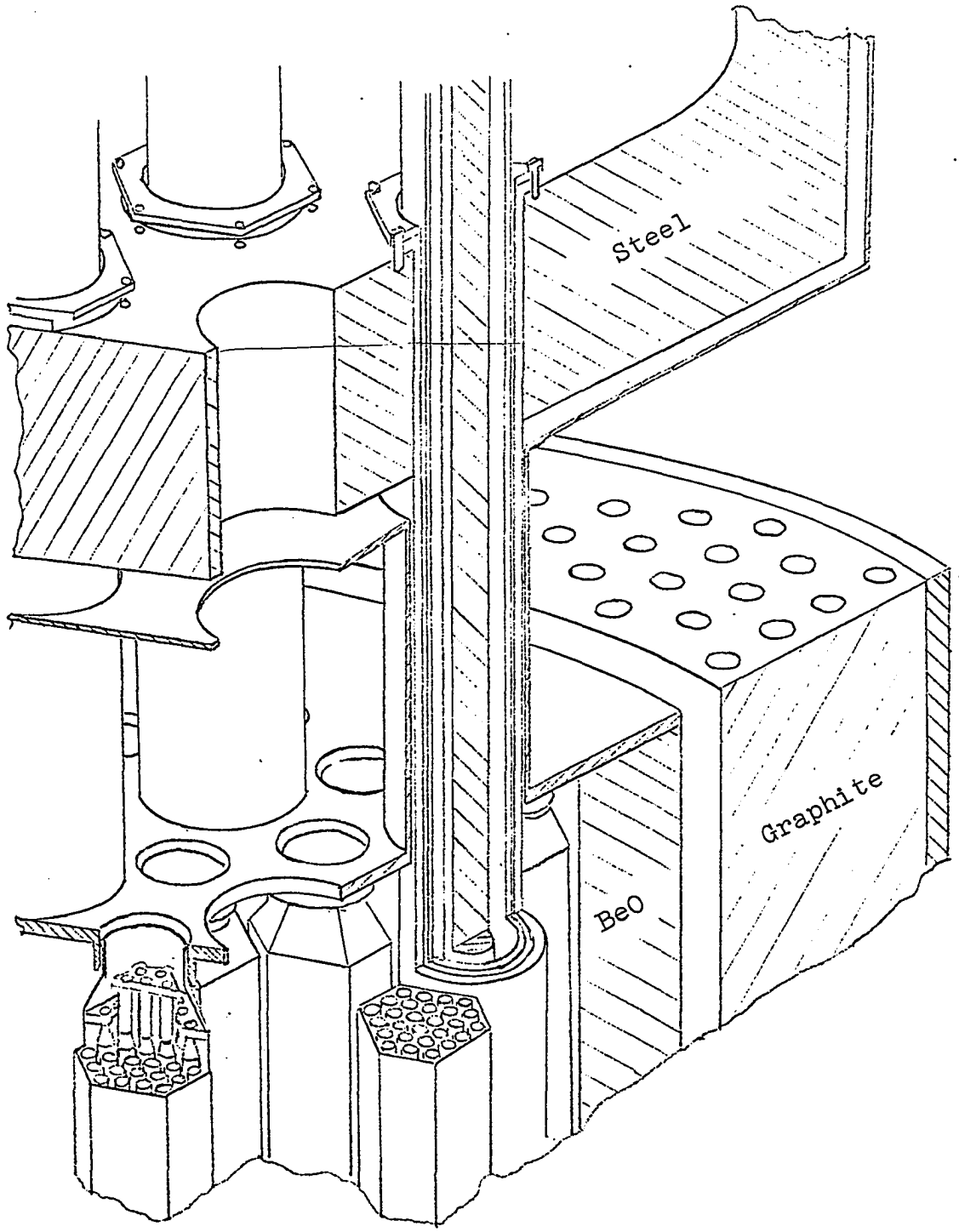

Fig. 4.3. Upper portion of reactor core (from GEMP-342, Reference 26).

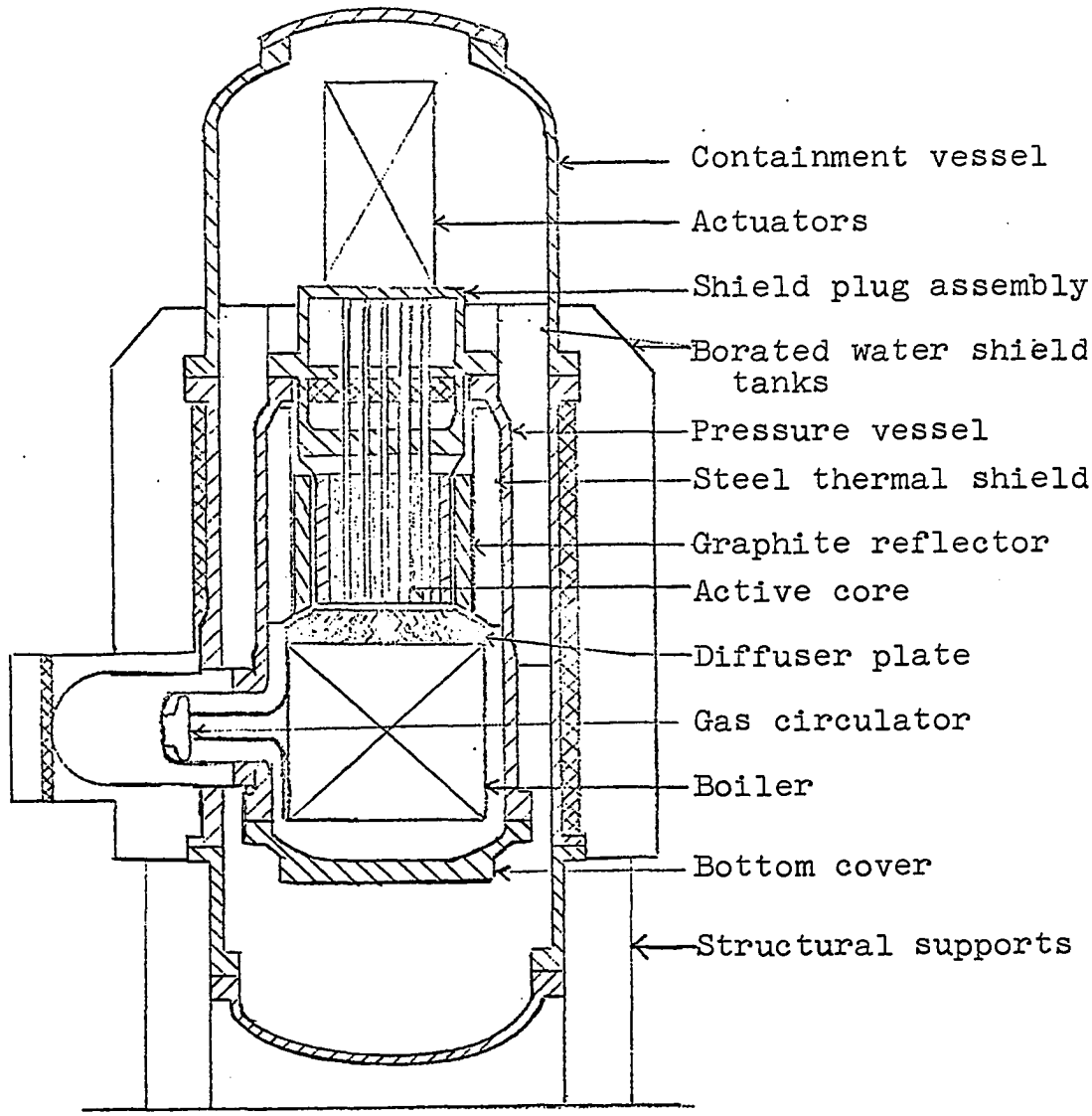

Fig. 4.4. Cross section of the 630A (from GEMP-342, Reference 26).

poison. Also, because each moderator tube can be shimmed separately, a method of gross radial power flattening is provided. In addition, poisoned safety rods, which are fully withdrawn during operation, are used for positive shutdown in the event of a scram signal. There are two types of control tubes, 48 of which have safety rods and 45 of which do not have safety rods. The two types of tubes are seen in Fig. 4.5.

A shield-plug assembly consisting of the active core, BeO reflector, shield plug, and control mechanism, is a single unit and can be removed from the reactor intact. This facilitates the refueling process and lends to unitizing the core structure. The shield-plug assembly supports the active core and provides shielding directly above the reactor. It also serves as the moderator inlet and outlet plenum, provides mountings for the control tubes and serves as the head of the pressure vessel. Neutron shielding is provided by the contained moderator, while seven inches of lead serves as the primary gamma shield. A cross section of the shield-plug is shown in Fig. 4.6.

Data for the 630A, pertinent to this design, are listed below:

number of fuel rods per element	27
number of fuel elements per core	216
number of moderator tubes per core	91
weight of UO_2 per fuel element	34.4 #
total weight of UO_2	$(7.43)10^3$ #
coolant free-flow area per element	1.933 in^2

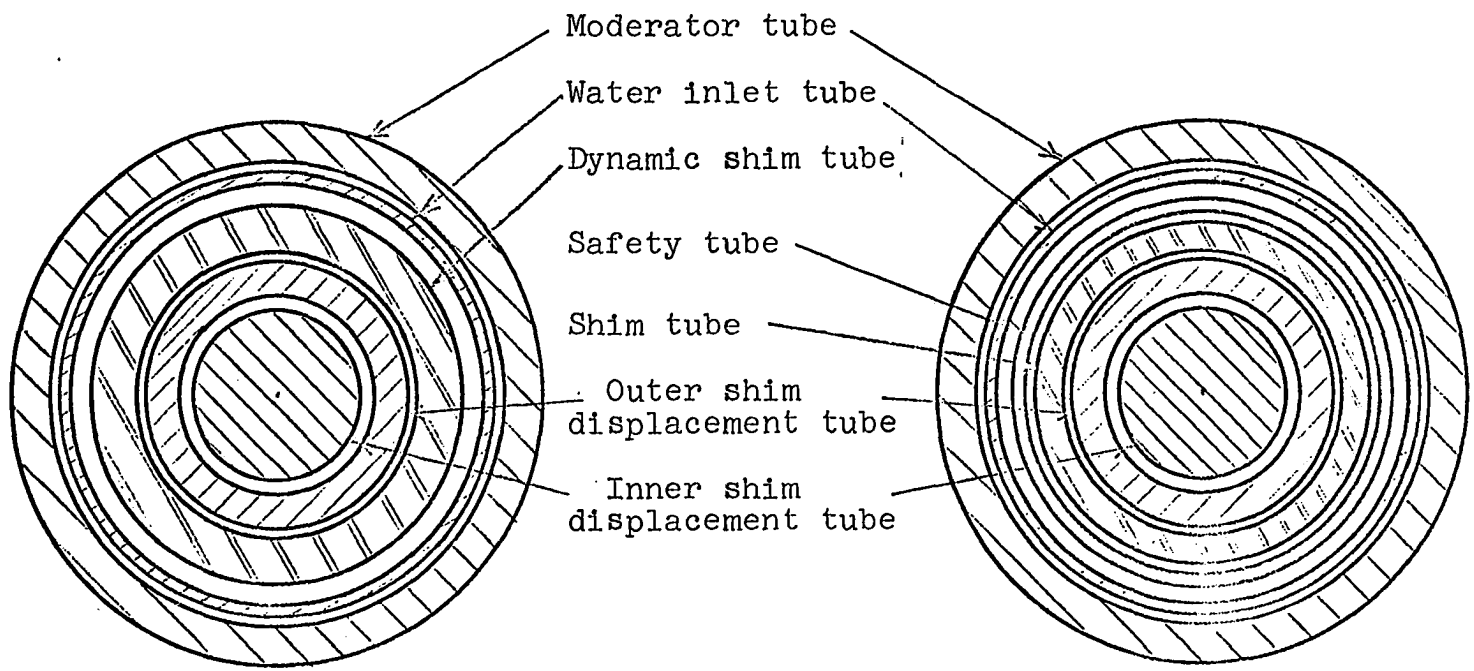

Fig. 4.5. Cross section of control tubes (from GEMP-342, Reference 26).

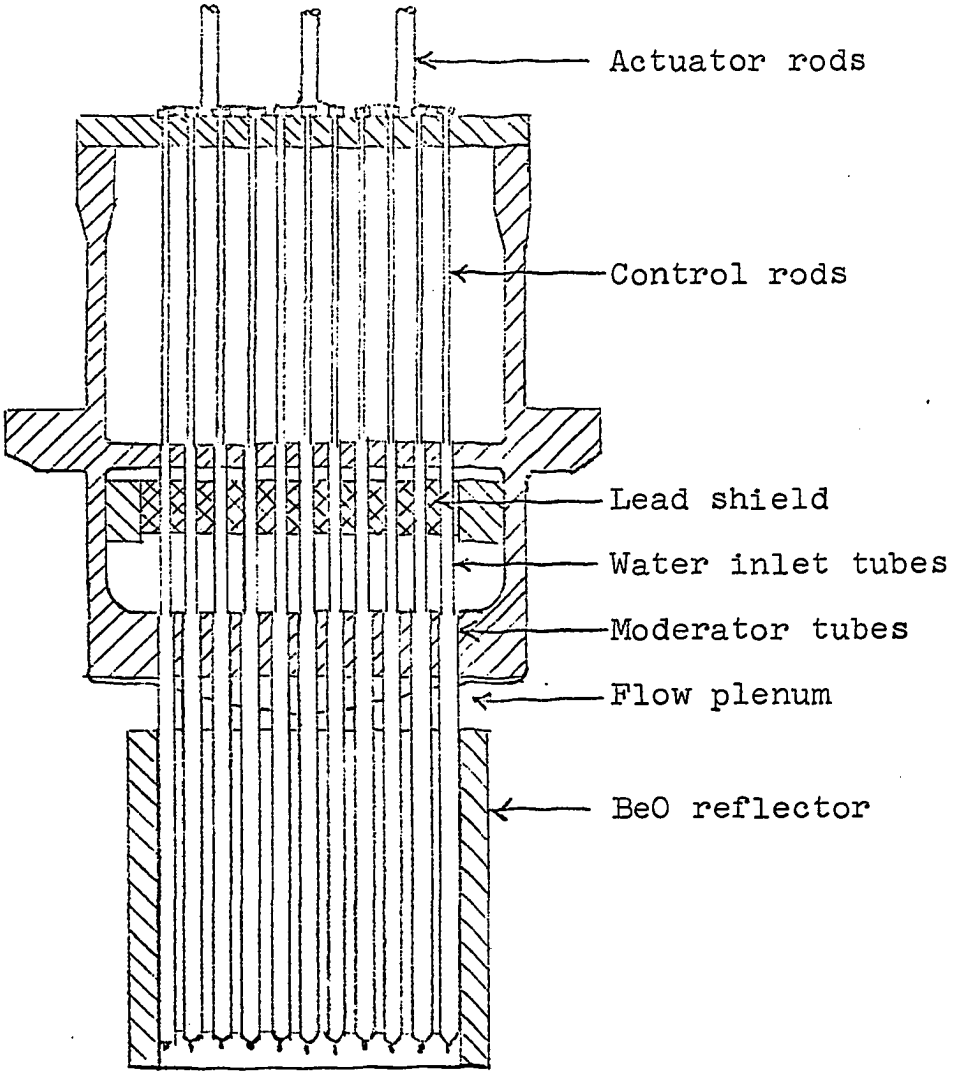

Fig. 4.6. Cross section of shield plug assembly (from GEMP-342, Reference 26).

total free-flow area		2.9 ft^2
heat transfer area per element		8.82 ft^2
total heat transfer area		1,910 ft^2
average heat flux @ 60.4 MW_t		$(1.026)10^5$ BTU/hr ft^2
total volume of fuel		12.1 ft^3
average power density @ 60.4 MW_t		$(1.7)10^7$ BTU/hr ft^3
coolant inlet temperature		553 °F
coolant outlet temperature		1,200 °F
mass flow rate		66.2 #/sec
maximum coolant pressure		830 psia
active core size:	length	42 in
	hexagonal side	26 in
over-all reactor size:		
	diameter	19.5 ft
	height	39.5 ft
reactor weight		600 long tons

core materials:
cladding, fuel element can and shim rods- incoly
moderator and water tubes - zircaloy-2
safety rods - stainless steel (1.25% B10)

structural materials:
pressure and containment vessels - carbon steel, SA-212-B
other structural materials - carbon steel.

Core Sizing

The design criteria were to maintain the same average heat flux of $(1.026)10^5$ BTU/hr ft^2 and the same average power density of $(1.7)10^7$ BTU/hr ft^3. A transmission efficiency of 86.5%, corresponding to that for the controllable pitch propeller, was used along with a cycle efficiency of 28.5%, corresponding to that of the intercooled and regenerative cycle at a pressure ratio of 3.0. These efficiencies resulted in a required heat rate of $(3.61)10^8$ BTU/hr and a coolant mass flow rate of 102.4 #/sec.

Thirty-six fuel elements and 36 moderator tubes were added circumferentially, maintaining the lattice spacing. The active core length was increased to 66 inches. This brought the total heat transfer surface up to 3,520 ft^2 and the fuel volume to 22.2 ft^3. Both the average flux and the average power density were maintained. The maximum gas outlet temperature was chosen at 1,250 ^oF. This is the maximum gas temperature which will yield the expected 20,000 hour life of the fuel elements, based on developments already performed[1].

Because information on the cross sections of Incoloy and Zircoloy-2 are lacking, these two materials were replaced with zirconium. This change has very little effect on the core physics. The above changes to the 630A gave rise to the following parameters of the design reactor:

number of fuel rods per element	27
number of fuel elements per core	252
number of moderator tubes per core	127
weight of UO2 per fuel element	54 #
total weight of UO2	$(1.362)10^4$ #
coolant free-flow area per fuel element	1.933 in^2
total free-flow area	3.38 ft^2
heat transfer area per element	13.9 ft^2
total heat transfer area	3,520 ft^2
average heat flux @ 106 MW	$(1.026)10^5$ BTU/hr ft^2
volume of fuel	22.2 ft^3
average power density @ 106 MW	$(1.625)10^7$ BTU/hr ft^3
coolant inlet temperature (approximate)	458 ^oF

[1]Delson, E. B., Manager, Applicational Operations, General Electric Company, Cincinnati, Ohio. 630A parameters. Private communication. 23 June, 1965.

coolant outlet temperature		1,250 °F
coolant mass flow rate		102.4 #/sec
maximum coolant pressure		1,000 psia
active core size:	length	66 in
	hexagonal side	28.75 in
over-all reactor size:		
	height	32 ft
	diameter	21.5 ft
reactor weight		740 long tons

core materials:
cladding, fuel element can, moderator tubes, water tubes and shim rods (0.074 vol. % Boron); all zirconium

structural materials:
pressure and containment vessels; carbon steel (SA-212-B)
other structural materials; carbon steel

Core Neutronics

The volume fractions of the materials within the active core region were determined for three possible conditions of rod position; all rods out, all shim rods in, and all shim and safety rods in. The resulting volume fractions are shown in Table 4.1.

An investigation into core reactivity with the various volume fractions was carried out. A computer program by Rohach (32) was modified for this investigation. The program is for the solution of the critical, one-dimensional, multi-group diffusion equation. It was used to obtain the initial enrichment and also to determine fuel depletion.

Table 4.1. Volume fractions of the active core materials

Material	Volume fraction		
	all rods out	all shim in	shim and safety in
UO_2	0.2650	0.2650	0.2650
He	0.3165	0.3165	0.3165
Zr	0.1900	0.3260	0.3260
H_2O	0.2290	0.0925	0.0795
Fe	0.0	0.0	0.0130
B_{10}	0.0	0.0	0.0001625

Four energy groups were used in this analysis and the values for the microscopic cross sections were obtained from References 33, 34, 35. The cross sections for the thermal group were corrected for temperature effects. Each material was corrected to the average temperature of that particular material in the active core. An equivalent cylinder was utilized based upon the active core dimensions. It was divided radially into three regions; the active core, the BeO reflector and the graphite reflector. The thicknesses of each prototype reflector were retained for this study.

Criticality was achieved at an enrichment of 1.68% with all shim rods inserted (minimum moderator) and at 1.058% with all rods out (maximum moderator). All of the shim rods could, therefore, control 0.522% of enrichment. With all the shim and safety rods inserted a shut-down margin of about

17% resulted.

From calculations a burnup of 0.908% enrichment per year is needed for 106 MW. The shim control over 0.522% enrichment corresponds to 210 days at full power or just under 14 round trips, Holland-U.S.A.-Holland. The expected 20,000 hour life of the fuel elements corresponds to 831 days or 55 round trips at full power. Based on the theoretical burnup and a 20,000 hour life, the enrichment was increased to 3.23%. To over-ride the added enrichment, 0.074 volume percent of Boron 10 was added to the shim rods.

To improve burnup and power density, the longitudinal flux was flattened by adding 16 centimeters of BeO, in the form of a slab pierced by the coolant and moderator tubes, at each end of the core. This gave rise to a chopped cosine with an average to maximum flux ratio of 0.766 as compared to 0.627 for the cosine distribution. The longitudinal thermal flux distribution is plotted in Fig. 4.7. The radial flux, for the four energy groups, is plotted in Figs. 4.8 and 4.9.

Core life was determined accounting for poison burnup, fission product buildup, moderator displacement and fuel depletion. At start-up, 47 sets of shim rods were withdrawn and criticality reached with poison content. As the Boron was depleted, the shim rods were inserted to maintain the critical state. The results of this study led to a plot of

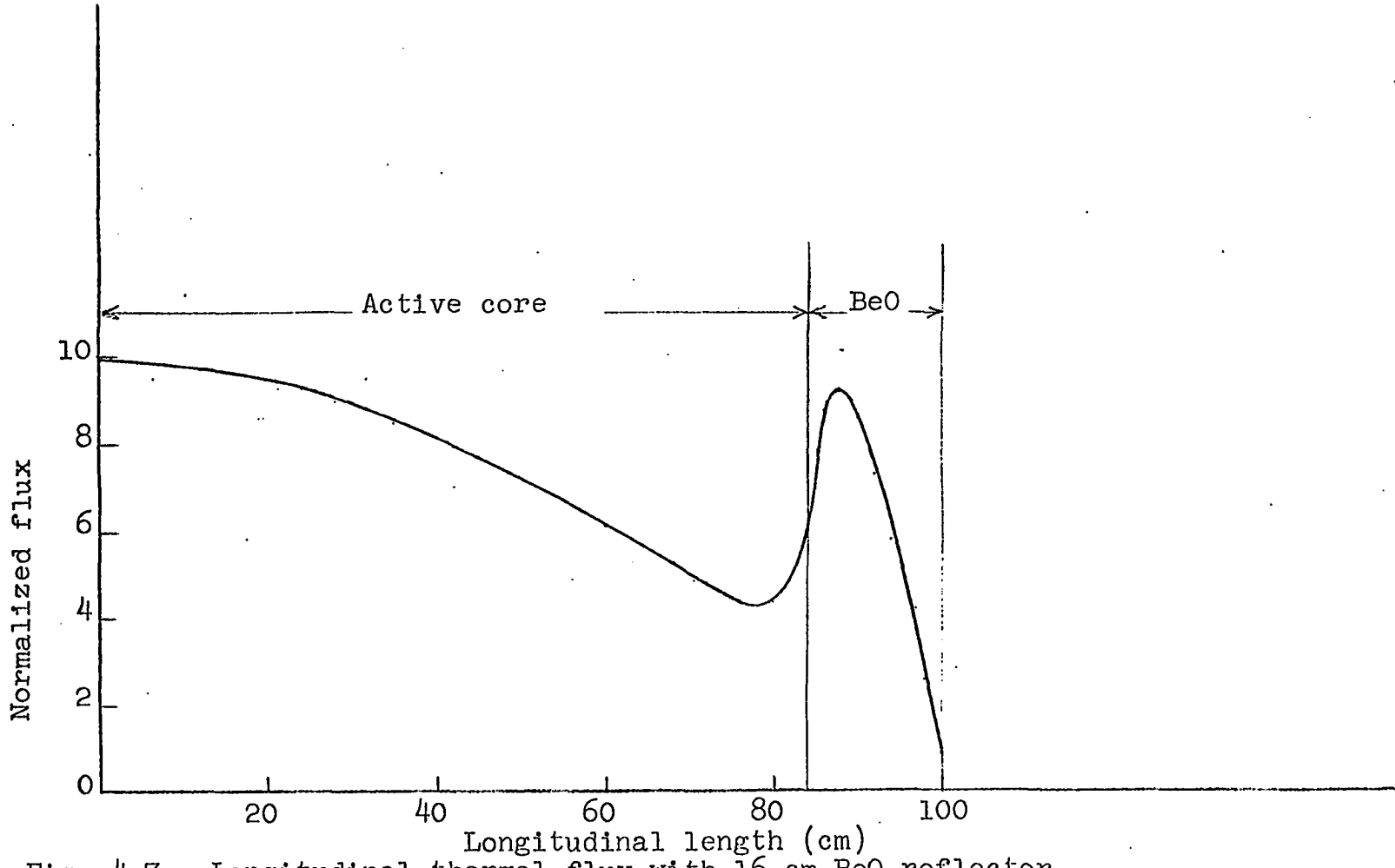

Fig. 4.7. Longitudinal thermal flux with 16 cm BeO reflector.

Fig. 4.8. Normalized flux versus core radius for three energy groups.

Energy Groups

A. 9.1 Kev to 1.35 Mev

B. 0.4 ev to 9.1 Kev

C. 1.35 Mev and above

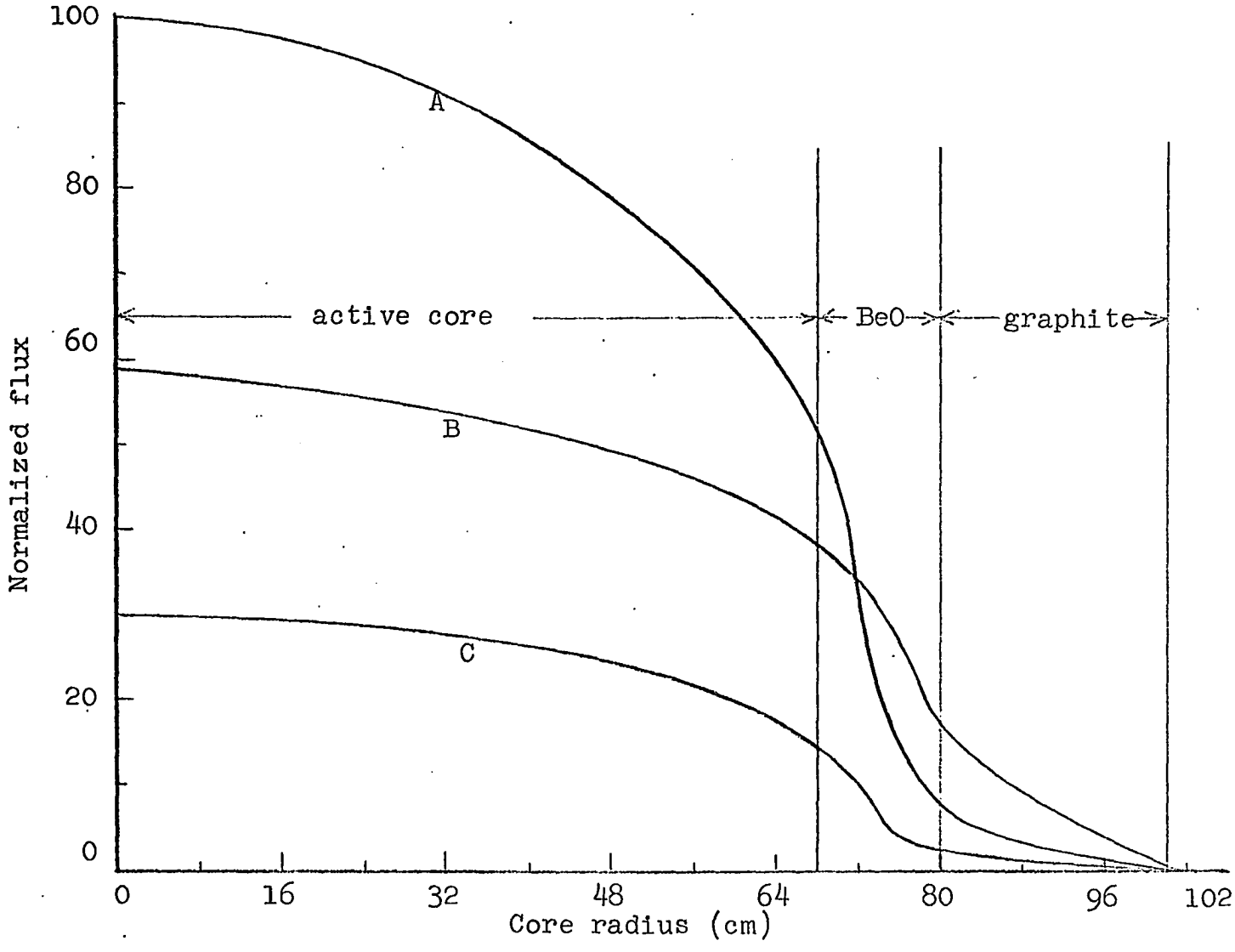
100
80
60
40
20
0
Normalized flux
A
B
C
active core
BeO
graphite
0
16
32
48
64
80
96
102
Core radius (cm)

Fig. 4.9. Normalized thermal flux versus core radius.

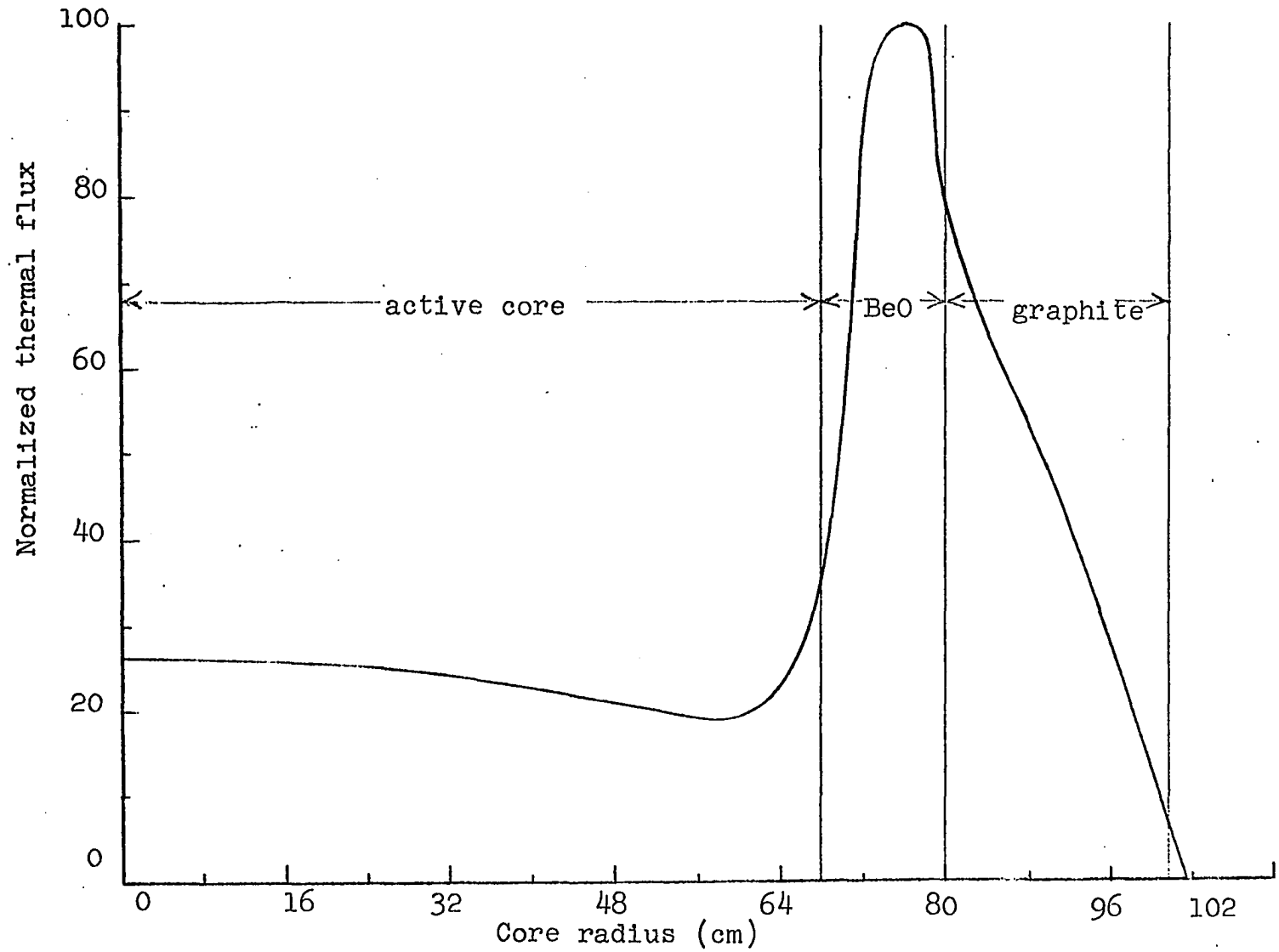
100
80
60
40
20
0
Normalized thermal flux
active core
BeO
graphite
0
16
32
48
64
80
96
102
Core radius (cm)

the amount of shim versus the number of days operation at full power, which can be seen in Fig. 4.10. All shim was withdrawn by 1815 days which corresponds to 1 1 round trips and a burnup of 31,100 MWD/MT.

The average thermal flux increased with time, going from a value of $(1.124)10^{13}$ at startup to a value of $(4.163)10^{13}$ at 1815 days. The power density at the core center never exceeded the value of $(6.3)10^{6}$ BTU/hr ft^3 which is below the design limit of $(1.7)10^{7}$ BTU/hr ft^3.

A unit cell was established utilizing an equivalent cylinder. A homogeneous mixture of zirconium, fuel and helium was assumed for the region outside of the moderator tube with the appropriate volume fractions applied. Two conditions were examined; all rods out and all shim rods in.

The multi-group diffusion theory computer program was utilized to determine the infinite multiplication and the thermal neutron flux distribution. To utilize fully the moderating effect of the water regions, all the boron was placed in the inner shim displacement rod. With all rods withdrawn, an infinite multiplication factor of 1.115 was obtained, along with a thermal flux distribution as seen in Fig. 4.11. With all rods inserted, an infinite multiplication factor of 1.069 was obtained and a thermal flux distribution as seen in Fig. 4.12.

Fig. 4.10. Amount of shim insertion versus number of days at full power. 100% equals "all in" position.

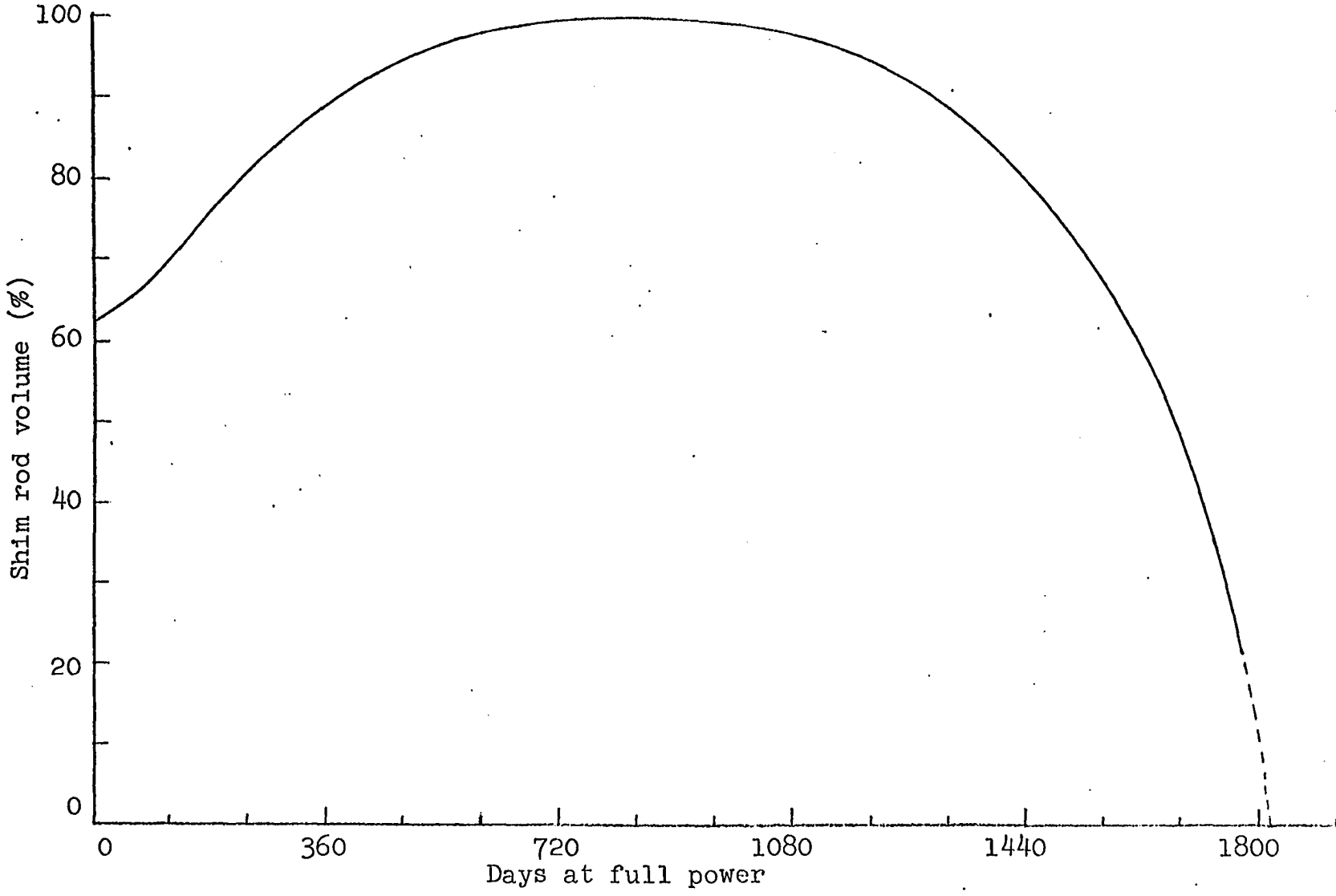
100
80
60
40
20
0
Shim rod volume (%)
0
360
720
1080
1440
1800
Days at full power

Fig. 4.11. Normalized thermal flux versus unit cell radius. Shim tube, all rods withdrawn.

Regions

I = zirconium water tube.

II = water moderator.

III = zirconium moderator tube.

IV = homogeneous region, UO_2, zirconium, and helium.

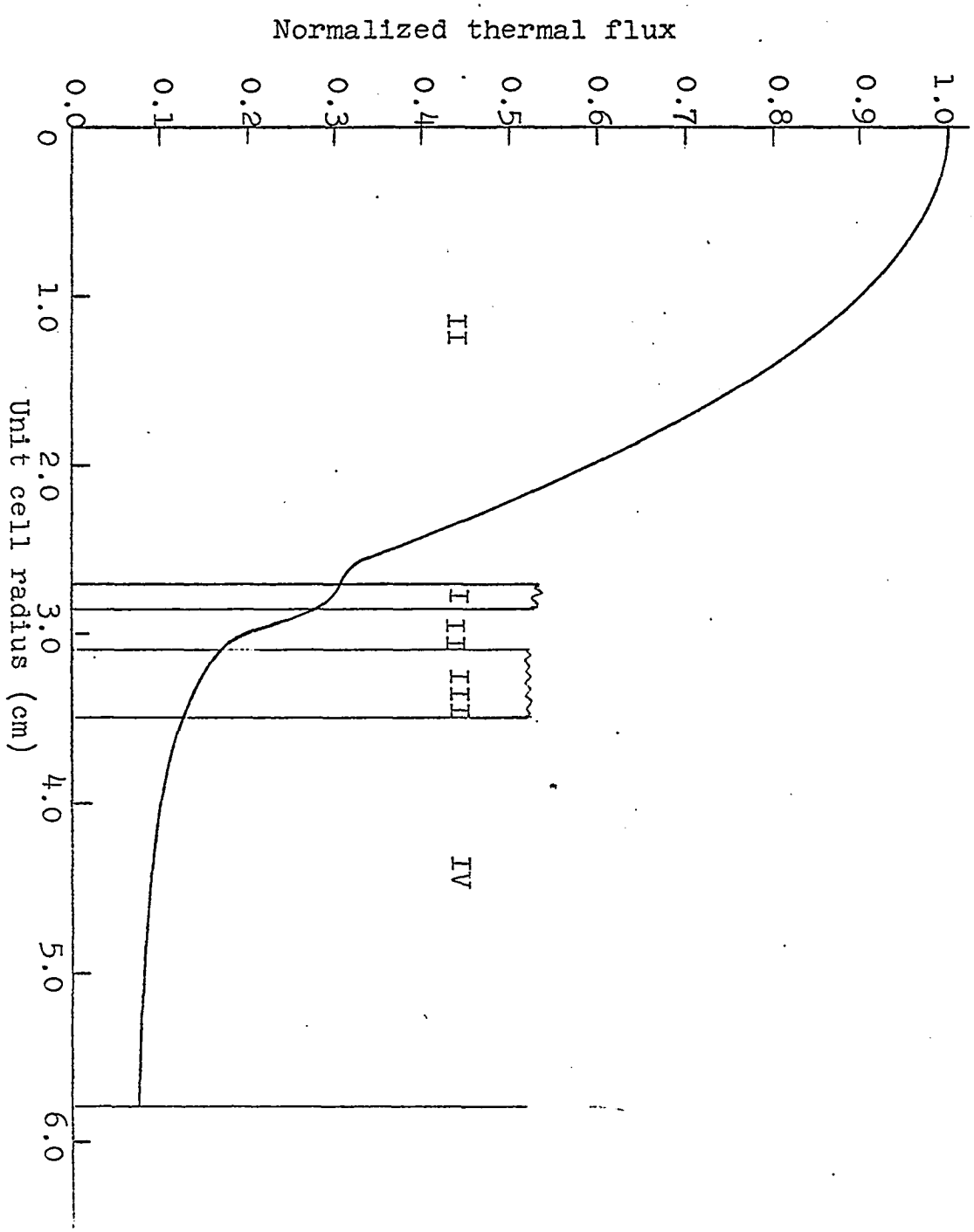
Normalized thermal flux
0.0
0.1
0.2
0.3
0.4
0.5
0.6
0.7
0.8
0.9
1.0
0
1.0
2.0
3.0
4.0
5.0
6.0
Unit cell radius (cm)
I
II
III
IV
I
II
III

Fig. 4.12. Normalized thermal flux versus unit cell radius. Shim tube, all rods in.

Regions

I = water moderator.

II = zirconium and boron inner shim displacement rod.

III = zirconium outer shim displacement rod.

IV = zirconium dynamic shim rod.

V = zirconium water inlet tube.

VI = zirconium moderator tube.

VII = homogeneous region, UO_2, zirconium and helium.

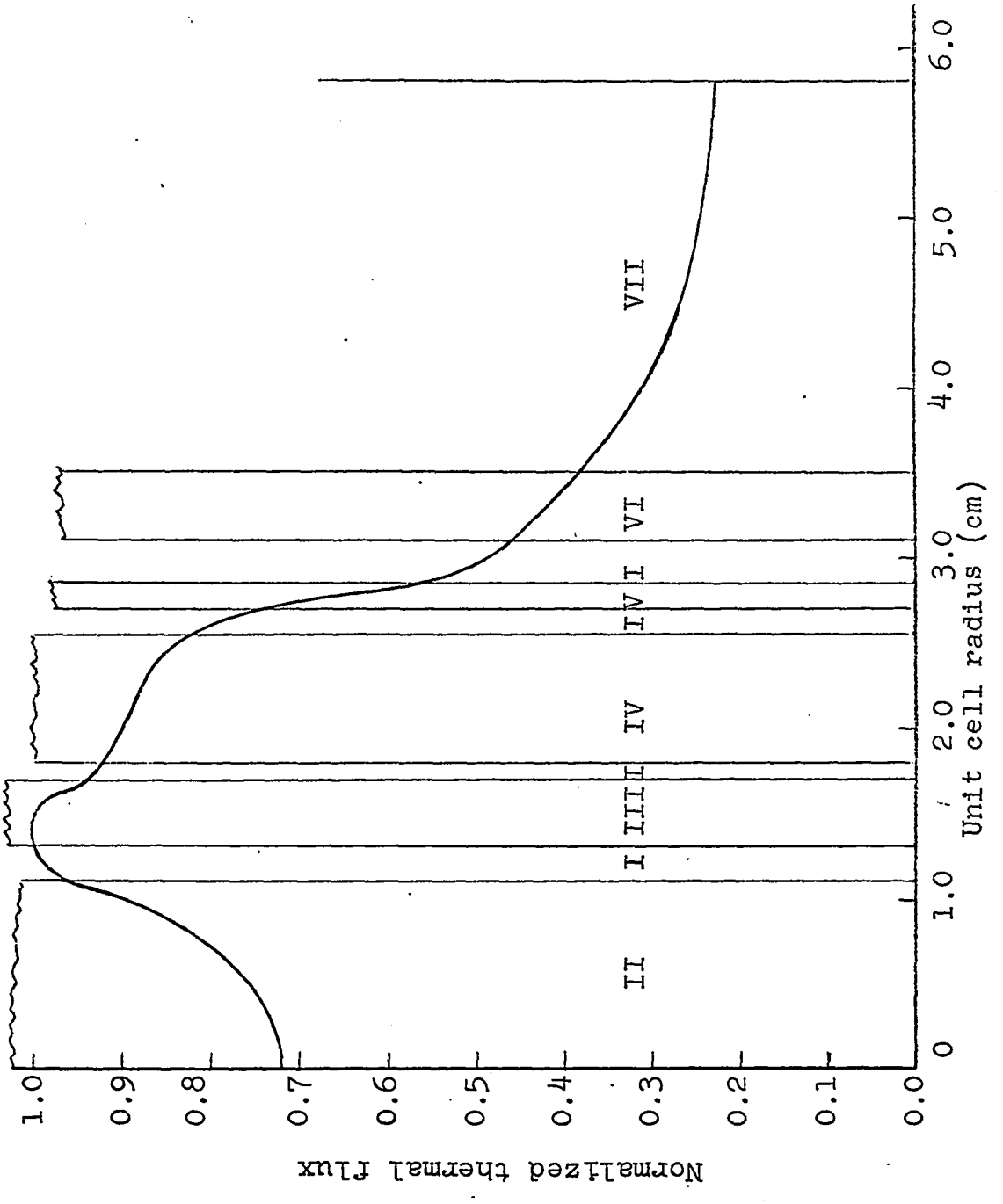
Normalized thermal flux
1.0
0.9
0.8
0.7
0.6
0.5
0.4
0.3
0.2
0.1
0.0
0
1.0
2.0
3.0
4.0
5.0
6.0
Unit cell radius (cm)
II
I
III
IV
V
VI
VII

Heat Transfer

The mass flow rate for the intercooled and regenerative cycle at a compression ration of 3.0 is 102.4 #/sec. The heat rate at full power is $(3.61)10^8$ BTU/hr and with a fuel volume of 22.2 ft^3, results in an average power density of $(1.625)10^7$ BTU/hr ft^3. The longitudinal flux distribution is a chopped cosine with an average to maximum ratio of 0.766. This function was utilized in determining the longitudinal temperature distribution in the central fuel element of the core.

Following the development of chapter six of (36), the coolant temperature, cladding surface temperature and the fuel centerline temperature were found as a function of the fuel element length.

The temperature difference between the coolant, at any point x, (t_m), and that at the inlet (t_{og}), is expressed as

$$t_m - t_{og} = \frac{QAL}{w\, c_p \pi} \left(1 - \cos \frac{\pi x}{L}\right) , \qquad (4.1)$$

where

Q = maximum power density (BTU/hr ft^3)

A = fuel cross sectional area (ft^2)

L = core and reflector length (ft)

w = coolant mass flow rate (#/hr)

c_p = specific heat at constant pressure (BTU/# ^oF)

For this design cycle t_{og} = 458 ^oF and Equation 4.1 becomes

$$t_m - 458 = (399)\left(1-\cos \frac{\pi x}{L}\right). \qquad (4.2)$$

The temperature difference between the cladding surface (t_s), and the coolant at any point x, is

$$t_s - t_m = \frac{QV}{h_x A_n} \sin \frac{\pi x}{L} , \qquad (4.3)$$

where

A_n = fuel element heat transfer surface area (ft^2)

V = fuel volume per element (ft^3)

h_x = heat transfer coefficient (a function of temperature taken from Fig. 3, p. 79 of Reference 26).

Substituting, Equation 4.3 becomes

$$t_s - t_m = \frac{(1.41)10^5}{h_x} \sin \frac{\pi x}{L} \qquad (4.4)$$

The temperature difference between the cladding surface at any point x, (t_s), and that at the inlet (t_{os}), is

$$t_s - t_{os} = \frac{QAL}{w\, c_p\, \pi} (1-\cos \frac{\pi x}{L}) + \frac{QV}{h_x A_n} \sin \frac{\pi x}{L} \qquad (4.5)$$

t_{os} is obtained from an energy balance at the first inch of fuel element length knowing

$$\Delta T = t_{os} - t_m = \frac{Q}{h_x A_n} . \qquad (4.6)$$

With $t_m = 458^\circ$ and $t_{os} = 732^\circ$, Equation 4.5 becomes

$$t_s - 732 = 399(1-\cos \frac{\pi x}{L}) + \frac{(1.41)10^5}{h_x} \sin \frac{\pi x}{L} . \qquad (4.7)$$

The fuel rod centerline temperature (t_f) minus the clad surface temperature is expressed as

$$t_f - t_s = \frac{Qa^2}{2} [\frac{1}{2k_f} + \frac{\ln(b/a)}{k_c}] \qquad (4.8)$$

where

a = fuel rod radius (ft)

b = cladding outside radius (ft)

k_f= thermal conductivity of the fuel (BTU/hr ft^2 ^oF-ft)

= (68.4) $T^{-0.498}$

k_c= thermal conductivity of the cladding (BTU/hr ft^2 ^oF-ft)

Equation 4.8 reduces to

$$t_f = t_s + 172^o \qquad (4.9)$$

Equations 4.2, 4.7, and 4.9 are plotted versus active core length in Fig. 4.13. The maximum cladding surface temperature is 1,643 ^oF occurring at 82% of the fuel element length. The maximum fuel centerline temperature is 1,822 ^oF and it occurs at 82% of the fuel element length also.

Shielding

The 630A meets the radiation protection specifications established by the Code of Federal Regulations, Title 10, part 20, "Standards of Protection Against Radiation". The primary requirements are:

1. Individuals with access to restricted areas;

a. A maximum of 3 rem of whole body dose during any one calendar quarter.

b. Whole body dose plus accumulated occupational whole body dose shall not exceed 5(N-18) rem, where N is the individual's age in years.

2. Dose levels in unrestricted areas shall be no more than 0.5 rem in any one calendar year; or in excess of 100 mrem

Fig. 4.13. Fuel core, cladding and coolant temperature versus active core length for a chopped cosine energy distribution.

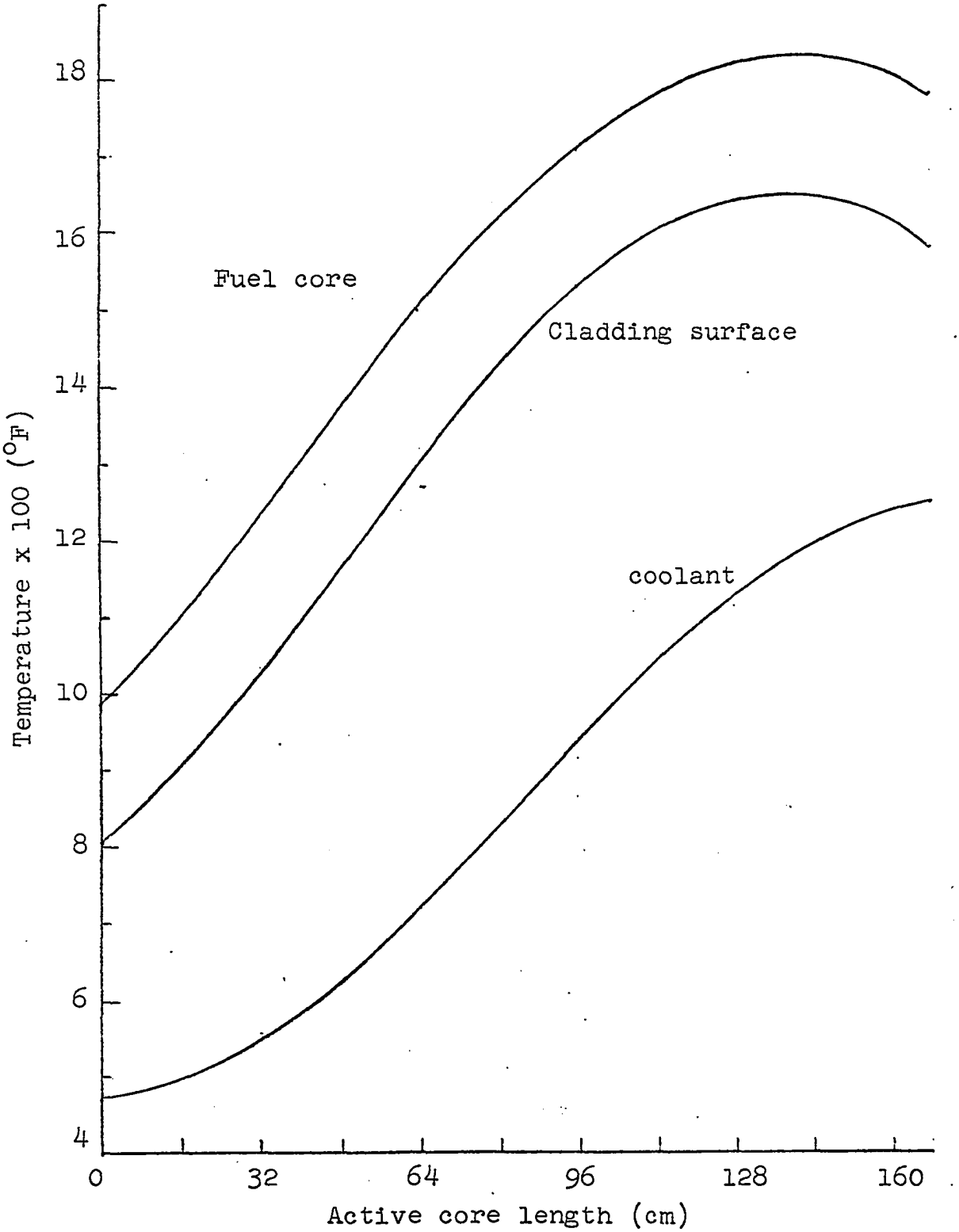
18
16
14
12
10
8
6
4
Temperature x 100 (°F)
Fuel core
Cladding surface
coolant
0
32
64
96
128
160
Active core length (cm)

in any seven consecutive days; or in excess of 2 mrem in any one hour of continuous occupancy.

Shielding is accomplished with steel thermal shields lead and borated water. A primary gamma dose rate of $(1.4)10^{-3}$ rads/hr, a secondary gamma dose rate of $(4.08)10^{-3}$ rads/hr and a fast neutron dose rate of $(4.4)10^{-5}$ rads/hr were calculated at the outer shield tank surface on the core midplane of the 630A at full power.

For this design the same shielding configuration was employed and the Comparison Method of shield design utilized (37). This method is based on known performance data as a basis for predicting the performance of a new design.

The dose rate of the prototype as compared to that of the new design is

$$\frac{D_p}{D_d} \cong \left(\frac{r_p}{r_d}\right) \left(\frac{T + r_d}{T + r_p}\right) \left(\frac{P_p}{P_d}\right) \qquad (4.10)$$

where

D = dose

r = core radius

T = shield thickness

P = power level

the subscripts are:

p = prototype

d = design

This resulted in a dose ratio of 0.488, with the shield thickness held constant.

The resulting dose rates at the outer shield tank surface are $(2.87)10^{-3}$ rad/hr for primary gamma, $(8.35)10^{-3}$ rad/hr for secondary gamma and $(9.22)\ 10^{-5}$ rad/hr for fast neutrons. The combined dose rate at the top of the reactor was found to be 0.146 mrem/hr as compared to 0.085 mrem/hr for the 630A.

The attenuation of the gamma dose rate in the outer borated water shield is $(0.3)10^{-3}$ rad/hr per cm of H_2O and that for the fast neutron dose rate is $(0.4)10^{-5}$ rad/hr per cm of H_2O. These values were taken from figure 7.2 page 149 of Reference 26. To bring the dose rates at the shield surface back to those of the 630A would require 26 cm of H_2O to be added to the shield thickness.

An investigation into the maximum dose rates at the shield surface that would give allowable limits in the adjoining compartments was carried out. If the source is assumed to be an infinite cylindrical surface and the bulkhead plating is 30-lb plate (0.75"), a dose rate of 3.58 mrem/hr exists at the opposite sides of the bulkheads of the adjoining compartments with the shield surface dose rate of 10.2 mrem/hr. To reduce this to the allowable limits 10 cm of thickness was added to the outer shield. A dose rate of $(2.95)10^{-2}$ mrem/hr was found to exist at the deck above the reactor assuming 20-lb plate for the deck.

The dose rate at the bottom shell plating was determined also. There is a 13 in. steel diffusion plate at the

bottom of the active core which has an effective thickness of 15 cm. Also below the core are the steel outlet plenum, inlet plenum, containment vessel, tank top and bottom shell plating. The double bottom was assumed filled with water. A surface source strength for fast neutrons of $(2.1)10^{13} n/cm^2$ sec was determined to exist at the bottom of the active core along with a surface source of $(1.58)10^{11}$ mev/cm^2 sec for gamma. The dose at the bottom of the diffuser plate, accounting for buildup, was $(1.58)10^{11}$ n/cm^2 sec and $(5.27)10^{10}$ mev/cm^2 sec. Assuming the diffuser plate surface to be a plane source and the materials below to be parallel plates, a dose rate of 0.068 mrem/hr was found to exist at the bottom side of the shell plating.

Dose rates at the outside of the side plating were not determined for several reasons. The plating is at least 40-lb plate (1.0"), the distance is three times that to the adjacent bulkheads and there will be longitudinal collision bulkheads placed outboard of the reactor which will add considerable material. No hazard is foreseen.

This study showed that 10 cm of borated water must be added to the outer shield tank to bring the dose rates to allowable limits in the fore and aft adjoining compartments and that no hazard exists in the living spaces above the reactor. Fig. 4.14 indicates distances and dose rates for the reactor compartment and adjoining areas. Fig. 4.15

Fig. 4.14. Shear plan of the reactor compartment showing reactor surface dose rates, dose rates in adjoining compartments, structural plate thicknesses and related dimensions.

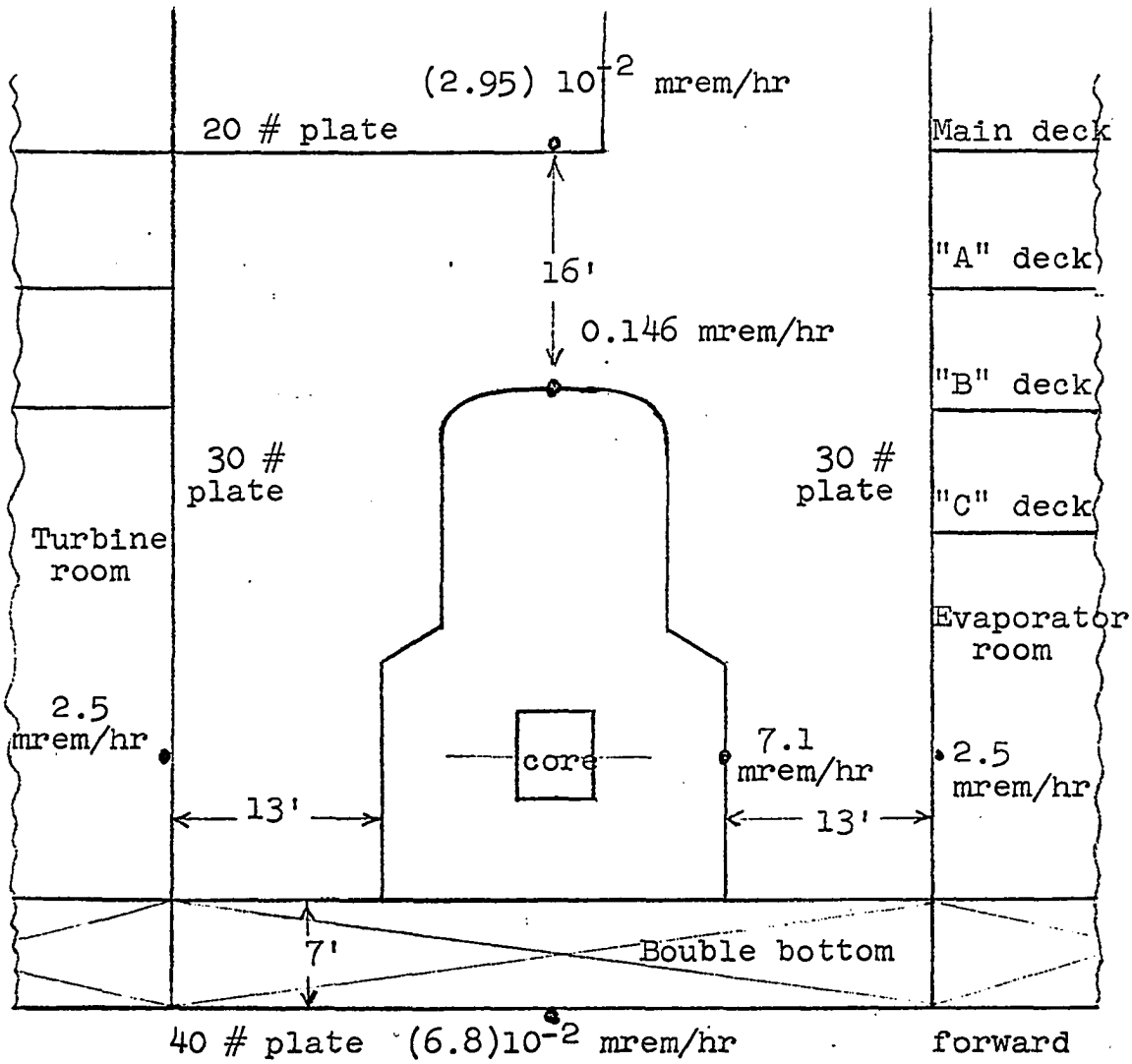
(2.95) 10⁻² mrem/hr
20 # plate
Main deck
"A" deck
16'
0.146 mrem/hr
"B" deck
30 # plate
30 # plate
"C" deck
Turbine room
Evaporator room
2.5 mrem/hr
core
7.1 mrem/hr
2.5 mrem/hr
13'
13'
7'
Bouble bottom
40 # plate
(6.8)10⁻² mrem/hr
forward

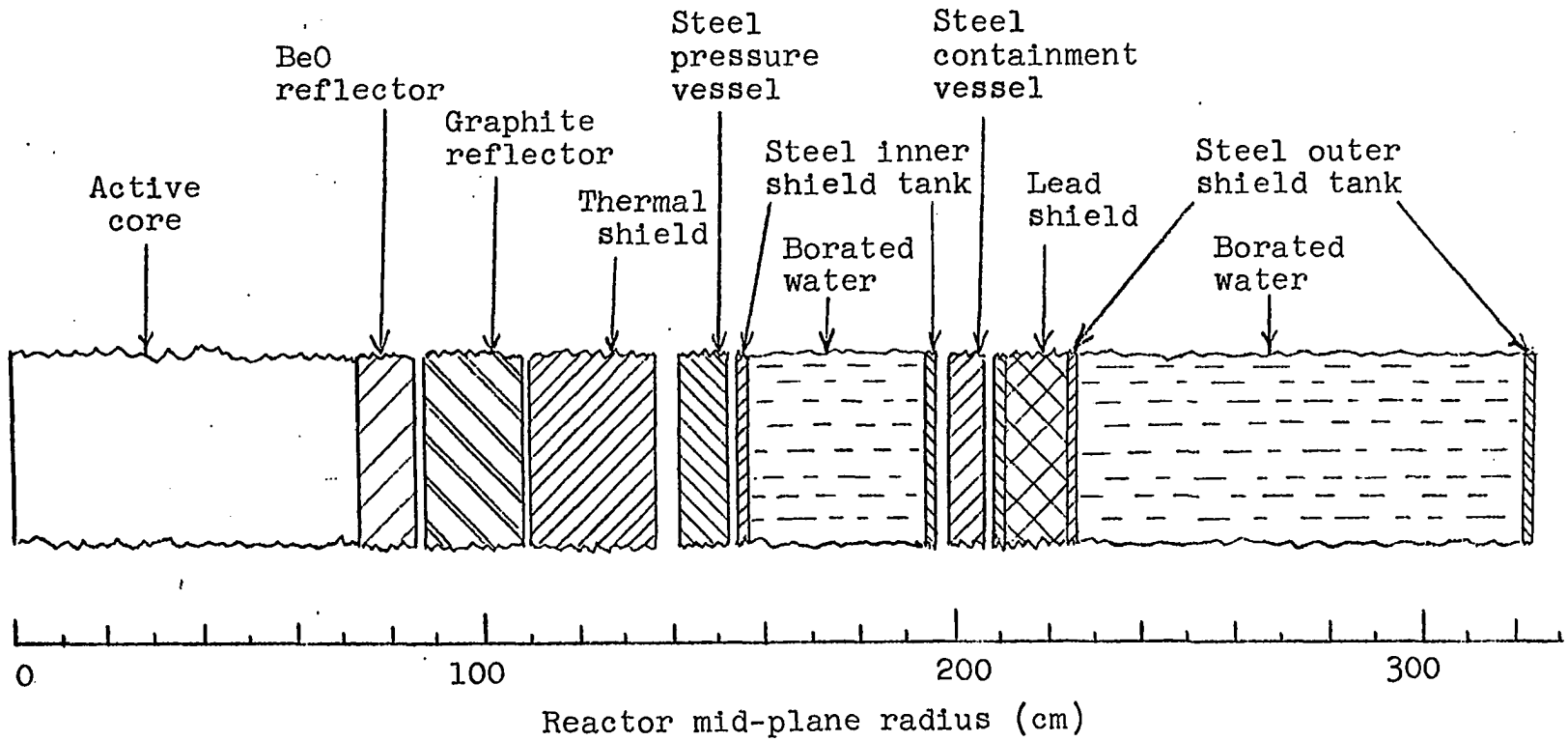

Fig. 4.15. Longitudinal cross section of the reactor at the core midplane.

shows a longitudinal cross section of the reactor at the core midplane.

Pressure Vessel

The 630A has 70 cm of reflector materials and helium between the active core and the pressure vessel. The inner radius of the pressure vessel is 130 cm. It is made of carbon steel, SA-212-B, is 2.75 in. thick and is designed for a maximum pressure of 900 psia at a temperature of 700 °F.

Retaining the reflector thickness, the new pressure vessel inner radius is 141 cm. It will be designed for a maximum pressure of 1,050 psia at a temperature of 700 °F. It will operate at a pressure of 1,000 psia and approximately 500 °F. Design procedure is based on maximum shear stress theory, as outlined in Chapter 11 of (36).

For thick-walled cylinders in the elastic range, the maximum stress is at the inner surface. Maximum circumferential or "hoop", tensile stress is

$$\sigma_{max} = \frac{P[(b/a)^2 + 1]}{(b/a)^2 - 1} , \qquad (4.11a)$$

where

P = internal pressure

b/a = radius ratio

and the minimum stress is

$$\sigma_{min} = -P . \qquad (4.11b)$$

The primary stress is

$$\sigma_P = \sigma_{max} - \sigma_{min} = \frac{2P\ (b/a)^2}{(b/a)^2-1} \tag{4.12}$$

The membrane stress is the average of the primary stress across the thickness of the vessel. The average of the maximum primary stress is

$$(\sigma_{max})_{ave} = \frac{Pa}{t}\ , \tag{4.13a}$$

and the average of the minimum primary stress is

$$(\sigma_{min})_{ave} = -\frac{P}{2}\ . \tag{4.13b}$$

The membrane stress is

$$S_m = \frac{P(2a + t)}{2t} \tag{4.14}$$

For this design the maximum allowable membrane stress intensity was based upon those listed in the ASME Pressure Vessel Code (38). From table N-421, page 21 of (38), $S_m(max)$ is given as 18,300 psia for SA-212-B carbon steel at 700 ^oF. Other properties are:

minimum tensile strength = 70,000 psia

minimum yield strength = 38,000 psia

yield strength = 27,400 psia

Thermal stress was also considered and for exponential internal heat generation in long thick-walled cylinders the maximum tangential stress is given as

$$S_T = \sigma_T = \frac{\alpha EQ}{k\ \mu^2(1-\nu)}\ , \tag{4.15}$$

where

α = coefficient of expansion (1/°F)

E = Young's modulus (psia)

k = thermal conductivity (BTU/hr ft^2 °F-ft)

Q = volumetric heat rate (BTU/hr ft^3)

ν = Poisson's ratio

μ = attenuation coefficient (1/ft)

σ_T= a factor obtained from a curve of μ a vis b/a (Fig. 11.12, p. 653 (36))

S_T and S_m are functions of wall thickness. The maximum allowable stress was established as the sum of S_T and S_m. Solving Equations 4.14 and 4.15 simultaneously for wall thickness resulted in a required thickness of 4.5 inches.

This thickness is based upon a volumetric heat rate of (1.555) 10^4 BTU/hr ft^3 which was determined, assuming that the design heat rate was 1/0.488 that of the prototype. The full power heat rate of the prototype pressure vessel was given as 0.01 watts/gm (26).

Reactor Containment Vessel

The containment vessel of the 630A will be retained for this design. It is made of carbon steel, type SA-201-B (A300). It is 3.4 inches thick and is designed for a maximum pressure of 555 psia and a maximum temperature of 650 °F.

Moderator Circuit

The moderator circuit of the 630A will also be retained. The moderator is maintained at a temperature between 210 and 240 ^{o}F, at a pressure of 250 psia. The moderator flow rate for the 630A is 1,000 gpm and assuming the same flow per moderator tube for the new design, the moderator flowrate will increase to 1,165 gpm.

Waste Handling

A charcoal adsorption bed is employed in the waste-gas system of the 630A. This system will be incorporated into the new design. The system is designed to handle the working fluid in the event that the pressure vessel has to be bled. The gas will flow into the containment vessel, then pass through the adsorption bed.

Reactor Size and Weight

The bottom cover, boiler, circulator, and circulator shield will be removed from the 630A, reducing its height from 39.5 feet to about 24 feet. An inlet-outlet plenum will be put in their place. The plenum inlet and outlet ducting were designed for a Mach number of less than 0.2 and a Reynolds number of greater than 10^{6} to keep the frictional losses to a negligible amount. The plenum will add about five feet to the reactor length. A cross section

of the plenum is seen in Fig. 4.16. It was seen in the core sizing section that the active core was lengthened by two feet and one foot of BeO reflector was added to its ends. This brings the overall height of the new reactor to approximately 32 feet.

The active core radius was increased by 12 cm, the pressure vessel thickness was increased 4.5 cm and 10 cm was added to the outer shield thickness. The reactor diameter for the new design is therefore, 21.5 feet.

The total weight of the 630A is $(1.245)10^6$ pounds, not including the auxiliary equipment outside of the reactor containment. Subtracting the combined weights of the bottom cover, boiler, circulator and shield left 1,102,330 pounds. The weight of the active core section of the 630A is approximately 227,430 pounds. A weight of 874,900 pounds remained which was assumed to be that of the moderator, moderator system, control rods and actuator equipment. It was further assumed that this equipment weight would increase as the ratio of the number of control rods, or by 1.39.

The weight of the new reactor core section was determined to be approximately 369,600 pounds. The inlet-outlet plenum was assumed to weigh twice that of the bottom cover or 80,000 pounds. This gave a total reactor weight of 1,669,600 pounds or 745 long tons, as compared to 555 long tons for the 630A.

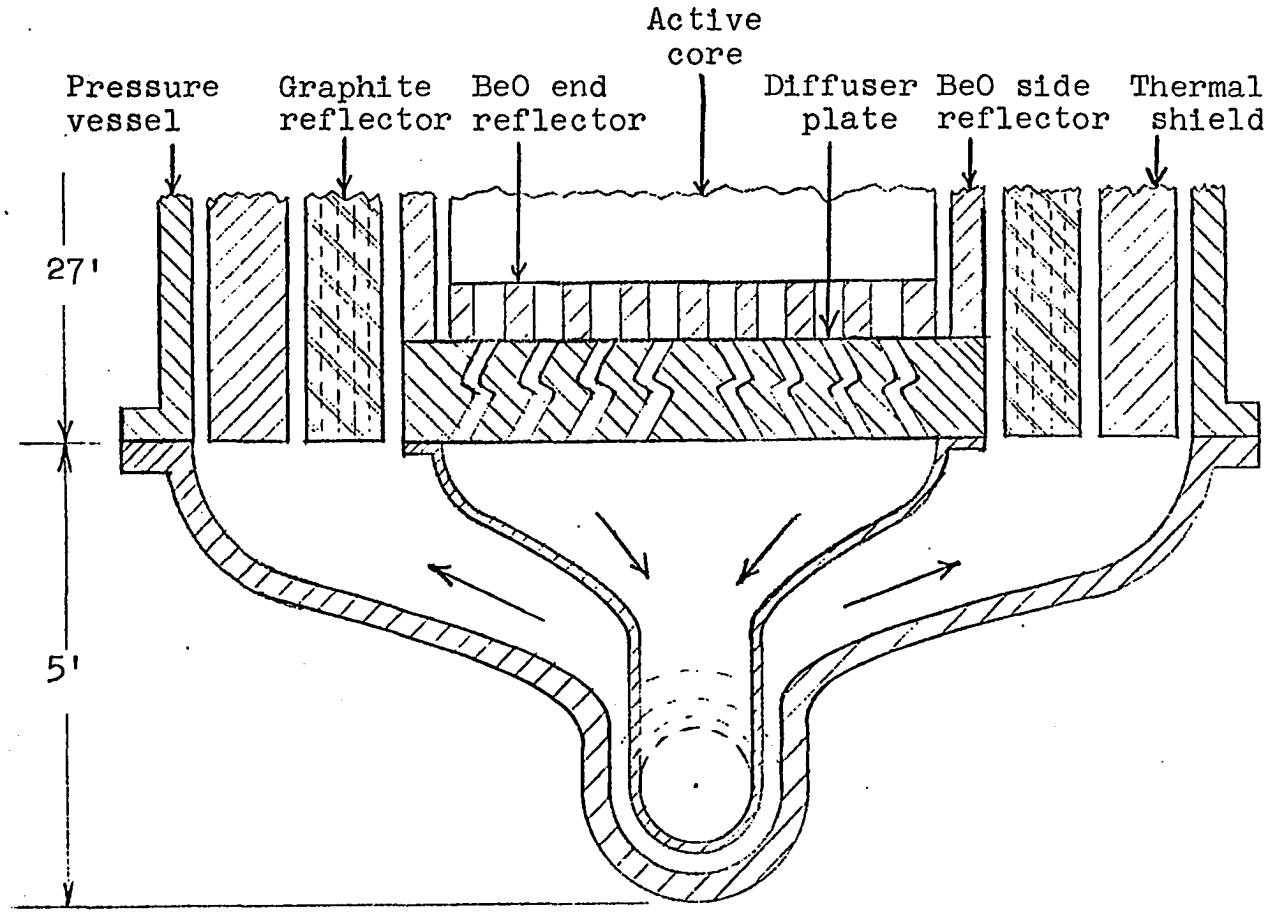

Fig. 4.16. Longitudinal cross section of the coolant inlet-outlet plenum.

The over-all dimensions for the reactor adopted for this design are 32 feet high and 20.5 feet in diameter. It weighs approximately 745 long tons and contains $(1.362)10^4$ pounds of UO2 enriched to 3.23%. It can operate at 106 MW for approximately 1815 days which amounts to a burnup of 31,100 MWD/MT.

CHAPTER V. FINAL CYCLE

To determine the final cycle parameters it is first necessary to establish the means by which the power is to be transmitted from the power turbine to the screw propeller. As mentioned in Chapter one, the gas turbine is unidirectional and in order to provide reversing capability for the propeller, one of three available methods must be employed; the electric drive, the reversing reduction gear or the controllable pitch propeller. These three methods were compared from the size, weight, cost and efficiency point of view.

Power Transmission Methods

Electric drive

The marine electric generators and motors are of two types; alternating and direct current. The D.C. motor offers better control but is larger and less efficient than a comparable A.C. motor. Typical motors in the 17,500 HP range, along with large capacity generators are compared in Table 5.1[1,2].

---

[1]Rowe, J. R., Large Motor and Generator Division, General Electric Company, Schenectady, New York. Marine motors and generators. Private communication. 13 January, 1966.

[2]Lory, M. R., Engineering Manager, Large Rotating Apparatus Division, Westinghouse Electric Company, East Pittsburgh, Pennsylvania. Marine motors and generators. Private communication. 10 December, 1965.

Table 5.1. Marine electric motor and generator data

Type	Rating	Length	Width	Height	Weight	Efficiency
D.C. motor	15,000 HP	28'	14'	18'	115 T	0.92
D.C. gen.	6,000 KW	24'	12'	14'	42 T	0.93
A.C. motor	15,000 HP	12'	20'	21'	67 T	0.975
A.C. gen.	11,500 KW	15'	6'	8'	29 T	0.975

Reversing reduction gears

There is a new reversing reduction gear being manufactured by the Falk Corporation which incorporates Airflex clutches. This unit is being designed for installation with an open cycle gas turbine[1](39). It has the following specifications:

Type: double-reduction; double helical; locked train.

Rating: 20,000 HP. Efficiency: 97%

Length: 16'; Width: 19'; Height: 18'; Weight: 111 Tons.

Controllable pitch propellers

A controllable pitch propeller can be designed to transmit 17,500 horsepower. One such design is 14 feet in diameter and weighs 11.6 tons[2]. It is four feet smaller and 12 tons lighter than the varying pitch propeller presently

---

[1]Dutton, E. B., Requirements Engineer, Pratt and Whitney Aircraft Company, East Hartford, Connecticut. Reversing reduction gears. Private communication. 18 July, 1966.

[2]Naulty, op. cit.

installed aboard the ROTTERDAM. A controllable pitch propeller is inherently less efficient and the one referred to above has an efficiency of 64% as compared to 71% for the one aboard the ROTTERDAM. To accomodate the control lines to the propeller, the tail shafting will have to be enlarged. This can be easily accomplished and the increase in shaft weight should not be excessive, at most double the existing weight or an increase of 7.5 tons. Regular marine reduction gears can be employed in conjunction with the controllable pitch propeller.

The varying pitch propeller operated at 134 RPM at 20 knots and the high pressure steam turbine operated at 4250 RPM for a reduction ratio of 31.7 to 1 with double reduction. The controllable pitch propeller operates at 240 RPM at 20 knots. Utilizing the same reduction ratio, a power turbine speed of 7500 RPM could be utilized which is well within the speed range of large gas turbines. It is felt that the reduction gears chosen for any specific power turbine speed would closely approximate the existing installation in size and weight, therefore, the existing reduction gears will be retained.

Comparison

To appraise each system properly a comparison on a unit horse power basis was carried out. The weight, volume and cost of the major components only were considered. The overall system efficiency, which accounts for the propeller

efficiency, was also compared. The investigation led to the results tabulated in Table 5.2.

Table 5.2. Comparison of power transmission methods

Type	Over-all efficiency	Tons/HP $x(10)^{-3}$	ft^3/HP	dollars/HP
D.C. drive	0.615	15.10	1.11	65.5
A.C. drive	0.674	6.80	0.70	41.5
Reversing reduction gears	0.680	7.65	0.312	Not Available
Controllable pitch propellers	0.615	5.65	0.231	29.0

The results show that the controllable pitch propeller is the most desirable in all categories except over-all efficiency. However, this system was chosen because it is felt that the volume, weight and cost advantages more than offset the low value of efficiency.

Cycle Parameters

The component pressure losses used in Chapter three are well within operating limits and so are the efficiencies of the compressor and turbine as varified by References 27 and 30. A total system pressure drop of 7.425%, along with a compressor efficiency of 88% and a turbine efficiency of 90%

were retained for the final cycle. Escher Wyss has improved recuperator effectiveness and values of 90% are possible (27). This value was incorporated in the final design.

The assumption made relative to the availability of cooling water to cool to an ambient of 60 ^{o}F was also retained. This would require a sea water temperature of about 48 ^{o}F which can be expected a great deal of the time. However, it is realized that as the cooling water temperature increases, so does the ambient temperature, with a resulting decrease in performance. However, this amounts to approximately one percent decrease in cycle efficiency for every ten degree increase in ambient temperature.

The 100 degree gas-to-steam temperature difference in the waste-heat boiler assumed for the preliminary studies was also retained.

Cycle study

Because the preliminary study indicated that the intercooled and regenerative cycle was the most efficient, it was investigated for the final cycle. The resulting cycle efficiencies and maximum degree of superheat are listed in Table 5.3 as functions of the pressure ratio.

The 324 degrees of superheat obtained at the pressure ratio of 2.0 is 24 degrees higher than that utilized on the ROTTERDAM for the turbo-generators. The higher the degree of superheat, the lower the steam rate. Based on the fact

Table 5.3. Intercooled and regenerative cycle efficiency and maximum degree of superheated steam

Pressure ratio	Cycle efficiency	Degree of superheat
2.0	29.6%	324
2.5	30.4%	221
3.0	30.3%	143
3.5	29.8%	83
4.0	29.2%	33

that there is only 0.8% difference in efficiency between that at the pressure ratio of 2.0 and that at the maximum efficiency, the pressure ratio of 2.0 will be utilized for the final design so as to take advantage of the higher degree of superheat.

Final Cycle

The final cycle for this design is seen in Fig. 5.1. To deliver 40,500 HP or its equivalent, $(2.86)10^4$ BTU/sec, a total mass flow rate of 144 #/sec was required.

Kinetic energy effects were ignored in the earlier cycle studies, but their effects were considered for the final design. Investigation of the low pressure compressor showed that the kinetic energy effects amounted to an enthalpy increase of one BTU/# if the inlet and outlet ducting areas were each one square foot. There was no

Fig. 5.1. Temperature Entropy diagram of the final cycle. Intercooled and regenerative with a compressor pressure ratio of 2.0.

State point properties

State point	Temperature (°R)	Pressure (psia)	Enthalpy (BTU/#)
1	520	500	-20.7
2	607	707	88.3
3	520	702	-20.7
4	607	993	88.3
5	1161	980	775.0
6	1710	973	1457.0
7	1537	722	1242.0
8	1357	525	993.0
9	1220	511	848.0
10	668	504	163.0

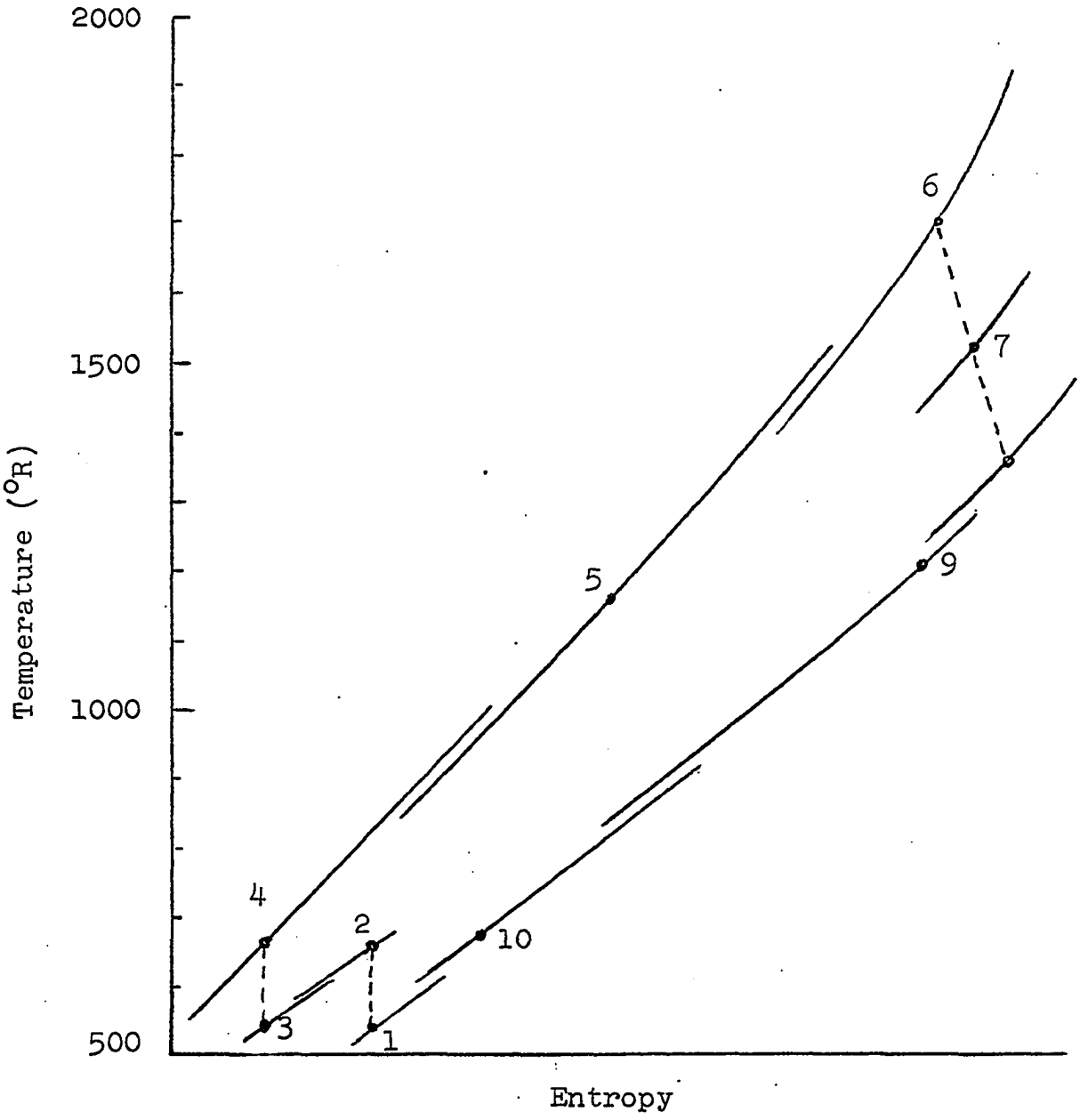
2000
1500
1000
500
Temperature (°R)
Entropy
1
2
3
4
5
6
7
9
10

increase in enthalpy across the compressor turbine (the high pressure turbine) if an inlet ducting area of one square foot was used along with an outlet ducting area of one and one half square feet. The pressure losses in the ducting will be low if the above ducting sizes are utilized because the Mach number is always less than 0.1 and, assuming smooth pipes, the Fanning friction factor is always less than 0.006 based on Reynolds number determination and the friction factor curves from Reference 23.

Energy Balance

The final cycle delivered $(2.56)10^4$ BTU/sec to the waste-heat boiler which produced 19.14 pounds of steam per second at 317 degrees of superheat. A boiler energy balance is seen in Fig. 5.2. The reactor supplied $(9.85)10^4$ BTU/sec and $(2.86)10^4$ BTU/sec were utilized for useful work. This gives rise to a cycle efficiency of 29.3% and a plant efficiency of 55%.

The final plant schematic, showing the helium system, is seen in Fig. 5.3. A schematic of the steam system is seen in Fig. 5.4. Only the major components are shown and no attempt was made to include pumps and associated auxiliary equipment.

Based on the new cycle state points, certain changes occurred which effected the heat transfer study conducted

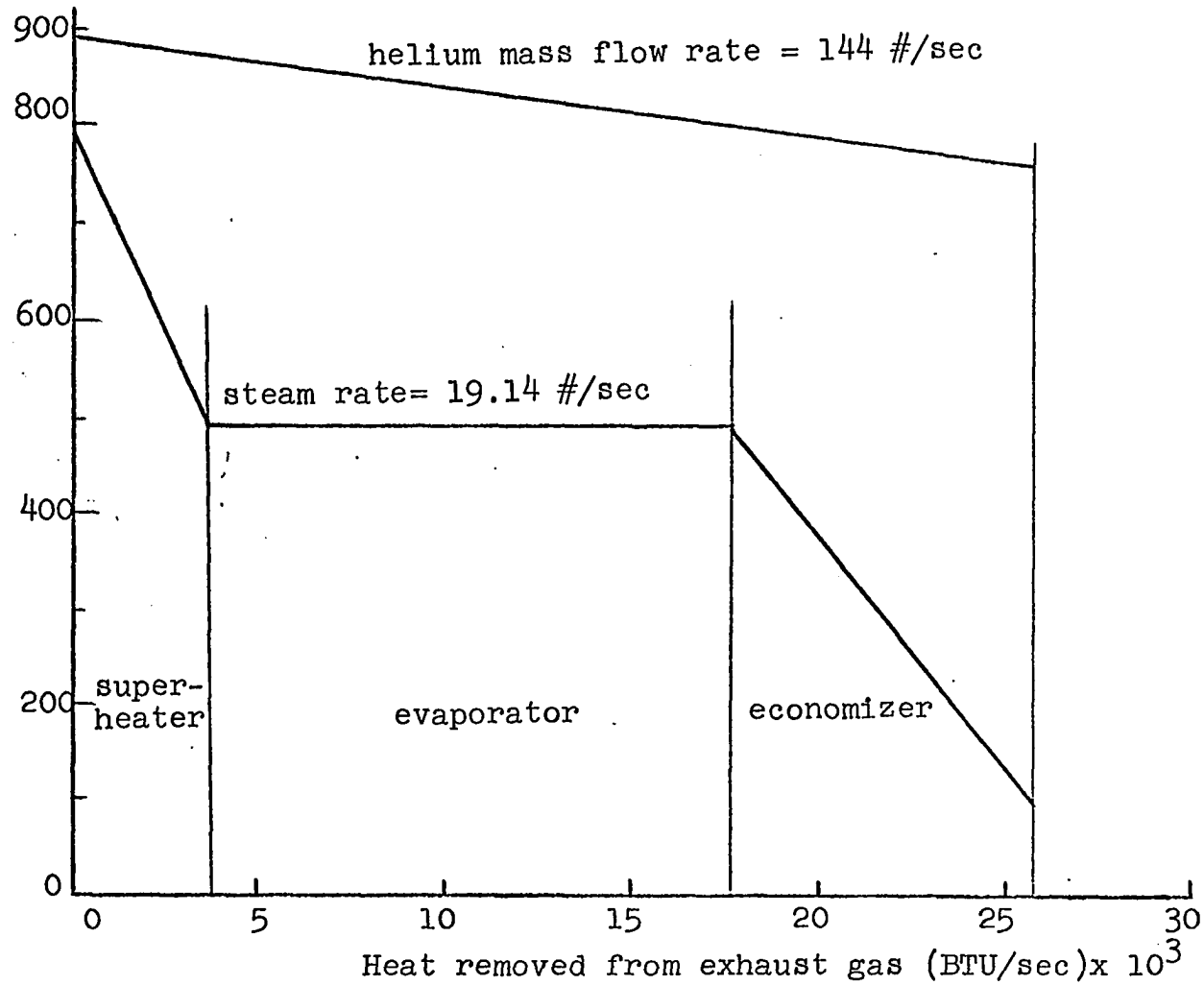

Fig. 5.2. Boiler energy balance.

Fig. 5.3. Helium flow schematic diagram with state points and transferred energy.

Legend

R = reactor
PC = precooler
IC = intercooler
B = waste-heat boiler
RC = recuperator
S = helium storage
LPC = low pressure compressor
HPC = high pressure compressor
HPT = high pressure turbine
PT = power turbine

$Q_r = (9.85)10^4$ BTU/sec
$Q_P = (1.32)10^4$ BTU/sec
$Q_I = (0.78)10^4$ BTU/sec
$Q_B = (2.56)10^4$ BTU/sec
$Q_{RC} = (9.82)10^4$ BTU/sec

State point	T (^{o}R)	P (psia)	h (BTU/#)	W_a (#/sec)
1	520	500	-20.7	72
2	607	707	88.3	72
3	520	702	-20.7	72
4	607	993	88.3	72
5	1161	980	715	72
6	1710	993	1457	144
7	1537	722	1242	72
8	1357	525	993	144
9	1220	511	848	144
10	668	504	163	72

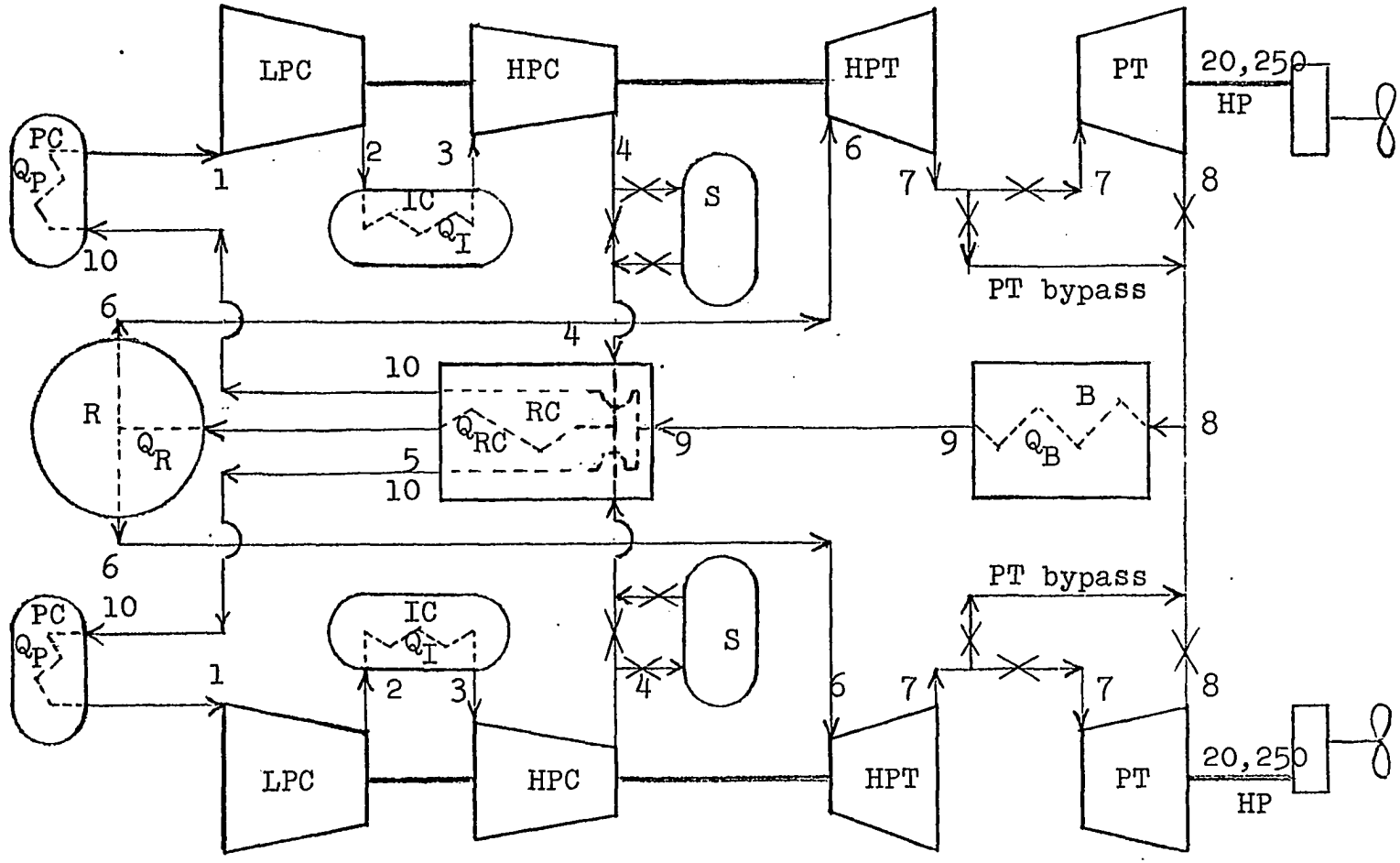
LPC
HPC
HPT
PT
20,250
HP
PC
Q_P
IC
Q_I
S
PT bypass
R
Q_R
RC
Q_{RC}
B
Q_B
1
2
3
4
5
6
7
8
9
10

Fig. 5.4. Steam flow schematic diagram with state points and flow rates.

State point	Temperature (°F)	Pressure (psia)	Enthalpy (BTU/#)	Flow rate (#/hr)
1	797	620	1405	46,500
2	750	620	1378	11,420
3	455	81	1258	11,000
4	226	5	1160	80
5	101	10	69	57,920
6	101	620	71	69,000
A	897	525	993	$(5.19)10^5$ # helium/hr
B	760	511	848	$(5.19)10^5$ # helium/hr

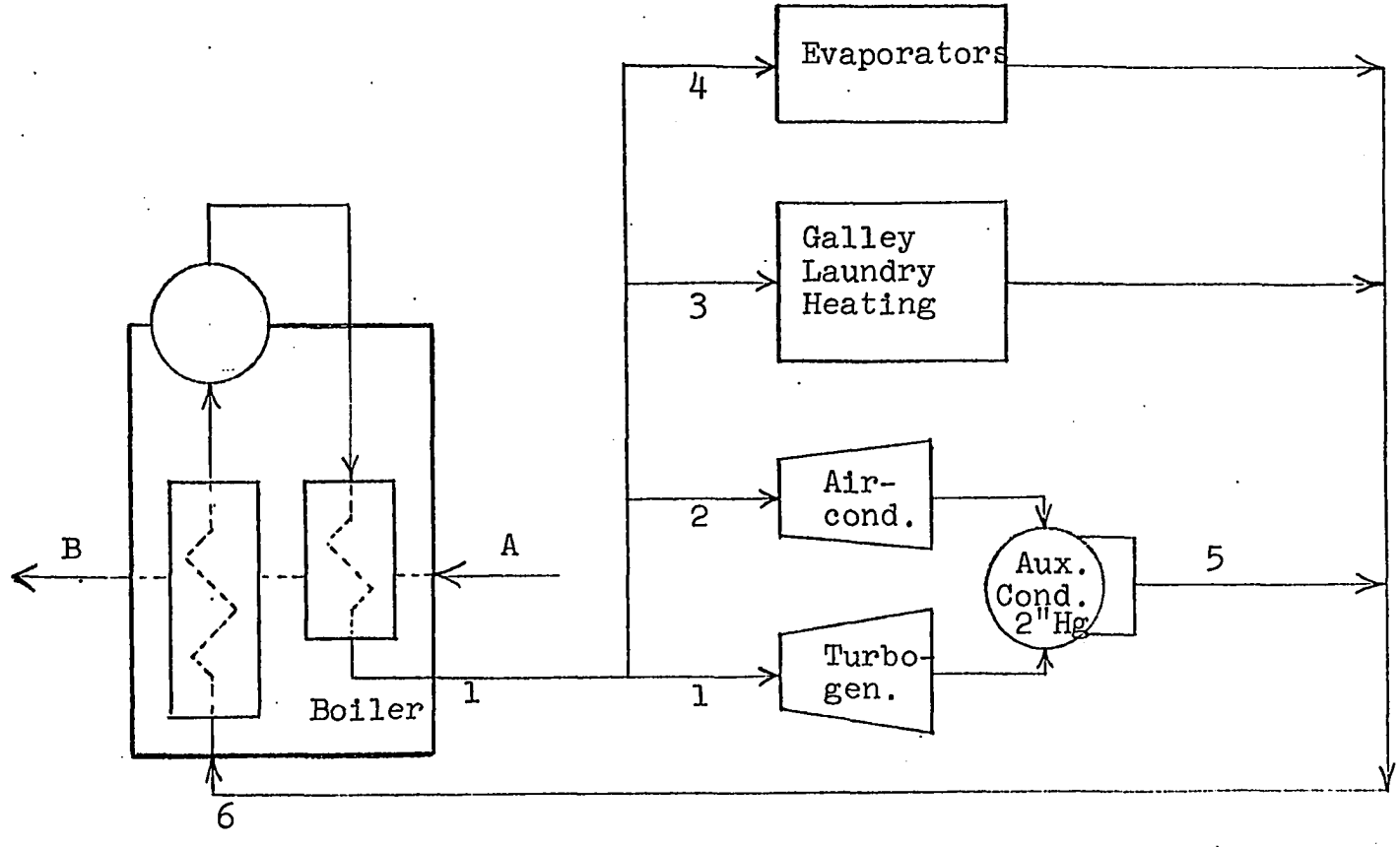
Evaporators
4
Galley
Laundry
Heating
3
Air-
cond.
2
Aux.
Cond.
2"Hg
5
Turbo-
gen.
1
1
B
A
Boiler
6

in Chapter four. The mass flow rate increased from 102 #/sec to 144 #/sec and the coolant inlet temperature increased from 458 °F to 701 °F. Both effect the coolant temperature difference, $t_m - t_{og}$, of Equation 4.1. The new expression becomes

$$t_m - 701 = (282)(1 - \cos \frac{\pi x}{L}) \qquad (5.1)$$

For the cladding surface temperature, with the new inlet surface temperature equaling 975 °F, Equation 4.7 becomes

$$t_s - 975 = 282(1 - \cos \frac{\pi x}{L}) + \frac{(1.41)10^5}{h_x} \sin \frac{\pi x}{L} \qquad (5.2)$$

The fuel centerline temperature can still be expressed as

$$t_f = t_s + 172 \qquad (5.3)$$

These changes brought about an increase in both the cladding surface and the core centerline temperatures. The maximum cladding surface temperature increased from 1643 °F to 1676 °F and the maximum core centerline temperature increased from 1822 °F to 1848 °F. These are not substantial increases and do not adversely affect the design.

CHAPTER VI. MACHINERY SELECTION AND PLANT ARRANGEMENT

Turbo-machines

The Escher Wyss company of Zurich, Switzerland has made many studies involving closed helium cycles. The turbines and compressors utilized for this design incorporated the Escher Wyss machines.

Size

Figure 12 on page eight of Reference 30 describes the turbo-machines for a 25-MW closed cycle helium plant. Twenty-five stages of compression are employed to attain a pressure ratio of 3.0. This amounts to a pressure ratio of 1.045 per stage. A pressure ratio of 2.0 is used for this design and assuming the same pressure ratio per stage, 17 stages will be required. The prototype unit has a nine stage low pressure compressor and an eight stage high pressure compressor, therefore, these units were incorporated into this design.

Eight stages of expansion are employed in the prototype for an expansion ratio of 2.4. This amounts to an expansion ratio of 1.156 per stage. The design expansion ratio for the compressor turbine is 1.34 and that for the power turbine is 1.38. Each turbine will require three stages assuming the same expansion ratio per stage as the prototype.

On a work-per-stage basis, the prototype delivers seven

megawatts per stage. The design compressor turbine delivers 15.9 MW and the power turbine delivers 15.0 MW. Three stages per turbine are, therefore, adequate. The maximum diameter for the whole turbo-compressor unit is six and one half feet and its length is thirty feet.

Weight

No specific information of the weight of the prototype machine is available, however, helium industrial gas turbine units generally weigh in the neighborhood of 5.3 #/HP[1]. This value will be used in this design and the resulting turbo-machine weight is 42.2 long tons.

Cost

Once again no specific cost information is available on the prototype machines, however estimates from industry are approximately 1.2 million dollars per unit[2].

Heat Exchangers

Size

Escher Wyss has also done extensive work in heat exchanger design for helium. Heat exchangers from a 60 MW

---

[1]Gentile, R. W., Engineer, Gas Turbine Department, General Electric Company, Schenectady, New York. Industrial gas turbines. Private communication. 13 June, 1967.

[2]Gentile, R. W., Engineer, Gas Turbine Department, General Electric Company, Schenectady, New York. Industrial gas turbines. Private communication. 21 June, 1967.

closed cycle plant will be used as the prototype for this design. These units are described on page 42 of Reference 27. A comparison of heat energy transferred and helium mass flow between the prototype and this design is seen in Table 6.1.

Table 6.1. Prototype and design heat transfer and mass flow rates

Component	Prototype		Design	
	heat transferred (BTU/hr)	mass flow (#/sec)	heat transferred (BTU/hr)	mass flow (#/sec)
Precooler	$(27.2)10^7$	305	$(4.80)10^7$	72
Intercooler	$(16.4)10^7$	305	$(2.84)10^7$	72
Recuperator	$(77.2)10^7$	305	$(35.4)10^7$	144

For heat exchanger heat transfer the total heat energy transferred is equal to

$$Q_T = U\ A\ \Delta t_{lm} \tag{5.1a}$$

where:

U = the over-all heat transfer coefficient for bare tubes based on the outside diameter.

$$U = \frac{1}{\frac{r_3}{r_2 h_{12}} + \frac{r_3 \ln(r_3/r_2)}{k_{23}} + \frac{1}{h_{34}}} \tag{5.1b}$$

A = the total outside tube surface area.

Δt_{lm} = the log mean temperature difference.

$$\Delta t_{lm} = \frac{\Delta t_{in} - \Delta t_{out}}{\ln\ (\Delta t_{in}/\Delta t_{out})} \tag{5.1c}$$

The heat transfer coefficient is a function of the inside and outside tube radii, the tube thermal conductivity and the inside and outside film coefficients. The tube diameter and material were held constant, therefore, the overall heat transfer coefficient is only a function of the film coefficient.

The film coefficient is defined by Equation 3.3 and is a function of thermal conductivity, tube diameter, Reynolds number and Prandtl number.

The thermal conductivity, and the Prandtl number, are both functions of type of gas, which is the same in both cases. They do vary with temperature and pressure, however. A comparison of the gas temperatures and pressures in the various components for the prototype and design conditions is seen in Table 6.2.

Table 6.2. Gas temperature and pressure for the prototype and design heat exchanger components

Component		Temperature (°F)		Pressure (atm)	
		prototype	design	prototype	design
Precooler	(in)	300	210	25	34
	(out)	100	60	25	34
Intercooler	(in)	220	140	39	47
	(out)	100	60	39	47
Recuperator high pressure	(in)	220	140	60	65
	(out)	815	700	60	65

Table 6.2 (Continued)

Component		Temperature (°F) prototype	Temperature (°F) design	Pressure (atm) prototype	Pressure (atm) design
Recuperator low pressure	(in)	880	760	25	34
	(out)	300	210	25	34

It is apparent that there are no large differences in temperature or pressure at any common point and therefore, it was assumed that the thermal properties are essentially the same in both situations and so is the Prandtl number. In addition, the tube diameter was considered to be the same in each case. For the film coefficients to remain constant, the Reynolds numbers must be equal. Reynolds number is expressed as

$$Re = v\, D \frac{\rho}{\mu} \tag{5.2a}$$

where

$$\rho = \frac{P}{WRT}\,, \tag{5.2b}$$

and

$$v = \frac{V}{A} = \frac{WRT}{PA}\,, \tag{5.2c}$$

therefore

$$Re = \text{constant } (\tfrac{1}{A})\,. \tag{5.3}$$

The film coefficient can be expressed as the product of the Reynolds number and a constant K_1 and utilizing Equation 5.3, h_c becomes

$$h_c = K_1 \text{ constant } (\tfrac{1}{A}) = k_2\ (\tfrac{1}{A}), \tag{5.4}$$

where K_2 is a new constant and A is the flow cross sectional area. For the flow areas to remain equal, the heat exchanger diameters will be kept constant. This then, will insure that the overall heat transfer coefficient will be the same in both the prototype and design cases.

When considering the log mean temperature difference, it is necessary to make an assumption regarding the temperature rise of the cooling water in the precooler and intercooler. For this comparison a coolant water temperature rise of 15 degrees will be assumed. Based on this and the data in Table 6.2, total surface areas can be compared as functions of total heat energy transferred and log mean temperature difference utilizing Equation 5.1a. The results of this comparison are seen in Table 6.3, remembering that the surface area is equal to πDL and D is being held constant, therefore, the length of the design heat exchangers can be found by establishing ratios of prototype to design lengths. This comparison was made and the results are seen in Table 6.4.

Table 6.3. Prototype and design heat exchanger surface areas

Component	Prototype ($A_p = Q_T/\Delta t_{lm}$)	Design ($A_d = Q_T/\Delta t_{lm}$)
Precooler	$(2.93)10^6$	$(0.92)10^6$
Intercooler	$(2.34)10^6$	$(0.81)10^6$
Recuperator	$(10.7)10^6$	$(5.2)10^6$

Table 6.4. Surface area ratios and prototype and design heat exchanger lengths and diameters

Component	Area ratio	Prototype length (ft)	Design length (ft)	Prototype diameter (ft)	Design diameter (ft)
Precooler	0.620	19.5	6.0	10	10
Intercooler	0.684	13.0	4.5	10	10
Recuperator	0.485	49.0	24.0	6.5	6.5

Weight

Information concerning weights of the specific components of the Escher Wyss design is lacking, however, approximate component weights were obtained from a study carried out by the General Electric Company on gas turbine power plants for ship propulsion (40). Resulting component weights were:

Precooler 15.5 long tons

Intercooler 12.0 long tons

Recuperator 208.0 long tons

Cost

Once again specific cost information for the Escher Wyss components is lacking but approximate heat exchanger costs were obtained from the General Electric study mentioned above. This estimate amounted to 1.492 million dollars for two precoolers, two intercoolers and one recuperator.

Waste-heat boiler

The waste-heat boiler is a sectional boiler manufactured by AMF Beaird Incorporated (41). The boiler has water walls and finned tubes placed horizontal and normal to the gas flow. To meet the demands of $(6.9)10^4$ pounds of steam per hour at 620 psia and 300 degrees of superheat, a boiler 12 feet wide, 10 feet high and 27 feet long was required. This unit also required a five foot diameter steam drum. It weighs 111 long tons and has an approximate cost of $350,000[1].

Inport boiler

The inport boiler is a typical marine auxiliary, oil-fired boiler of the water tube type. It was designed to produce 75% of the normal steam load at the design conditions, or $(5.2)10^4$ #/hr. Its estimated size is 10 feet wide, 10 feet high and 15 feet long. Its estimated weight is 60 long tons and its estimated cost is $250,000[1].

Plant Arrangement

Machinery

The machinery space is 65 feet long, has an average width of 85 feet at the 44 foot waterline and 66 feet at the 12 foot waterline, and has a height of 34 feet. To obtain the maximum available space, the reduction gears were moved

---

[1]Clay, op. cit.

aft 16 feet and the thrust bearings were located in the after compartment. The location of the turbo-machines was dictated by the shaft line and the reduction gear pinion. Because the recuperator and the waste-heat boiler are about the same length and because the latter feeds the former, they were placed one above the other, fore and aft, along the centerline where maximum vertical clearance was available

The inport boiler was located just forward of the waste-heat boiler to minimize steam piping and the precooler and intercooler were located adjacent to each other to simplify and reduce cooling water piping.

A balanced plant layout resulted with the gas piping reduced to a minimum. The machinery arrangement is seen in Figs. 6.1, 6.2, and 6.3. The scale in each case is one inch equals ten feet.

There is adequate space within the compartment to accommodate all auxiliary equipment. The helium storage tanks, although not shown, can be placed outboard of the turbo-machinery with no difficulty.

Reactor

A side elevation of the reactor compartment is seen in Fig. 4.14. The reactor is centrally located within the compartment. Longitudinal collision bulkheads are not shown but would amount to a thickness of approximately five feet of laminated concrete, steel and wood, if the SAVANNAH design

Fig. 6.1. Machinery compartment. Looking forward from frame 48, on the starboard side.

Legend

A Power turbine
E Intercooler
F Precooler
G Recuperator
H Waste-heat boiler
J Inport boiler
→ gas flow

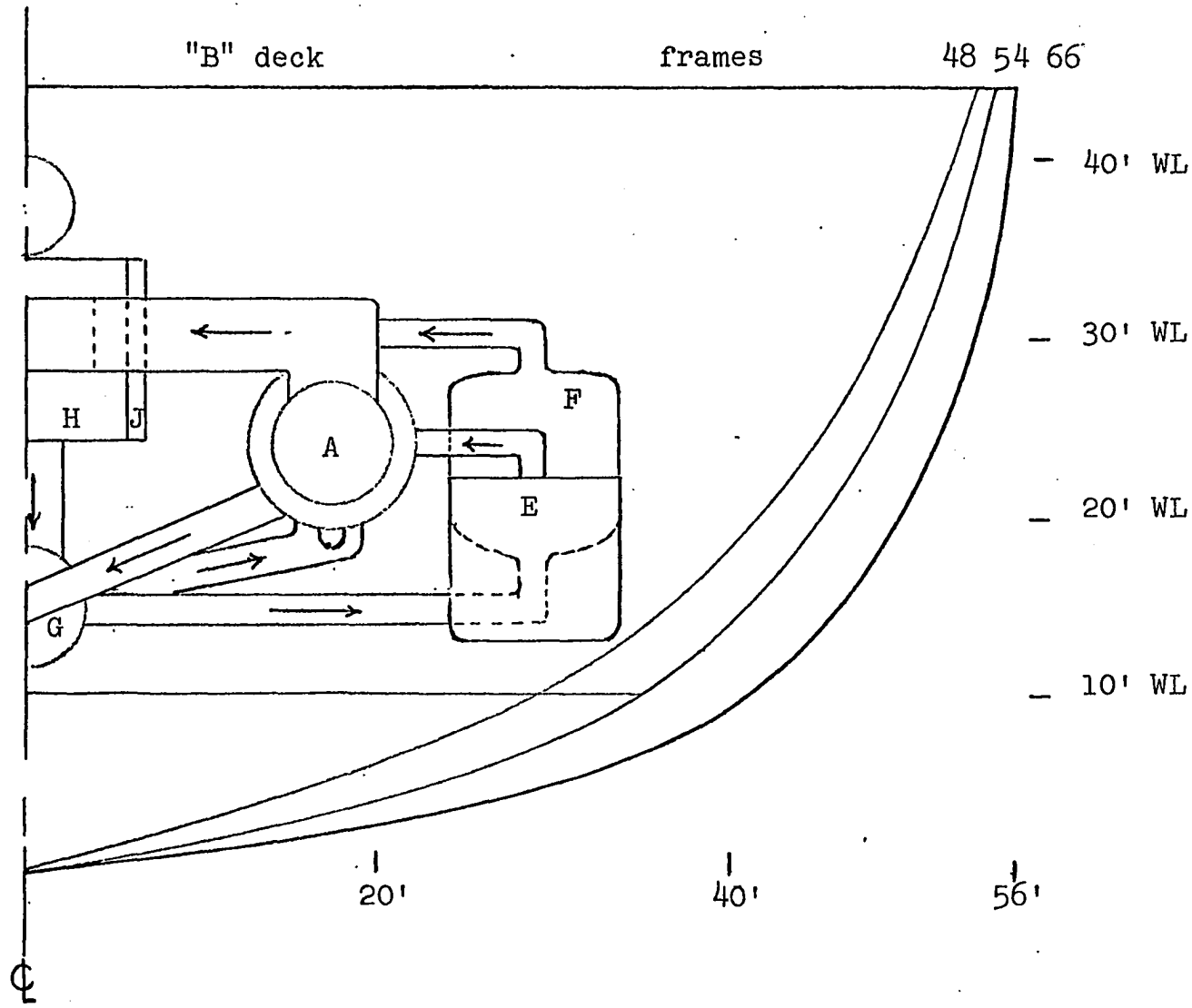
"B" deck
frames
48 54 66
40' WL
30' WL
20' WL
10' WL
H
J
A
F
E
G
20'
40'
56'
℄

Fig. 6.2. Machinery compartment. Half breadth plan.

Legend

A Power turbine
B Compressor turbine
C High pressure compressor
D Low pressure compressor
E Intercooler
F Precooler
G Recuperator
H Waste-heat boiler
I Reduction gears
J Inport boiler
→ gas flow

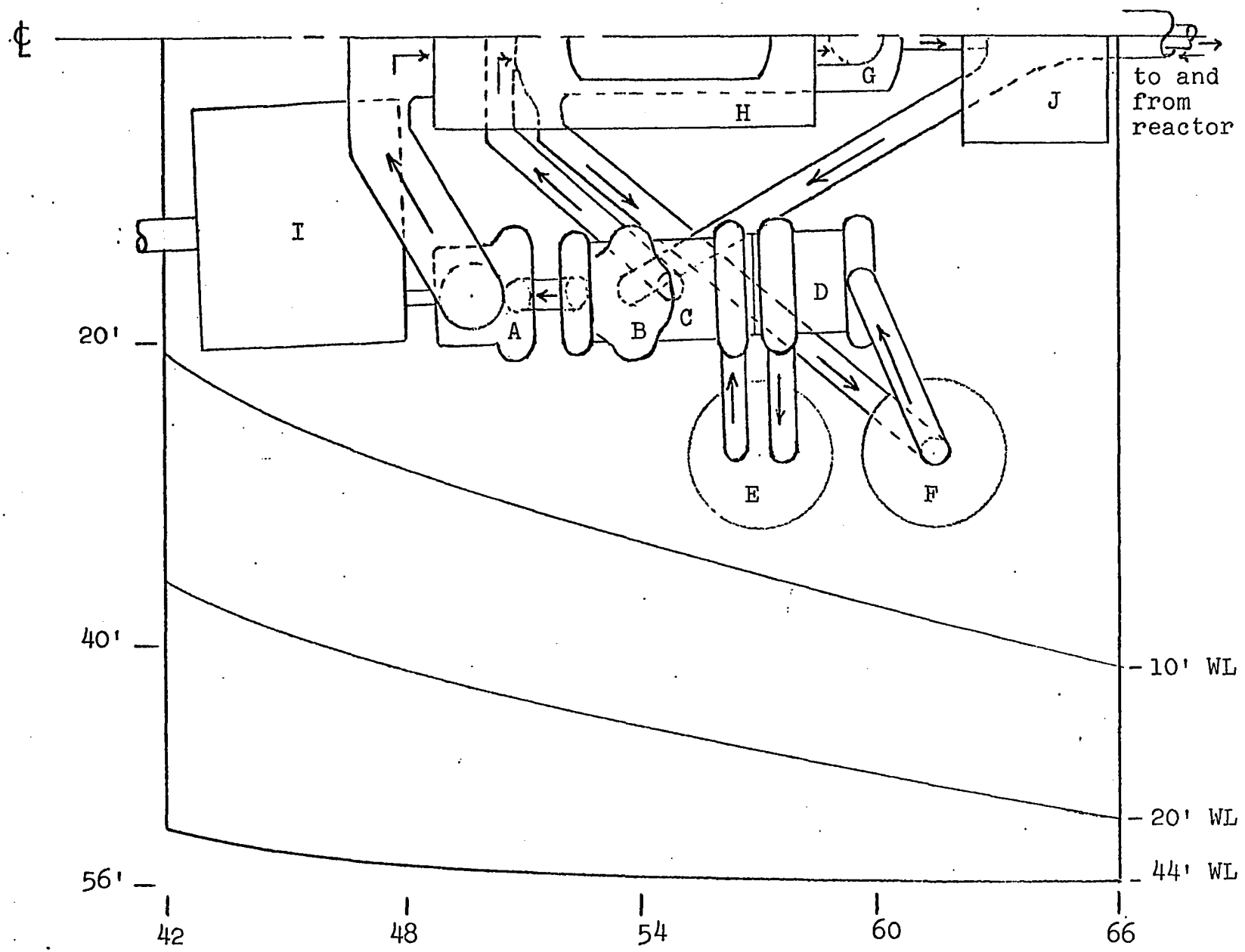
℄
I
A
B
C
D
E
F
G
H
J
to and from reactor
20'
40'
56'
10' WL
20' WL
44' WL
42
48
54
60
66

Fig. 6.3. Machinery compartment. Shear plan.

Legend

A Power turbine
B Compressor turbine
C High pressure turbine
D Low pressure turbine
E Intercooler
F Precooler
G Recuperator
H Waste-heat boiler
I Reduction gears
J Inport boiler
→ gas flow

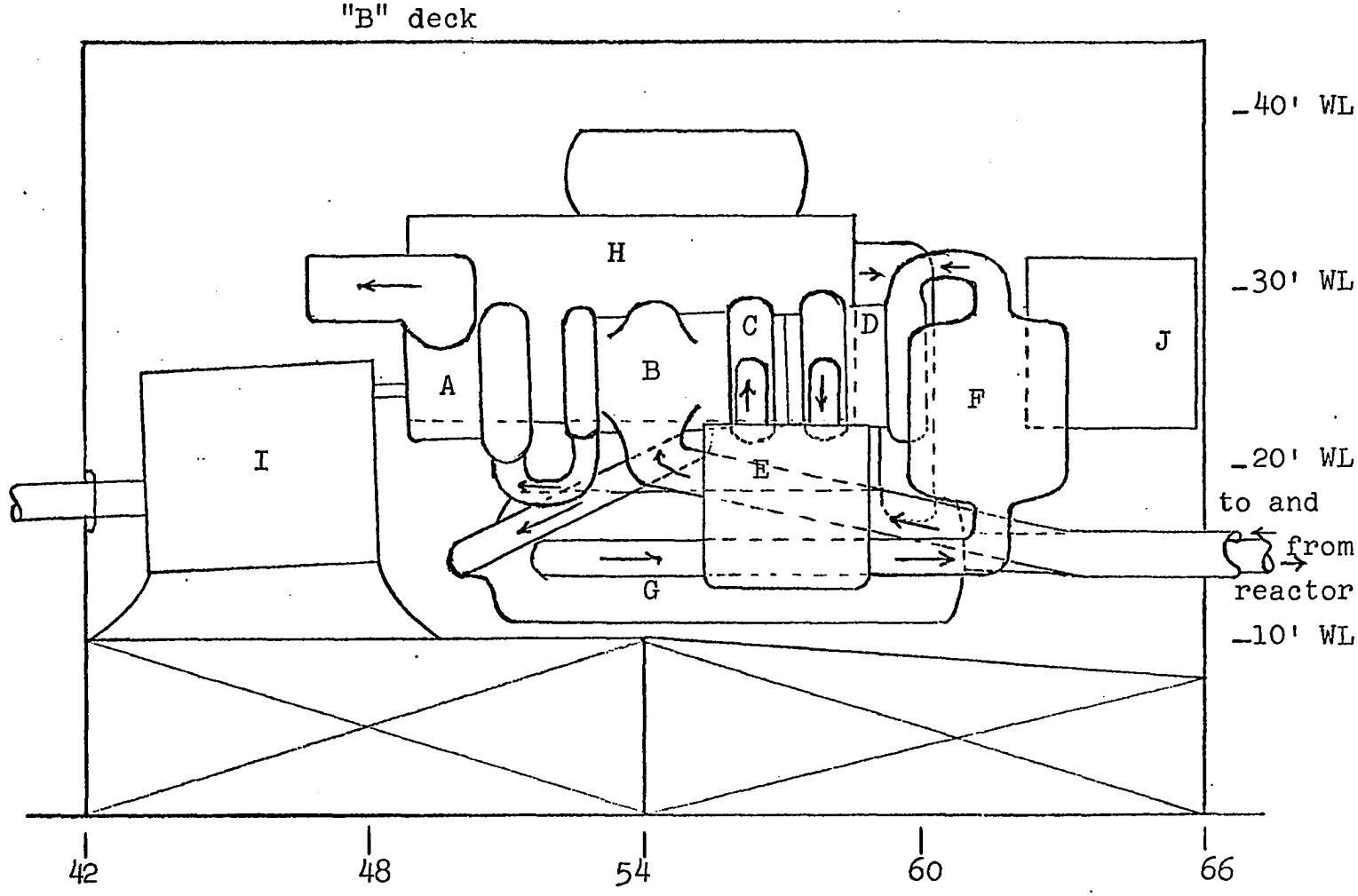
"B" deck
-40' WL
-30' WL
-20' WL
-10' WL
to and from reactor
H
A
B
C
D
E
F
G
I
J
42
48
54
60
66

is followed. A collision bulkhead to protect the 630A was designed by the marine consultant firm of George G. Sharp. Its weight was estimated to be 102 long tons and this value will be used in this design.

With a reactor diameter of 21.5 feet and allowing ten feet for the collision bulkheads, there is still approximately 70 feet of compartment width at the 20 foot waterline that is available for the location of the associated reactor auxiliary equipment.

Statical Stability

The initial condition of the ship was with the draft forward equal to the draft aft at nine meters, corresponding to a displacement of 31,037 metric tons in salt water. The height of the center of gravity above the keel was 11.25 meters in this fully loaded condition, and the height of the metacenter above the keel was 12.49 meters resulting in a metacentric height of 1.24 meters.

Removing the boilers, turbines, condensers, propellers, tail shafting and 3,400 metric tons of fuel amounted to a total weight removal of 4,148 metric tons. This weight resulted in a vertical moment about the keel of 13,346 meter-tons and a trimming moment, about the center of flotation, of 20,318 meter-tons, by the bow. Adding the reactor, turbo-machines, heat exchangers, waste-heat and

auxiliary boilers, collision bulkhead, propellers and tail shafting amounted to an added weight of 1,425 metric tons. This weight addition resulted in a vertical moment about the keel of 8,793 meter-tons and a trimming moment about the center of flotation of 55,480 meter-tons, by the stern. The trimming moment caused by the movement of the reduction gears aft 16 feet produced an additional moment of 760 meter-tons, by the stern.

The weight changes brought about a final displacement of 28,314 metric tons, a draft forward of 7.90 meters, a draft aft of 8.75 meters and a trimmed condition of 0.85 meters by the stern. The final height of the center of gravity above the keel was 12.20 meters which resulted in a metacentric height of 0.427 meters.

The ship's trim can be corrected by filling the forward three fuel tanks. This would add 1,137.5 metric tons to the ship's displacement but increase the metacentric height to 0.96 meters.

CHAPTER VII. PLANT SIZE, WEIGHT, COST AND EFFICIENCY COMPARISONS

In this chapter the power plant of the prototype ship and that of this design will be compared considering size, weight, cost, operating costs and efficiency. For this particular study only those items that were replaced will be considered. All other machinery is common to both the prototype and the design and can, therefore, be ignored here.

The primary source of information of the cost values for the conventionally powered ship was the Atomic Energy Commission's report, "Economics of Nuclear and Conventional Merchant Ships" (2). In this report the passenger ship class is broken down into two types based upon speed and size. The pertinent data for the type of ship most closely approximating that of the ROTTERDAM are listed in Table 7.1 along with comparable data for the ROTTERDAM.

Table 7.1. Comparison between economic prototype and ROTTERDAM

Item	Prototype	ROTTERDAM
Length between perpendiculars	750 ft	748 ft
Molded beam	100 ft	112 ft
Molded draft	34.5 ft	30 ft
Debth (to strength deck)	75 ft	76 ft
Block coefficient	0.54	0.434
Machinery weight (total) (boilers, turbines, condensers, reduction gears)	1,341 tons	892 tons
Displacement	39,632 tons	31,048 tons
Number of passengers	1,115	1,456

Table 7.1 (Continued)

Item	Prototype	ROTTERDAM
Normal shaft horsepower	31,400 HP	35,000 HP
Sustained speed	21.9 kts	20.5 kts
Speed/length ratio	0.80	0.75
Fuel consumption	0.3219 Ton/mi	0.48 Ton/mi
Machinery cost	$6,500,000	------

The economic study was conducted in 1957 with projected values to 1965 and 1970. Interpolation of the data was carried out to obtain 1967 values wherever applicable. The sizes and weights of the prototype machinery aboard the ROTTERDAM are known but their costs are not and many assumptions had to be made. It is with this in mind that the comparisons in this chapter are made.

Machinery Size Comparison

The equipment for the nuclear plant was placed in the existing machinery spaces aboard the ROTTERDAM. Each of the four boilers occupying the boiler room has a deck area of 375 square feet and a volume of 9,400 cubic feet. In the new design this space is occupied solely by the reactor which requires 365 square feet of deck area and has a volume of 11,500 cubic feet. This amounts to one fourth the deck area and one third the volume. However, space will be utilized by the longitudinal collision bulkheads. Based on

the Savannah design, these bulkheads should be approximately five feet thick, which will still provide a 25 foot wide space outboard of the reactor, at the ten foot waterline, or an area of 1,150 square feet, both port and starboard, for the auxiliary equipment.

The equipment that was replaced in the turbine room was the steam turbines, condensers and all the auxiliary piping and associated pumps. The steam turbines occupied an area of approximately 420 square feet each and the condensers each occupied an area of 230 square feet.

All of the propulsion machinery and the boilers of the new design were placed in this compartment, as was seen in Chapter VI with considerable room to spare outboard of the coolers. It is anticipated that this space will be occupied by all the necessary auxiliary equipment and the helium storage tanks. A summary of the machinery sizes is given in Table 7.2.

This comparison shows that the main propulsion machinery of the new design occupies approximately 754 square feet less deck area and 31,566 cubic feet less volume than the main propulsion machinery aboard the ROTTERDAM.

Table 7.2. Machinery size comparisons

ROTTERDAM

Item	Length (ft)	Width (ft)	Height (ft)	Number	Total area (ft^2)	Total volume (ft^3)
Boiler	25	15	25	4	1,500	37,550
Steam turbines	19	22	10	2	840	8,400
Condenser	19	12	11	2	456	5,000
			Totals		2,796	50,950

Design

Item	Diameter (ft)	Length (ft)	Number	Total area (ft^2)	Total volume (ft^3)
Reactor	21.5	32	1	365	11,650
Gas turbines	6.5	30	2	390	1,980
Recuperator	6.5	24	1	156	780
Precoolers	10	6	2	35.6	214
Intercoolers	10	4.5	2	35.6	160

Item	Length (ft)	Width (ft)	Height (ft)	Number	Total area (ft^2)	Total volume (ft^3)
Waste-heat boiler	26	12	10	1	310	3,100
Inport boiler	15	10	10	1	150	1,500
			Totals		2,042	19,384

Machinery Weight Comparison

The weights of the ROTTERDAM machinery that were replaced, as well as the weights of the design machinery are tabulated in Table 7.3.

Table 7.3. Machinery weight comparison

ROTTERDAM			Design		
Item	Number	Total weight (tons)	Item	Number	Total weight (tons)
Boiler	4	540	Reactor	1	745
Turbine	2	108	Turbine	2	84
Condenser	2	84	Precooler	2	31
Propeller	2	47	Recuperator	1	208
Tail shaft	2	15	Intercooler	2	24
Fuel		3,400	Waste-heat boiler	1	111
	Totals	4,194	Inport boiler	1	60
			Propeller	2	23
			Tail shaft	2	30
			Collision Bulkhead	2	102
			Totals		1,418

The fuel and the collision bulkheads must be considered in this comparison because they both contribute to the total displacement of the ship. This comparison shows a reduction in main propulsion machinery weight of approximately 2,776

long tons incorporating the new design.

Machinery Cost Comparison

To obtain the cost estimates of the equipment removed from the ROTTERDAM, the data presented on the study prototype listed in Table 7.1 can be utilized. The total cost of the machinery was 6.5 million dollars and the total machinery weight was 1,351 tons. This amounts to $4,800 per ton of machinery, and it is on this value that the ROTTERDAM machinery cost is based. The weight of the machinery removed from the ROTTERDAM was 794 tons which amounts to a cost of 3.81 million dollars.

The cost of the items used in this design are listed below, in millions of dollars:

Reactor (1)	3.10
Turbine (2)	2.20
Intercooler (2), precooler (2), and recuperator (1)	1.49
Waste-heat boiler (1)	0.35
Inport boiler (1)	0.25
Controllable pitch propeller	0.36
Total	7.75

The reactor cost is based on the cost of the first twenty units and was obtained from Table 3.1 of Gemp-326 (42). The cost values of the turbines were taken from Gentile[1]

[1]Gentile, op. cit.

and those for the heat exchangers were taken from (40). The costs for the boilers were obtained from Clay[1] and those for the controllable pitch propeller from Naulty[2].

The difference in main propulsion machinery costs, namely 3.94 million dollars, affects the capital cost of the ships and for this comparison, it will be assumed that this is the only capital cost item that is different between the prototype and the design. The one major item not included is the installation cost which is not readily available. This, then, gives rise to a capital cost for the prototype of 57.7 million and 61.6 million dollars for the design ship.

Operating Costs

The operating costs, as defined here, will include fixed costs, fuel costs, and depreciation and interest costs.

Fixed costs

The fixed costs are listed in Table 7.4 on a daily basis and all values are for 1967.

Based on the information in Table 7.4, the annual fixed costs are 17.6 million dollars for the conventional ship and 18.75 million for the nuclear ship.

---

[1] Clay, op. cit.

[2] Naulty, op. cit.

Table 7.4. Daily fixed costs comparison between conventional and nuclear ship

Item	Conventional	Nuclear
Wages	21,360	21,695
Subsistance	6,355	6,355
Stores, supplies, equipment	1,420	1,420
Maintenance and repairs	2,130	2,130
Insurance	2,980	3,811
Miscellaneous ship expenses	250	250
Amortization	13,825	15,780
Totals	48,324	51,441

Depreciation and interest cost

The depreciation and interest cost for the conventional ship is determined by assuming 9.5% of the capital costs and 10% of the capital costs for the nuclear ship. This cost amounts to 5.48 million dollars per year in the case of the conventional ship and 6.16 million dollars in the case of the nuclear ship.

Fuel cost

The round trip, Holland-U.S.A.-Holland, was assumed to take 15 days; six days at sea, one and one half days in port, six days at sea, one and one half days in port.

Conventional fuel The cost for bunker "C" fuel oil was taken as $3.10 per barrel or $21.7 per metric ton. The fuel consumption is ten tons per hour at full speed and the ship is assumed to travel at full speed all of its operating time. Therefore, for the 24.35 round trips per year the fuel cost is 1.52 million dollars.

Nuclear fuel The nuclear fuel cost will be made up of the following charges: use; depletion; reprocessing; fabrication; and plutonium credit. The parameters used in this study are:

type of fuel	UO_2
average exposure	31,100 MWD/MT
gross power	106 MW
shaft horsepower	35,000 SHP
initial uranium loading	5,600 Kg
initial U235 loading	180 Kg
initial enrichment	3.23%
initial fuel cost	$280/Kg
discharge uranium 1 loading	5,044 Kg
discharge U235 loading	19.35 Kg
discharge enrichment	0.384%
discharge cost	$3/Kg
total burnup	556 Kg
plutonium concentration	0.6%
plutonium content	30.4 Kg

plutonium credit $10/gm

years of operation 6.27 yr

The nuclear fuel cost is broken down in Table 7.5. The sub-item costs were determined utilizing the methods and price schedules as outlined (43), and the cost of the fuel is from (44).

Table 7.5. Itemized nuclear fuel cost, 31,100 MWD/MT

Item	Sub-item	sub-total ($x10^3)	total ($x10^3)
Use			
	fabrication.	81.5	
	cooling, shipping, storage and processing.	0.3	
	annual.	35.7	
			117.5
Depletion			14,000.0
Reprocessing			
	reprocessing.	171.5	
	turnaround.	171.5	
	loss in processing.	2.2	
	reconversion.	19.2	
	shipping.	80.6	
			445.0
Fabrication			785.0
Plutonium credit			302.0
		final total	15,045.5

The annual nuclear fuel cost is 2.40 million dollars which is 58% higher than the 1.52 million for conventional fuel.

The annual operating costs are compared in Table 7.6.

Table 7.6. Comparison of annual operating costs with a burnup of 31,100 MWD/MT

Item	Conventional (millions)	Nuclear (millions)
Fixed costs	17.60	18.75
Depreciation and interest	5.48	6.16
Fuel	1.52	2.11
Totals	24.60	27.02

The annual operating costs for the nuclear ship are 2.42 million more or just 10% higher than those for the conventionally fueled ship. But if a plot is made of the final enrichment and plutonium content versus the number of days at full power, certain factors become evident. The plutonium content peaks and it may be possible to achieve a lower fuel cost if the core is not allowed to operate to complete depletion. Such a plot is seen in Fig. 7.1. The plutonium peaks at 1,340 days or 23,000 MWD/MT, which is 4.75 years of operation. The fuel cost is itemized in Table 7.7 and the parameters used in this study are the same as before with the exception of the final discharge conditions, which are listed below.

discharge uranium loading	5,181 Kg
discharge U235 loading	40.9 Kg

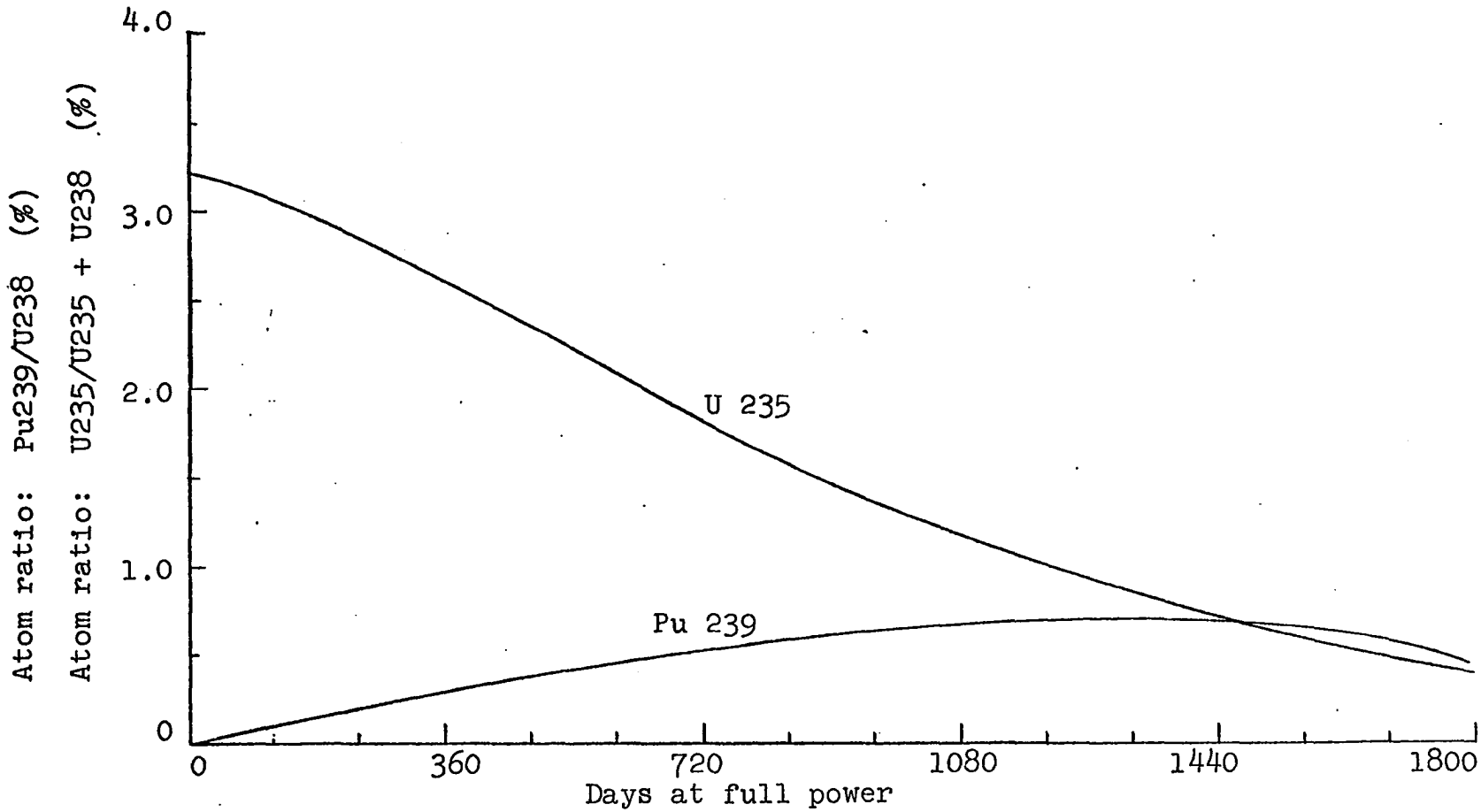

Fig. 7.1. Plotunium 239 and Uranium 235 content versus days at full power.

discharge enrichment	0.8%
discharge cost	30.5 $/Kg
total burnup	460 Kg
plutonium concentration	0.69 %
plutonium content	35.4 Kg
plutonium credit	10 $/gm
years of operation	4.75 yr

Table 7.7. Itemized nuclear fuel cost, 23,000 MWD/MT

Item	sub-items	sub-total ($x10^3)	total ($x10^3)
Use			
	fabrication.	75.0	
	cooling, shipping, storage and processing.	3.12	
	annual.	39.6	
			117.7
Depletion			4,600.0
Reprocessing			
	reprocessing	175.0	
	turnaround	175.0	
	loss in processing	4.6	
	reconversion	40.5	
	shipping	83.0	
			478.1
Fabrication			785.0
Plutonium credit			354.0
		final total	5,626.8

The annual nuclear fuel cost is 1.185 million dollars which is 22% less than the 1.52 million for conventional fuel.

It is now obvious that a more economical plant can be achieved if the core is not allowed to operate to depletion. With a 4.75 year life the annual operating expenses are 26.1 million dollars which is just 1.5 million or 6% more than that for the conventional ship.

Plant Efficiency

The estimated plant efficiency of the ROTTERDAM, as obtained from the Chief Engineer, is about 21% whereas it was seen in Chapter V that the plant efficiency for this design is 55%.

This study has revealed certain factors regarding the comparison of a conventional power plant with that of a direct cycle nuclear plant. The nuclear plant is considerably lighter, occupies less deck area and less compartment volume than a comparable oil-fired plant, however, it is more expensive and has a higher operating cost.

CHAPTER VIII. SUMMARY OF RESULTS

The maximum open cycle efficiency occurred at a pressure ratio of 5.0 for the intercooled and regenerative cycle, with the minimum total system pressure loss. Incorporating a waste-heat boiler reduced the cycle efficiency but it did lead to a higher over-all plant efficiency.

An air filtering system can effectively clean and dry the air of an open cycle but it is impractical to clean the radioactive effluent. No large-scale system has yet been developed. Scaling-up pilot plants leads to excessive size, weight and pressure drop.

The closed cycle is as efficient as the open cycle and it has some advantages over it. The ambient pressure can be increased giving rise to smaller equipment. It gives a flatter efficiency curve for large operating ranges. The working fluid best suitable for a closed nuclear cycle is helium.

The 630A nuclear steam generator can be redesigned to deliver 106 MW and it can be incorporated into the closed Brayton cycle. A fuel loading of $(1.362)10^4$ pounds of UO_2, enriched to 3.23% has a maximum operating life of 6.37 years and a burnup of 31,100 MWD/MT. The completely contained and shielded reactor is 32 feet high and 21.5 feet in diameter.

The final cycle incorporated into the design was the intercooled and regenerative cycle with a pressure ratio of

2.0. Its maximum efficiency is 29.5% which gives rise to a plant efficiency of 55%.

The turbo-machinery chosen was of the Escher Wyss design with 17 stages of compression and six stages of expansion for each unit. These units are 30 feet long and 6.5 feet in diameter. The heat exchangers are also of the Escher Wyss design.

The comparison between the conventional steam plant and the nuclear plant showed that the nuclear plant occupied 750 square feet less deck area and 31,566 cubic feet less volume. It also weighed 2,776 tons less. It did cost 3.94 million dollars more, however. The nuclear ship had an annual operating cost of 1.5 million dollars more than the conventional ship, but its fuel costs were 0.335 million dollars less each year.

CHAPTER IX. CONCLUSIONS AND RECOMMENDATIONS

Conclusions

The open cycle is not technically feasible at this time because the radioactive effluent cannot be controlled.

The closed cycle, with intercooling and regeneration, can give cycle efficiencies of upwards of 39% utilizing nitrogen and no waste-heat boiler. It is higher than a comparable steam plant.

The use of a waste-heat boiler can be utilized to advantage with the closed cycle, especially when large quantities of steam are required.

The closed, direct Brayton cycle plant is lighter and more compact than a comparable steam plant. This system can be employed for any horsepower, but when used in conjunction with a controllable pitch propeller the maximum shaft horsepower is limited to about 25,000 horsepower. Larger shaft horsepowers will require the use of a varying pitch propeller and electric drive.

Plant efficiencies of 55% and higher can be readily obtained with this system.

Present day machinery can be utilized for this type of system.

High burnup is possible with the 630A, however, in this study no consideration was given the higher isotopes of plutonium which have large absorption cross sections and

would tend to decrease the burnup. Also the burnup predicted may be possible from the nucelonics point of view, but the large quantity of fission products may prove very troublesome from the engineering point of view.

A smaller quantity of nuclear fuel could be utilized if the heat transfer limitations could be eliminated. The core was initially sized based upon the maximum heat flux and power density of the prototype. Raising these values would result in a smaller core. Also a higher core temperature would permit higher cycle temperatures with resulting higher cycle efficiencies.

The cost of nuclear fuel could be lowered if the final plotunium content and final fuel enrichment were optimized.

Better ship's stability could be obtained if the shaft line was lowered two feet, which is possible with the smaller diameter controllable pitch propeller. This would lower the center of gravity of the main propulsion machinery.

The use of the inport boiler could be eliminated by having an all-electric hotel service and utilizing shore ties when in port. However, this method would be more expensive.

Recommendations

It is recommended that further study be carried out on the direct, nuclear Brayton cycle and its many innovations. The knowledge gained from the high temperature gas-cooled

reactor program should be applied to the direct cycle. General Atomics Corporation has a 40 MWe reactor at Peach Bottom, New Jersey (45) that is a good example of the high temperature gas-cooled reactor. Gas temperatures of 1380 °F are predicted. The fuel elements have coated fuel dispersed in a highly impermeable graphite permitting high surface temperatures and good fission product retention.

The author is of the opinion that this system is technically feasible and should be employed in a large passenger ship.

CHAPTER X. LITERATURE CITED

Introduction

1. Kramer, A. W. Nuclear propulsion for merchant ships. U.S. Atomic Energy Commission. Technical Information Service Extention. 1962.

2. Conklin, D. L., editor. Economics of nuclear and conventional merchant ships. Washington, D.C., U.S. Government Printing Office. 1958.

Chapter I

3. Hendrickson, R. L. and Mangan, J. L. Heat recovery from gas turbine exhaust. Amer. Soc. Mech. Engr. Paper 63-PWR-19. 1963.

4. Mund, M. G. and Murphy, T. E. The gas turbine air-cleaning dilemma. Amer. Soc. Mech. Engr. Paper 63-AHGT-63. 1963.

5. Paterson, J. R. Calculating the combined cycle. Gas turbine Reference Library Report GER-2227 [General Electric Company, Schenectady, New York] 1965.

6. Seward, H. L., editor. Marine engineering. Vol. 1. The Society of Naval Architects and Marine Engineers. New York, New York. 1942.

7. Labberton, J. M., editor. Marine engineer's handbook. New York, New York. McGraw-Hill. 1945.

8. Keenan, J. A., and Kaye, J. Gas tables. New York, New York. John Wiley and Sons. 1961.

9. Keenan, J. H. and Keyes, F. G. Thermodynamic properties of steam. New York, New York. John Wiley and Sons. 1951.

Chapter II

10. Ernst, T. Air filter application on gas turbines. Amer. Soc. Mech. Engr. Paper 66-GT-114. 1966.

11. Mund, M. G. and Wright, T. E. Design, development and application of air cleaners for gas turbines. Soc. Auto. Engr. Paper 538B. 1962.

12. Dalton, C. A. Sulfur and sea-water attack of turbine blades. Amer. Soc. Mech. Engr. Paper 65-GTP-7. 1965.

13. Weinert, E. P. and Carlton, G. A. Salt-water problems in marine gas turbines. Amer. Soc. Mech. Engr. Paper 65-GTP-18. 1965.

14. Krusen, G. C. and Silverman, L. Evaluation of proposed krypton-xenon adsorption system designs for the PL-2 reactor. U.S. Atomic Energy Commission Report NYO-4815 [New York Operations Office, AEC] 1962.

15. Adams, R. D. and Browning, W. E. Removal of radioiodine from air streams by activated charcoal. U.S. Atomic Energy Commission Report ORNL-2872 [Oak Ridge National Laboratory, Oak Ridge, Tennessee] 1960.

16. Ackley, R. D., Adams, R. E. and Browning, W. E. The disposal of radioactive fission gases by adsorption. U.S. Atomic Energy Commission Report TID-7593 [Technical Information Service Extention, AEC] 1959.

17. Ackley, R. D. and Browning, W. E. Equilibrium adsorption of krypton and xenon on activated carbon and linde molecular sieves. U.S. Atomic Energy Commission Report ORNL-CF-61-2-32 [Oak Ridge National Laboratory, Oak Ridge, Tennessee] 1961.

Chapter III

18. Lewis, A. D. Gas power dynamics. Princeton, New Jersey, D. Van Nostrand. 1962.

19. Senoo, Yasutoshi. Gas medium selection and turbomachinery matching for closed-Brayton-cycle-space power system. Amer. Soc. Mech. Engr. Paper 63-WA-86. 1963.

20. Frieder, A. Turbine cycles with ideal gases. [Zurich, Switzerland] Sulzer Technical Review Research Number 1961. 1961.

21. Frutschi, H. The influence of the properties of real gases on the closed-cycle process. [Zurich, Switzerland] Escher Wyss News Number 23046(e). 1960.

22. Chapman, A. J. Heat transfer. New York, New York, Macmillan. 1960.

23. McAdams, W. H. Heat transmission. 3rd edition. New Yord, New York. 1954.

24. Chart of the nuclides. 6th edition. Richland, Washington, Knolls Atomic Laboratory. 1961.

25. Evaluation of coolants and moderators for the maritime gas-cooled reactor. U.S. Atomic Energy Commission Report GA-570 [General Dynamics Corporation, California] 1958.

26. 630A Mark V maritime nuclear steam generator. U.S. Atomic Energy Commission Report GEMP-342 [General Electric Company, Cincinnati, Ohio] February, 1965.

27. Closed-cycle gas turbines for all fuels. [Zurich, Switzerland] Escher Wyss News 39, Number 1. 1966.

28. Table of thermal properties of gases. U.S. National Bureau of Standards Circular, Number 564. Washington, D.C., Government Printing Office, U.S. Department of Commerce. 1955.

29. Thermodynamic properties to 6,000 °K for 210 substances involving the first 18 elements. National Aeronautics and Space Administration Report SP-3001. 1963.

30. Keller, C. and Schmidt, D. Industrial closed-cycle gas turbines for conventional and nuclear fuels. Amer. Soc. Mech. Engr. Paper 67-GT-10. 1967.

Chapter IV

31. Nuclear-powered tanker, design and economic study. U.S. Atomic Energy Commission Report GA-1500 [General Atomic Division, General Dynamics Corporation, San Diego, California] 1960.

32. Rohach, A. F. Unpublished computer program from the Numerical Methods of Reactor Analysis course. N.E. 583. Ames, Iowa, Nuclear Engineering Department, Iowa State University. 1967.

33. Reactor physics constanta. U.S. Atomic Energy Commission Report ANL-5800 [Argonne National Laboratory, Argonne, Illinois] 1963.

34. Radkowsky, A., editor. Naval reactors physics handbook. Vol. 1. U.S. Atomic Energy Commission. Washington, D.C. U.S. Government Printing Office. 1963.

35. Bondarenko, I. I., editor. Group constants for nuclear reactor calculations. New York, New York. Consultants Bureau. 1964.

36. Glasstone, S. and Sesonske, A. Nuclear reactor engineering. Prinston, New Jersey. D. Van Nostrand. 1963.

37. Blizard, E. P., editor. Reactor handbook. 2nd edition. New York, New York. 1962.

38. American Society of Mechanical Engineers Boiler and pressure vessel code. Section III, rules for the construction of nuclear vessels. New York, New York, The Society. 1965.

Chapter V

39. Caldera, D. L. and Hoch, C. E. Gas turbine propulsion machinery for the MSTS roll-on/roll-off ship. Amer. Soc. Mech. Engr. Paper 67-GT-31. 1967.

Chapter VI

40. White, A. O. A study of gas turbine power plants for ship propulsion. Quincy, Massachusetts. The Society of Naval Architects and Marine Engineers, New England Section. October, 1963.

41. Clay, P. E. Heat recovery for gas turbine- an advanced design. Amer. Soc. Mech. Engr. Paper 67-GT-22. 1967.

Chapter VII

42. 630A maritime nuclear steam generator. U.S. Atomic Energy Commission Report GEMP-108 [General Electric Company, Cincinnati, Ohio] April, 1962.

43. Guide to nuclear power cost evaluation. U S. Atomic Energy Commission Report TID-7025 Vol. 4 [Technical Information Service Extention, AEC] March, 1962.

44. Eschbach, E. D. and Kanninen, M. F. Uranium price schedules and bred fuel value. U.S. Atomic Energy Commission Report HW-72219 [General Electric Company, Richland, Washington] December, 1964.

Chapter VIII

45. LeClair, T. G. Status of the high-temperature gas-cooled reactor. Amer. Inst. Engr. Educ. Paper 62-166. 1962.

CHAPTER XI. ACKNOWLEDGEMENTS

The author wishes to express his sincere appreciation to the following peopel:

Dr. Glenn Murphy, Head of the Nuclear Engineering Department and major professor, for providing me the opportunity to pursue this course of study and for his academic guidance, moral support and patient understanding throughout.

Dr. Alfred F. Rohach, for his tireless assistance in programming the neutronics phase of this design and for his helpful advice throughout its preparation.

Dr. George K. Serovy, Dr. Richard A. Danofsky and Dr. Donald F. Young, the other members of my advisory committee, for their assistance in answering questions whenever called upon to do so.

The Ford Foundation, for providing me with a financial grant which permitted me to complete my work.

My wife, Carol Faye, who assumed full responsibility of our family for fifteen months and whose unselfish sacrifices allowed me to complete the requirements for the advanced degree.